

**EPIDERMAL GROWTH FACTOR RECEPTOR AND JANUS KINASE 2
REGULATION OF PROGRAMMED CELL DEATH LIGAND 1 EXPRESSION AND
IMMUNOESCAPE IN HEAD AND NECK CANCER**

By

Fernando Concha-Benavente

MD. Universidad Nacional de San Agustín, 2007

Submitted to the Graduate Faculty

Of the School of Medicine in partial fulfillment

of the requirements for the degree of

PhD in Immunology

UNIVERSITY OF PITTSBURGH

2016

UNIVERSITY OF PITTSBURGH

SCHOOL OF MEDICINE

This dissertation was presented

by

Fernando Concha-Benavente MD

It was defended on

March 16, 2016

and approved by

Michael T. Lotze, MD, PhD, Professor

Walter Storkus, PhD, Professor

Sarah Gaffen PhD, Professor

Alexander Sorkin PhD, Professor

Dissertation Advisor: Robert L. Ferris, MD, PhD, Professor

Copyright © by Fernando Concha-Benavente

2016

**EPIDERMAL GROWTH FACTOR RECEPTOR AND JANUS KINASE 2
REGULATION OF PROGRAMMED CELL DEATH LIGAND 1 EXPRESSION AND
IMMUNOESCAPE IN HEAD AND NECK CANCER**

Fernando Concha-Benavente, MD, PhD.

University of Pittsburgh, 2016

Co-inhibitory immune checkpoint receptors (ICR) are novel targets for cancer immunotherapy. Programmed death ligand 1 (PD-L1), expressed in many cancers, including head and neck cancers (HNC), interacts with its receptor, programmed death 1 (PD-1), resulting in an exhausted phenotype. As yet, the stimuli and pathways that induce PD-L1 expression in tumor cells are not fully understood. Interferon gamma ($IFN\gamma$) and the epidermal growth factor receptor (EGFR) utilize Janus kinase 2 (JAK2) as a common signaling node transmitting tumor cell-mediated extrinsic or intrinsic signals, respectively. We investigated the mechanisms by which these factors upregulate PD-L1 and immunosuppressive cytokine expression in HNC cells in the context of EGFR/JAK/STAT pathway activation. We found that wild type overexpressed EGFR significantly correlated with JAK2 and PD-L1 expression. Furthermore, PD-L1 expression was induced in an EGFR- and JAK2-dependent manner, and specific JAK2 inhibition prevented PD-L1 upregulation in HNC, enhancing their immunogenicity. HNC tumors have higher expression of immunosuppressive cytokines including $TGF\beta$, IL-10, VEGF-A and IDO and lower expression of inflammatory cytokines such as IL-12A and IL-17A than controls. EGFR/JAK2 inhibition downregulated secretion of these STAT3-dependent cytokines *in vitro*, suggesting that targeting the EGFR/JAK2/STAT3 suppressive pathway may reverse tumor immunoescape. This view is supported by *in vivo* findings where HNC patients unresponsive to cetuximab therapy had significantly higher concentrations of immunosuppressive cytokines.

NK cells are crucial for promoting T cell responses against cancer. However, NK cell PD-1 expression remains largely undefined. Cetuximab-activated NK cells constitute the major effector cell subset that lyses tumor targets via antibody dependent cellular cytotoxicity (ADCC). We demonstrate that expression of PD-1 in HNC tumors correlates with NK cell activation markers. HNC patients exhibit higher levels of circulating PD-1⁺ NK cells, which are further enriched in the tumor. Interestingly, cetuximab treatment increased this frequency *in vitro* and *in vivo*. Inhibition of the PD-L1/PD-1 axis increased cetuximab-mediated NK cell activation and cytotoxicity.

Collectively, our findings suggest a novel role for JAK2 in EGFR-mediated PD-L1 upregulation and immunosuppressive cytokine secretion. Importantly, combined inhibition of the EGFR and PD-L1/PD-1 axis presents a potential strategy to reverse cetuximab-resistant immune evasion of HNC by enhancing NK cell cytotoxicity.

TABLE OF CONTENTS

PREFACE.....	XVI
1.2 INTRODUCTION.....	1
1.1 THE HALLMARKS OF CANCER.....	1
1.2 CANCER IMMUNOSURVEILLANCE.....	3
1.3 CANCER IMMUNOEDITING.....	3
1.4 CANCER IMMUNOTHERAPY.....	7
1.5 SIGNALS 0, 1, 1.5, 2 AND 3 IN IMMUNE CELL ACTIVATION AND ABERRANT SIGNALS 1, 2 AND 3 IN TUMOR IMMUNE ESCAPE.....	8
1.5.1 SIGNAL 0: Damage-associated molecular pattern molecules (DAMP).....	9
1.5.2 SIGNAL 1: Antigen processing machinery (APM) and HLA class I mediated antigen presentation.....	10
1.5.2.1 Normal antigen processing and presentation.....	10
1.5.2.2 Defects of APM machinery components ad antigen presentation in tumor cells.....	12
1.5.3 SIGNAL 1.5: CD40/CD40L.....	14
1.5.4 SIGNAL2: Co-stimulatory/co-inhibitory molecules, the PD-L1/PD-1 axis.....	15
1.5.5 SIGNAL 3: Tumor derived cytokines and chemokines.....	18
1.6 HEAD AND NECK CANCER (HNC)	22
1.6.1 The EGFR/JAK2/STAT3 pathway activation.....	22
1.6.2 Cetuximab-mediated EGFR blockade.....	23
1.6.3 Cetuximab-mediated NK cell activation.....	23
1.6.4 EGFR-mediated immune escape.....	24

1.7 HYPOTHESIS.....	25
1.8 SPECIFIC AIMS.....	26
1.8.1 SPECIFIC AIM 1: Determine the in vitro effect of EGFR and JAK2 inhibition to reverse PD-L1 upregulation and correlate with patient tumor expression data from The Cancer Genome Atlas (TCGA) and pre- and post-single agent cetuximab clinical trial UPCI 08-013.....	26
1.8.2 SPECIFIC AIM 2: Determine the in vitro effect of EGFR and JAK2 inhibition downregulating STAT3 dependent tumor derived cytokines and correlate with TCGA tumor expression data and patient serum specimens from pre- and post- single agent cetuximab clinical trial UPCI 08-013.....	26
1.8.3 SPECIFIC AIM 3: Determine the effect of EGFR and JAK2 inhibition in order to enhance NK cell mediated tumor lysis in vitro and correlate with patient tumor expression data from TCGA and pre- and post- single agent cetuximab clinical trial UPCI 08-013.....	26
2.2 IDENTIFICATION OF THE CELL-INTRINSIC AND EXTRINSIC PATHWAYS DOWNSTREAM OF EGFR AND IFNγ THAT INDUCE PD-L1 EXPRESSION IN HEAD AND NECK CANCER.....	27
2.1 INTRODUCTION.....	27
2.2 MATERIALS AND METHODS.....	29
2.2.1 Tumor cell lines.....	29
2.2.2 Antibodies and treatments.....	30
2.2.3 Flow cytometry analysis.....	32

2.2.4	Western blotting.....	33
2.2.5	siRNA knockdown.....	33
2.2.6	Quantitative PCR (qPCR)	34
2.2.7	Chromatin immunoprecipitation assay (ChIP)	34
2.2.8	Immunohistochemistry (IHC) protocol.....	35
2.2.9	Cellular cytotoxicity assay.....	36
2.2.10	The cancer genome atlas (TCGA) data retrieval analysis.....	37
2.2.11	IPA Ingenuity pathway software analysis.....	37
2.3	RESULTS.....	38
2.3.1	PD-L1 protein expression is higher in HPV positive HNC tumor specimens.....	38
2.3.2	HPV positive tumor specimens show higher Th1 type expression profile.....	41
2.3.3	PD-L1 expression correlates with that of JAK2, EGFR, IFNγ and a Th1 profile regardless HPV status.....	43
2.3.4	STAT1 but not STAT3, PIK3CA or MAPK1 expression is higher in tumor tissue and strongly correlates with PD-L1, EGFR and IFNγ regardless of HPV status.....	46
2.3.5	IFNγ-mediated PD-L1 upregulation is JAK2/STAT1 dependent.....	51
2.3.6	EGFR-mediated PD-L1 upregulation is JAK2/STAT1 dependent.....	57
2.4	DISCUSSION.....	62
2.5	SUPPLEMENTARY DATA.....	69
3.2	DOWNREGULATION OF IMMUNOSUPPRESSIVE CYTOKINE SECRETION BY EGFR AND JAK2 INHIBITION IN HEAD AND NECK CANCER.....	79

3.1 INTRODUCTION.....	79
3.2 MATERIALS AND METHODS.....	81
3.2.1 Patient plasma specimens collection and storage.....	81
3.2.2 Tumor cells and treatments.....	82
3.2.3 Antibodies and other reagents.....	82
3.2.4 ELISA.....	83
3.2.5 Flow cytometry analysis.....	83
3.2.6 Luminex assay.....	84
3.2.7 TCGA database analysis.....	84
3.3 RESULTS.....	85
3.3.1 HNC tumors have higher expression of signature immunosuppressive cytokines than control tissues.....	85
3.3.2 HNC tumors have lower expression of immunostimulatory cytokines than control mucosa.....	87
3.3.3 EGFR and JAK2 inhibition downregulate STAT3 activation in tumor cells.....	88
3.3.4 EGFR and JAK2 inhibition downregulate production of TGFβ and other signature immunosuppressive cytokines in tumor cells.....	89
3.3.5 EGFR and JAK2 inhibition diminish secretion of soluble PD-L1.....	93
3.3.6 Cetuximab resistant HNC patients have significantly lower concentrations of Th1 cytokines in plasma than responders.....	94
3.3.7 Cetuximab resistant patients have higher concentration of TGFβ in plasma.....	97

3.4 DISCUSSION.....	98
4.2 DISRUPTION OF THE PD-L1/PD-1 AXIS INTERACTION BY JAK2 INHIBITION AND/OR anti-PD-1 mAb BLOCKADE ENHANCES CETUXIMAB MEDIATED NK CELL CYTOTOXICITY IN HEAD AND NECK CANCER.....	102
4.1 INTRODUCTION.....	102
4.2 MATERIALS AND METHODS.....	105
4.2.1 Patients and specimens.....	105
4.2.2 Tumor infiltrating lymphocyte (TIL) isolation.....	106
4.2.3 PBMC and NK isolation from peripheral blood.....	106
4.2.4 Co-culture of NK cells using hIgG1 or PD-L1-coupled beads.....	106
4.2.5 Tumor cell lines.....	107
4.2.6 Antibodies and treatments.....	107
4.2.7 Flow cytometry analysis.....	108
4.2.9 Cellular cytotoxicity assays.....	109
4.2.10 The Cancer Genome Atlas (TCGA) data retrieval and analysis.....	109
4.3 RESULTS.....	110
4.3.1 HNC patients have higher PD-1+ circulating NK cells in healthy individuals, which are enriched in HNC tumors, and predict better survival.....	110
4.3.2 Elevated expression of NK activation markers correlates with that of PD-1 in HNC tumors.....	113
4.3.3 PD-1 expressing NK cells display an activated phenotype.....	115

4.3.4	Cetuximab induces NK cell activation, PD-1 expression and IFN γ -dependent PD-L1 upregulation in HNC.....	118
4.3.5	PD-1 blockade enhances NK cell cytotoxicity and cetuximab mediated ADCC in PD-L1 high tumor targets.....	121
4.3.6	JAK2 inhibition prevents tumor PD-L1 expression and enhances cetuximab mediated NK cell cytotoxicity.....	124
4.4	DISCUSSION.....	127
4.5	SUPPLEMENTARY DATA.....	132
	BIBLIOGRAPHY.....(0000).....	135

LIST OF FIGURES

Figure 1.1	2
Figure 1.3	6
Figure 1.5	9
Figure 1.5.1.2	14
Figure 1.5.2	18
Figure 1.5.3	21
Figure 2.3.1	41
Figure 2.3.2	42
Figure 2.3.3	45
Figure 2.3.4	50
Figure 2.3.5	56
Figure 2.3.6	61
Figure 2.5.1	69
Figure 2.5.2.....	70
Figure 2.5.3	70
Figure 2.5.4	71
Figure 2.5.5	72
Figure 2.5.6	73
Figure 2.5.7	73
Figure 2.5.8	74
Figure 2.5.9	75
Figure 2.5.10	75
Figure 2.5.11	76
Figure 2.5.12	76

Figure 2.5.13	77
Figure 2.5.14	77
Figure 2.5.15	78
Figure 2.5.16	78
Figure 3.3.1	86
Figure 3.3.2	88
Figure 3.3.3	89
Figure 3.3.4	92
Figure 3.3.5	94
Figure 3.3.6	96
Figure 3.3.7	97
Figure 4.3.1	112
Figure 4.3.2	115
Figure 4.3.3	117
Figure 4.3.4	121
Figure 4.3.5	124
Figure 4.3.6	126
Figure 4.5.1	132
Figure 4.5.2	133
Figure 4.5.3	134

LIST OF TABLES

Table 2.3.3.1.....	46
Table 2.3.4.1	51

PREFACE

When I was a little kid, my mom used to ask me, what do you want to be when you grow up? I always answered -while holding my colorful toy stethoscope in one hand and a small plastic microscope on the other hand-, a doctor mom! I want to be a doctor! ... And here I am, a few years later. Medicine and science are wonderful, truly captivating, enticing, rewarding, but not easy. They require a lot of motivation, commitment, endurance and most importantly passion, the kind of passion that makes you leave everything behind -even your beloved ones- to pursue your dreams! ... I am a dreamer, a very passionate one. I am infinitely thankful to God -and life itself- for giving me the opportunity to discover the beauty of nature and science, and of course, my dear mother for her unconditional support of my passion, for letting me follow my dreams.

I am very fortunate to have met so many amazing mentors during the past years of my life, brilliant minds who I admire and consider exemplary and honorable, the ones who showed me how wonderful medicine and science is and taught me those attributes that make a great scientist. First, I want to thank my mentor Dr. Robert L. Ferris - or Doc, how I always call him- for believing in me, for opening the doors of his laboratory and giving me a home to start my scientific journey, for his wise advice and encouragement even during the most difficult times of my thesis project, for giving me the freedom a creative researcher needs in order to explore new ways to go around experimental obstacles. I am sure immunology research would have never been as exciting without his support and amiable mentorship. I am also grateful to Dr. Michael T. Lotze, my laboratory rotation mentor and thesis committee member, I admire your work, scientific ethics, kindness, and joyful personality. I will always remember how such a great

motivator you are, your words of encouragement even when experiments fail and your wise advice for my future medical and scientific career plans. I am also thankful to Dr. Nikola Vujanovic whose sharp scientific advice was always helpful, his respectful yet friendly personality always made him really approachable. I am honored to have learned some experimental techniques from him and collaborate -at least in part- in the research he conducts. Finally, I am also indebted to Doctors Russell Salter -my first lab rotation mentor and initially part of my thesis committee-, Walter Storkus, Sarah Gaffen and Alexander Sorkin for their patience, insightful guidance and helpful scientific suggestions with my thesis project during the past years.

I should also make a special mention to my very first mentor and friend Dr. Jorge Ballón Echegaray, I will always be grateful for the opportunity he gave me to work in the immunology research group he still directs at the Universidad Nacional de San Agustín-Peru. I am indebted to him for introducing me to the fascinating world of immunology and for fueling my passion for research that now burns stronger than ever.

Finally, I want to thank all the Ferris lab members who helped me in more than one way. Also, all the friends and kindhearted people from all around the world I have met in this wonderful city, Pittsburgh! A place that now I call home away from home. And last but not least, my close family, especially Delfina and Jorge -mom and dad-, Toribio and Lourdes -my beloved grandpa and aunt- and all those who were there for me since the very beginning, some are still around. *Gracias totales!!!*

1.0 INTRODUCTION

1.1 THE HALLMARKS OF CANCER

Cancer arises in eukaryotes when normal cells develop genomic instability transforming their timely and biologically organized growth and function. This oncogenic multistep transformation is caused by intrinsic and extrinsic disturbances that lead to tumor transformation. These capabilities include, in addition to genomic instability, uncontrolled and sustained proliferation, evasion of growth suppression, resistance to cell death by enabling mitogenic immortality, activation of an invasive phenotype, stimulation of angiogenesis and metastasis. These capabilities common to the majority of tumors are recognized as the initial “Hallmarks of Cancer” (1). Recent work has yield evidence for enlarging this list of tumor transforming competences where re-conditioning of cellular metabolism, inflammation promoting tumor development and evasion of immune destruction become important new hallmarks of cancer (Figure 1.1). Importantly, another important factor that adds complexity to this set of tumor characteristics is the recruitment and interaction of tumor cells with surrounding stromal cells and immune infiltrating cells forming the intricate network called the tumor microenvironment. Focusing on inflammation and immune recognition by the host has increased our therapeutic strategies targeting the process of oncogenic transformation and enabled new and curative approaches.

Recognition of the immune escape capabilities of cancer cells as one important factor inducing and maintaining tumor formation has provided a framework to understand the interaction of the host’s immune system with cancer cells in the setting of immune surveillance.

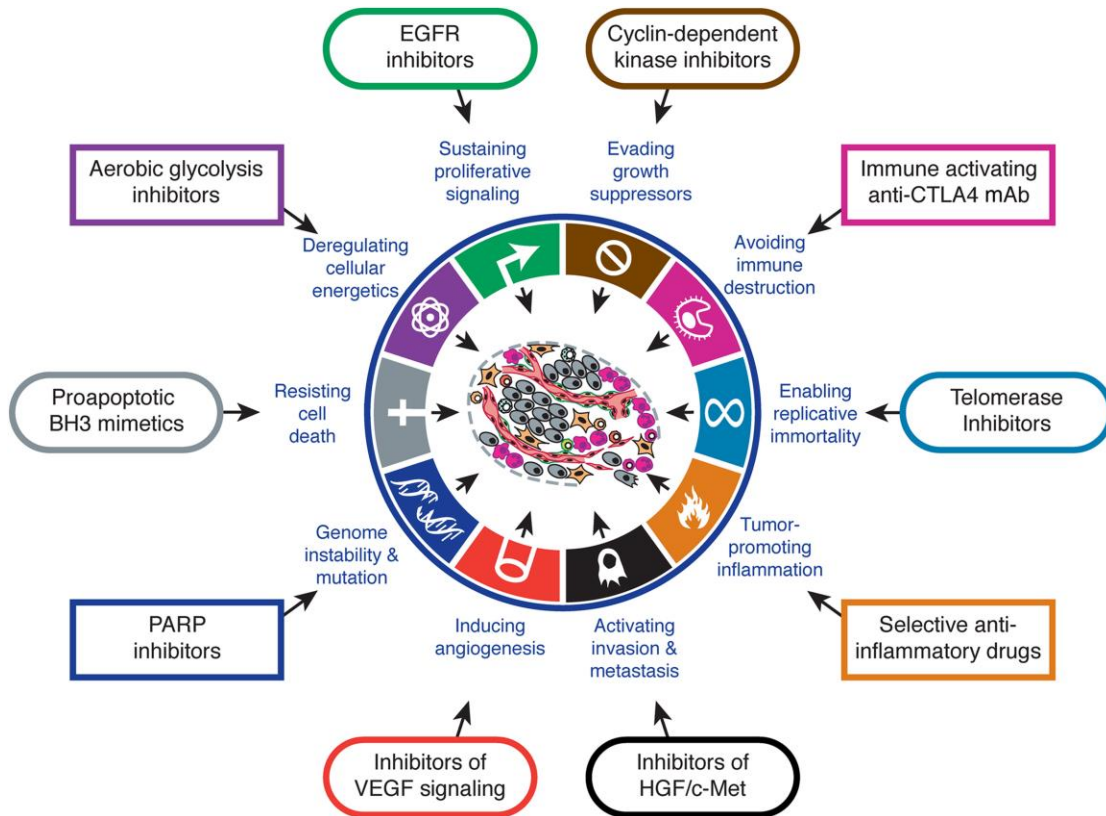


Figure 1.1 The hallmarks of cancer: The illustration lists the up-to-date hallmarks of cancer development, which include the four recently added: tumor promoting inflammation, genome instability and mutation, deregulation of cellular energetics and escape from immune destruction. We include as well the therapeutic strategies that target each of the different cancer capabilities that aim ultimately to reverse cancer progression. [Adapted from Hallmarks of Cancer: The Next Generation. Hanahan D and Weinberg R. Cell, 2011 (1)].

1.2 CANCER IMMUNE SURVEILLANCE

The cancer immune surveillance theory was originally proposed in 1957 by Burnet M. (2-4) when he predicted that the host's immune system could actively detect and eliminate nascent tumor cells. These seminal insights were confirmed and extended in transplantation models of nude athymic mice in 1970 that allowed researchers to investigate how tumors arise in immunocompromised hosts (5). As the field of tumor immunology evolved, studies showing the pivotal role of IFN γ in control of tumor growth in mice provided irrevocable evidence of the role of the immune system in cancer suppression. The question of how tumors still appear and progress in immunocompetent hosts is still an unresolved conundrum (6). Extensive work over the past 30 years revealed that this immunosurveillance function was only part of a larger, more complex setting that included "cancer immunoediting", which more accurately temporally defines the tumor-immune system interactions and cross-talk.

1.3 CANCER IMMUNOEDITING

Cancer immunoediting comprises all the dynamic multifactorial processes where the immune system, through activation of innate and adaptive immune mechanisms, not only protects against cancer development but also shapes or "edits" the phenotype of emerging cancer cells in three temporally well-defined stages: elimination, equilibrium and escape. A large body of evidence supports this notion; first, chronic inflammation promotes cancer development (7) and second, previous work showed that an intact immune system could prevent or promote cancer depending on the stage of the immunoediting sequence (6, 8).

Elimination, is characterized by immune destruction of transformed cells, which are highly immunogenic, a small subset of these transformed cells survive immune destruction and enter the “editing” phase termed equilibrium. The elimination phase is sufficiently supported by evidence where immunodeficient mice develop more carcinogen-induced and spontaneous cancers than wild type mice and tumors derived from immunodeficient mice are more immunogenic than those from immunocompetent mice. The role of type I and II interferons, dendritic cells, and CD8 T cells are underlined in the immunogenic process and rejection of tumors that involve the adaptive immune system (9-11) (Figure 1.3). More recently, new pathways of tumor rejection involving the innate immune system have been described whereby NK cells play a crucial role eliminating senescent tumors that expressed NKG2D ligands upon DNA damage and overactive Ras signaling (12, 13). The *equilibrium* stage is characterized by tumor dormancy where strong immune pressure causes tumor cell destruction, culling and Darwinian selection of tumor cells that are progressively more resistant to immune attack. Dormant tumor cells have higher proportion of resident CD8+ T cells, NK cells and gamma delta T cells but low NKT, Tregs and MDSCs (14). What tilts the balance to either elimination or escape is still not well understood, since editing occurs during dormancy, such cells evolve in an environment that the immune system is unable to contain, leading to escape. Tumor immune *escape* occurs through several different mechanisms including resistance to cell death and increasing certain intrinsic survival signals including STAT3, Bcl-2, Bcl-xl, IAPs and surviving. Tumors evade immune recognition by downregulating signal 1, constituted by antigen processing and HLA class I presentation, by providing aberrant signal 2, characterized by overexpression of immune checkpoint receptor ligands including PD-L1, Tim3, LAG3 and Galectin 9, or providing an abnormal signal 3,

characterized by secreting immunosuppressive cytokines such as VEGF, TGF β , IL-10 and IDO among others rather than IL-12 family members (15-17).

Recognizing that the immune system is not ignorant of the presence of cancer but rather sculpts its progress or rejection, underpins the need of investigating and understanding the individual mechanisms by which these complex phenomena occur and justifies the development of strategies to manipulate the host immune system in order to promote tumor control and elimination.

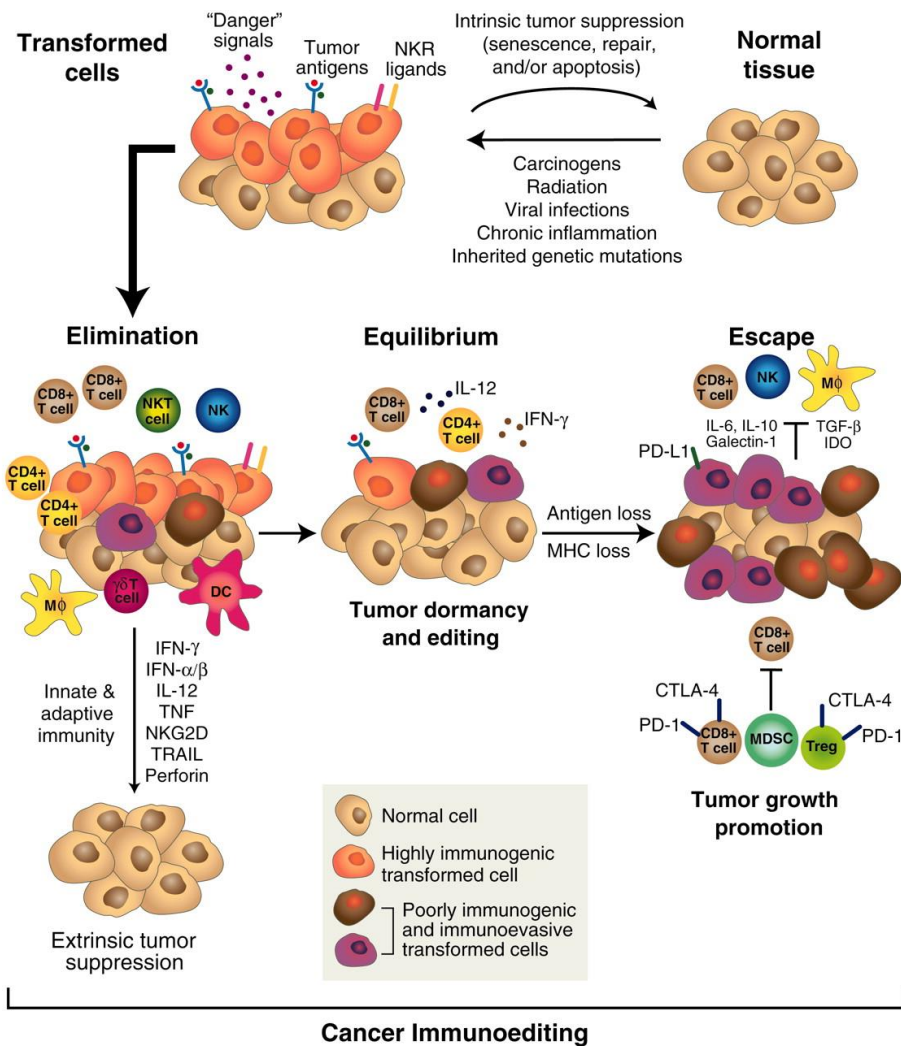


Figure 1.3 The cancer immunoediting concept: Only after cellular transformation has occurred and intrinsic tumor suppressor mechanisms have failed, an extrinsic tumor suppressor mechanism is engaged in which the host immune system edits or sculpts tumor development. Cancer immunoediting consists of three sequential phases: elimination, equilibrium, and escape. In the escape stage many mechanisms of immune evasion are triggered, characterized by aberrant signals 1-antigen presentation-, 2 -co-inhibitory molecules and 3-immunosuppressive soluble cytokines. [Adapted from Schreiber RD, Old LJ, Smyth MJ. Cancer immunoediting: integrating immunity's roles in cancer suppression and promotion. *Science*. 2011 (9)].

1.4 CANCER IMMUNOTHERAPY

We have described numerous studies that support the immune system as a major modulator of cancer growth. Immunotherapy of cancer has emerged as a viable and transformative approach for treatment of patients. Current immunotherapies are focused on either stimulating the activities of specific components of the immune system or counteract signals produced by cancer cells that suppress immune responses. Adoptive cell transfer, therapeutic tumor-antigen specific monoclonal antibodies, cancer vaccines, immune modulators and immune checkpoint blocking antibodies are among the different types of immunotherapy. Importantly, approaches that involve combinations and target multiple pathways may prove to be synergistic and generate stronger antitumor immune responses. It is noteworthy to mention the recent clinical success of antibodies targeting programmed death ligand 1/programmed death 1 (PD-L1/ PD-1) axis, especially in the setting of melanoma where PD-1 mediated monoclonal antibody blockade has revolutionized conventional treatment strategies of patients (18-20). Investigating the immunosuppressive pathways that tumor cells have across different types of cancers is important in order to understand their biology, rationalize and personalize treatments in order to increase efficacy of current therapies. One major advance in the field of immunotherapy has been the increasing capabilities to undertake genomic studies of tumors to measure the effect of antitumor immunotherapy and evaluate its efficacy. This defines key parameters that allow us to differentiate tumor gene profiles from responders and non-responders, identify mutations, stratify patients and develop new approaches that will ultimately enhance response rates.

**1.5 SIGNALS 0, 1, 1.5, 2 AND 3 IN IMMUNE CELL ACTIVATION AND
ABERRANT SIGNALS 1, 2 AND 3 IN TUMOR IMMUNO ESCAPE**

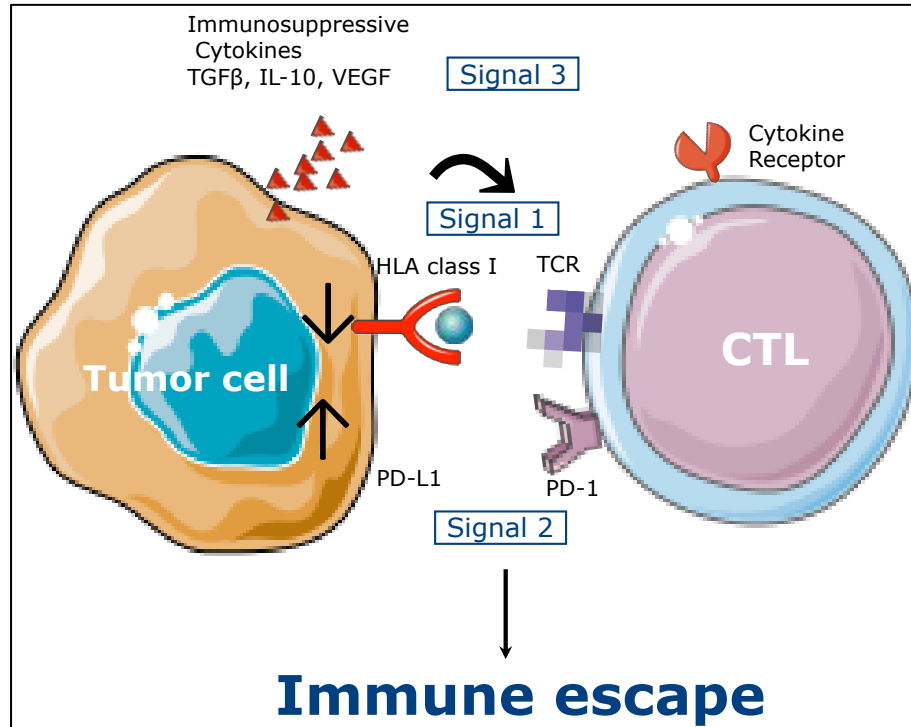
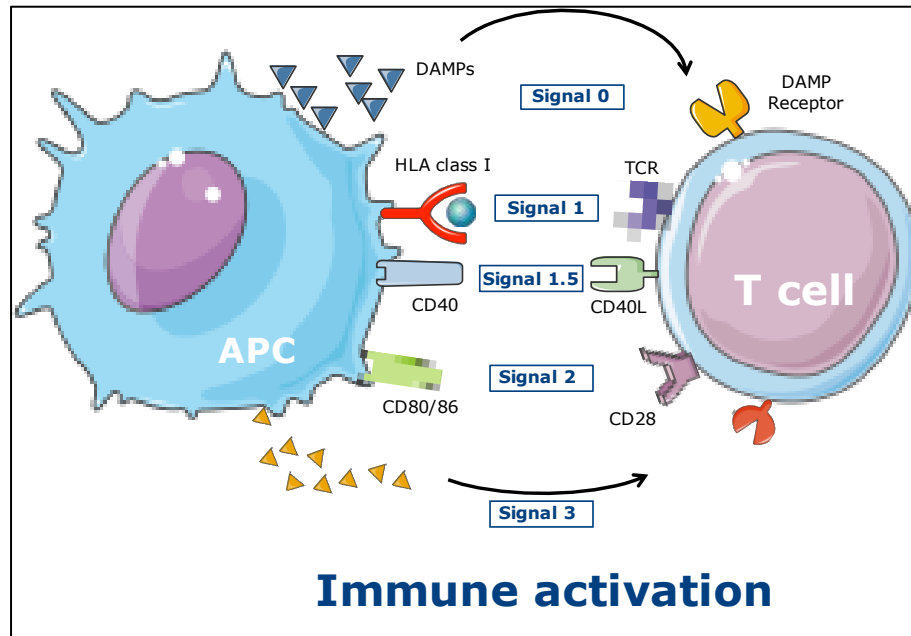


Figure 1.5 Signals 0, 1, 1.5, 2 and 3 in normal immune cell activation and aberrant signals 1,2 and 3 in tumor immune escape: In a normal immune cell activation 3 signals are required. Signal 1 mediated by MHC class I antigen presentation to the T cell receptor on CD8⁺ T cell, following this event CD40L is upregulated on the T cell and ligates CD40 on the antigen presenting cell promoting CD80/CD86 upregulation, this constitutes what we call signal 1.5. Signal 2 is mediated by co-stimulatory molecules CD80/CD86 expressed on antigen presenting cells such as dendritic cells that engages CD28 on T cells providing a second activating signal. Finally signal 3, mediated by known stimulating soluble cytokines secreted by antigen presenting cells namely: IFN γ , IFN α , IL-12, IL-1, TNF α . (**Top panel**). Conversely, in the setting of cancer, suppressed antigen presenting cells or tumor cells themselves provide aberrant signals 1, 2 and 3. Characterized by downregulation of HLA class I mediated antigen presentation, aberrant co-inhibitory molecules such as PD-L1, also known as immune checkpoint ligands and finally soluble suppressive cytokines such as TGF β , IL-10, IL-6, and IDO among others, these three aberrant signals favor immune escape of tumor cells (**Bottom panel**).

1.5.1 SIGNAL 0: Damage-associated molecular pattern molecules (DAMP)

Damage-associated molecular pattern molecules (DAMPs) are cell-derived molecules that initiate the immune response, thus called herein signal 0. DAMPs are secreted from cells that suffer traumatic or ischemic damage, either in the absence or presence of microbial infection. DAMPs bind specific receptors such as Toll-like receptors (TLRs), NOD-like receptors (NLRs), RIG-I-like receptors (RLRs), AIM2-like receptors, and the receptor for advanced glycation end products (RAGE). The ligation of these receptor induces autophagy in the target cell. Autophagy is a process whereby soluble cytoplasmic components and organelles are degraded by the lysosome, most likely as a cell stress response to starvation and subsequently to limit damage and maintain cellular homeostasis as a means to exert protein/organelle quality control. Importantly, autophagy constitutes one of the “Hallmarks of Cancer” and is linked to both tumor cell survival and death. Indeed, severely stressed cancer cells (by nutrient starvation, radiotherapy or cytotoxic drug therapy) induce cell shrinkage via autophagy to a state of reversible dormancy (21). This survival strategy of tumor cells may lead to an eventual regrowth and persistence of late stage tumors.

The concept of DAMPs initiating immune responses as what we call signal 0, starts with the idea that the immune system detects danger when tissues have been damaged either by microbes or sterile inflammation. In this model, DAMPs such as HMGB1, HSP, ATP, hyaluronic acid bind specific receptors and activate antigen-presenting cells (APCs) from stressed or damaged tissues. These activation stimuli in turn switch on pathways such mitogen-activated protein kinases (MAPKs), NF- κ B, and PI3K/AKT which provide potent responses to cell survival, proliferation and immune activation (22).

1.5.2 SIGNAL 1: Antigen processing machinery (APM) and HLA class I mediated antigen presentation

1.5.2.1'Normal antigen processing and presentation "Proteins are degraded by two major pathways: the ubiquitin-proteasome pathway and the lysosomal pathway (23). In APCs the lysosomal pathway primarily degrades external proteins taken up by endocytosis or recycled internal proteins loading the final peptides onto HLA class II molecules, the proteasomal pathway degrades intracellular proteins through ubiquitination and loads the final peptide product generated by the proteasome onto HLA class I molecules (24, 25). A major exception to this rule is a process called cross-presentation, whereby external proteins taken up by professional antigen presenting cells entering the lysosomal pathway attain access to the HLA class I pathway (26).

The complex process of ubiquitination is a multi-step tandem enzymatic enzymatic reaction involving 3 crucial catalytic proteins: E1 (ubiquitin activating enzyme), E2 (ubiquitin conjugating enzyme) and E3 (substrate specific ubiquitin ligase) that covalently link a 76-residue polypeptide to free amino groups on the target protein (27).

Once tagged, the target proteins are degraded by the proteasome. The proteasome is a multimeric protein complex formed by the 20S catalytic core, which has two outer rings of 7 α -subunits (α 1- α 7) and two inner rings of 7 β -subunits (β 1- β 7); two regulatory 19S particles sit on both ends of the core regulating ingress and egress of cargo. Importantly, 3 β -subunits: β 1, β 2 and β 5 are replaced by the interferon- γ (IFN γ) inducible subunits: low molecular weight protein-2, 7 and 10 (LMP2, LMP7 and LMP10), respectively. The replacement of these subunits at the catalytic core forms the immunoproteasome (28, 29). This structure generates different antigenic peptides with high affinity for HLA class I alleles (30, 31). Once these immunogenic peptides are generated, they are transported to the endoplasmic reticulum (ER) by transporter of antigen processing (TAP), which is formed by two non-covalently linked subunits TAP1 and TAP2. The assembling of TAP1 and TAP2 forms a pore on the ER membrane allowing the protein to enter the ER lumen (32-34). Peptides that enter the ER lumen are loaded onto nascent HLA class I heavy chains, which are associated with β 2-microglobulin chains, with the assistance of four chaperones: calnexin, ERp57, calreticulin and tapasin. The HLA class I complex is subsequently loaded with the peptide by tapasin (Figure 1) (35-38). The stabilized trimeric complex: HLA class I heavy chain, β 2-microglobulin and peptide, now transverses the Golgi apparatus, shuttles to the cell membrane and fuses with it so the HLA class I peptide complex is exposed extracellularly and can be recognized by the cognate T cell receptor (TCR) on CD8⁺ T cells. An intact, stepwise progression of this pathway is required in order for the immunogenic peptide to reach the surface loaded onto HLA class I molecules and interact with CD8⁺ T cells. If any of the steps is disrupted in tumor cells, antigen presentation does not occur, leading to an impaired TA-specific CTL recognition and subsequent lysis (39).

1.5.2.2 Effects of APM machinery components and antigen presentation in tumor cells

Abnormalities of the APM machinery have been identified in many types of cancer including HNC. Most of them take place at the genetic or epigenetic level, however, there is also evidence of defects at the transcriptional and post-translational level, as follows:

Proteasome defects: Abnormalities in expression and function of the IFN γ inducible subunits LMP2, LMP7 and LMP10 have been described in HNC (40, 41) as well as in other cancers such as esophageal (42-44), stomach (45), colorectal (46-48), bladder (49, 50), prostate cancer (51) as well as melanoma (52, 53). The molecular basis for these defects has been described for certain types of cancer. For instance, gastric cancer shows microsatellite mutations at the gene encoding *LMP7* and single nucleotide polymorphisms for *LMP2* and *LMP7* have been detected in the case of cervix malignancies (54). Loss of LMP2 upregulation after IFN γ treatment has been associated with defects in transcription factors such as interferon response factor 1 (IRF1) and signal transducer and activator of transcription (STAT1) binding to promoter sequences (55). Furthermore, defects in Janus kinase 2 (JAK2) expression have been linked to lack of interferon-mediated upregulation of LMP2 and LMP10 in melanoma (56).

Defects in TAP1, TAP2 and chaperones: Downregulation of TAP1 and TAP2 at the mRNA and protein level in cell lines and primary tumors has been documented for HNC (40, 41, 57-59) as well as for esophageal (42-44), stomach (45), pancreatic (60), colorectal (46-48), prostate cancers (51) and melanoma (52, 53, 61-63). Interestingly, IFN γ treatment restored TAP

expression in several cell lines where it was downregulated (64-66). However, this effect was impaired in those cells with loss of JAK2 expression (56). Therefore, JAK2 presents as a crucial mediator in IFN γ pathway activation and HLA class I upregulation. Additionally, genetic mutations at the *TAP* loci that impair normal protein expression or function have been reported in cervix, colorectal, gastric and lung carcinomas (45, 46, 48, 67-69).

As for chaperones expression and function, calnexin, tapasin and ERp57 have been shown to be downregulated in HNC (maxillary sinus and larynx carcinomas) as well as in esophagus, colon, prostate, cervix and breast cancer and melanoma (41, 44, 46, 48, 51, 54, 61, 70, 71). Additionally, a defective IFN γ signaling has been associated with low tapasin expression in melanoma cells (56). However, more interesting is the finding of an irreversible tapasin frameshift mutation in metastatic melanoma cells that is associated with *HLA-A3* gene expression selective epigenetic unresponsiveness to IFN γ , which is reversible only after DNA methyltransferase I depletion (72). Thus, these results suggest the rational use of demethylating agents in order to increase HLA class I antigen presentation and stimulate CTL specific responses.

Defects in HLA class I molecules: Complete absence of HLA class I expression on the cell membrane has been linked with β 2-microglobulin mutations and defects in peptide synthesis and transport that are concomitantly found with defects in expression of LMP, TAP and chaperones, leading to a defective peptide loading of HLA molecules and instability of the HLA class I-peptide trimolecular complex. Interestingly, HLA class I and β 2-microglobulin defects can only be overcome with gene transfection, and defects in APM components can induce a very marked downregulation in HLA class I expression which can be corrected with IFN γ treatment. Defects in HLA class I expression have been described in HNC, esophagus,

gastric and colon carcinomas as well as in melanoma (43, 45, 48, 73-79). Likewise, partial mutations in the *HLA* loci have been detected in laryngeal cancer (80, 81) colon, cervical carcinoma and melanoma (68, 77, 82).

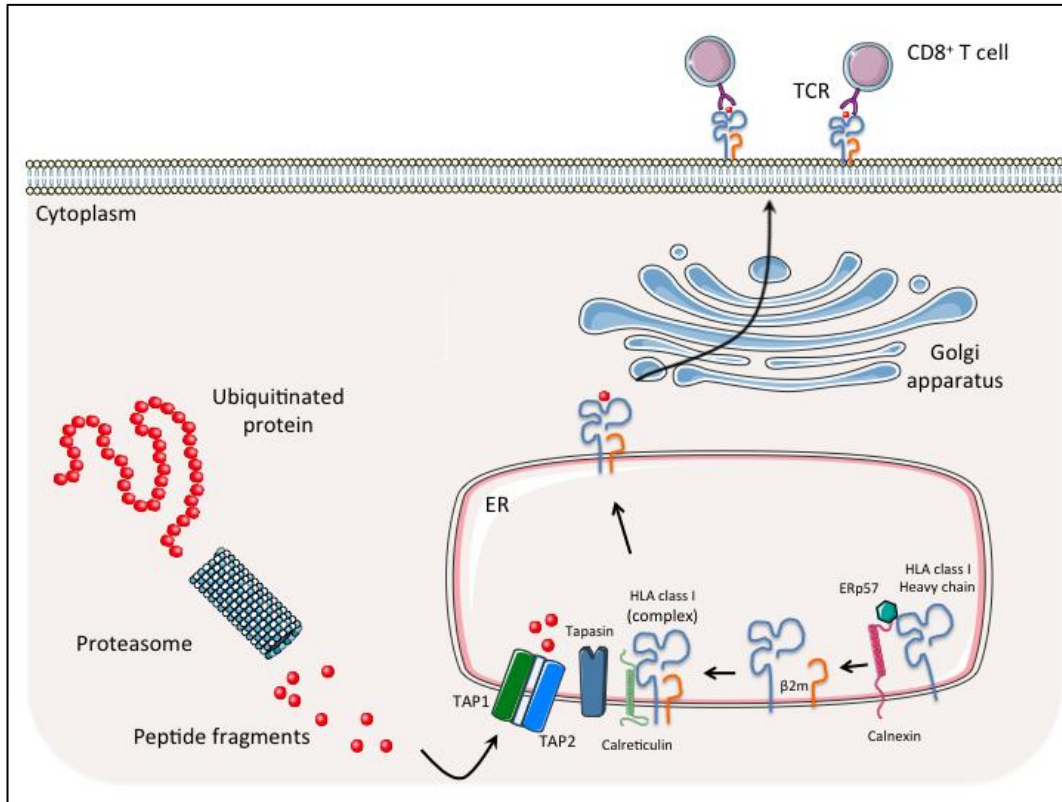


Figure 1.5.1.2 Antigen processing machinery components: Normal cells process intracellular ubiquitinated proteins tagged for degradation via the proteasome generating peptide fragments that are loaded onto nascent HLA class I molecules inside the endoplasmic reticulum (ER). Antigen presentation on the cell surface requires intact APM machinery in order to stimulate specific CD8⁺ T cell effector responses.

1.5.5 SIGNAL 1.5: CD40/CD40L

CD40 is a receptor member of the tumor necrosis factor (TNF) receptor family, is expressed by antigen-presenting cells, as well as non-immune cells and tumors. CD40 binds its ligand CD40L, which is transiently expressed on T cells and other non-immune cells under inflammatory

conditions. A wide spectrum of molecular and cellular processes is regulated by CD40 engagement including the initiation and progression of cellular and humoral adaptive immunity. We coined the concept of CD40/CD40L interaction as signal 1.5 since ligation of CD40 on APCs increases expression of co-stimulatory molecules CD80/CD86, which provide an activating signal 2.

CD40L/CD40 interactions exert profound effects on dendritic cells (DC), B cells, and endothelial cells, among many cells of the hematopoietic and non-hematopoietic compartments. It has been demonstrated that CD40 engagement on the surface of DCs promotes their cytokine production, the induction of co-stimulatory molecules on their surface, and facilitates the cross-presentation of antigen. Overall, the impact of CD40 signaling ‘licenses’ DCs to mature and achieve all of the necessary characteristics to effectively trigger T-cell activation and differentiation (83).

1.5.4"IGNAL 2: Co-stimulatory/co-inhibitory molecules, the PD-L1/PD-1 axis

T cell activation not only depends on MHC class I mediated antigen presentation but also on second signal characterized by co-stimulatory molecules. This co-stimulatory signal 2 is antigen independent and is provided by the B7 family of molecules and is expressed on antigen presenting cells: B7.1 (CD80) and B7.2 (CD86), which bind to CD28 expressed on T cells (84). Interestingly, these same ligands bind the immune checkpoint receptor cytotoxic T lymphocyte antigen 4 (CTLA4) providing inhibitory signals downstream preventing T cell receptor activation (85). In addition to B7 receptors other members of this family have been identified and named B7-homologs (B7-H) due to their structural resemblance to the former ones: B7-H1/CD274 or programmed death ligand 1 (PD-L1), B7-DC/CD273 or programmed death ligand

2 (PD-L2), B7-H2/CD275, B7-H3/CD276 and B7-H4. From these, PD-L1 and PD-L2 bind to their surrogate receptor molecule programmed death 1 (PD-1) delivering inhibitory signals (Figure 1.5.2) (86).

PD-L1 and PD-L2 are type I transmembrane glycoproteins composed of IgC- and IgV-type extracellular domains (84, 87). PD-L1 shares 20% amino acid identities with B7.1 and B7.2 that are ligands for CD28 and CTLA-4. PD-L1 and PD-L2 share 40% amino acid identity while human and murine orthologs of PD-L1 or PD-L2 share 70% amino acid identity. Both PD-L1 and PD-L2 have short cytoplasmic tails with no known motif for signal transduction, suggesting that these ligands do not transduce any signal upon interaction with PD-1. However, one group reported that cross-linking of PD-L2 induces stimulatory signal in DCs, resulting in the augmented antigen presentation (88).

PD-L1 is expressed under homeostatic conditions in many non-immune tissues including endothelial cells, heart, skeletal muscle and placenta to name a few (87) and in immune cells such as activated B and T cells and dendritic cells (DC). Additionally, PD-1 is expressed on double-negative $\alpha\beta$ and $\gamma\delta$ T cells in the thymus and induced on peripheral T and B cells upon activation (89, 90). In homeostatic immune system development and function PD-L1/PD-1 interaction delivers inhibitory signals that regulate both peripheral and central tolerance. In the thymus, PD-L1 is expressed on thymocytes in the cortex and in the medulla, participating in positive as well as negative selection (91). Likewise, tolerogenic dendritic cells express PD-L1 and PD-L2, and reduce the initial phase of activation and expansion of self-reactive T cells, it is also involved in limiting the reactivation, expansion and effector functions of T cells (92, 93). PD-1/PD-L1 interaction inhibits T cell proliferation, survival, cytotoxicity and cytokine release, induces apoptosis of tumor-specific T cells (94, 95), promotes the differentiation of CD4⁺ T cells

into Foxp3⁺ regulatory T cells (96), and resistance of tumor cells to CTL attack (97). Upon PD-L1 ligation, PD-1 recruits SH2-domain containing protein tyrosine phosphatases (SHP-1 and SHP-2) to the immunoreceptor tyrosine based switch motif within the PD-1 cytoplasmic tail and inhibits positive signaling events downstream of the TCR. Importantly, PD-L1 has also been shown to mediate differentiation and maintenance of FOXP3⁺ regulatory T cells (Tregs) via downregulation of the Akt/mTOR pathway (98).

In addition, the PD-1/PD-L1 axis may also regulate NK cell function. In a murine model, tumor derived IL-18 promoted the differentiation and accumulation of immature NK cells, which overexpressed PD-L1 and killed lymph node resident DC in a PD-1/PD-L1-dependent manner (99). These results suggest a NK/DC crosstalk in a PD-1/PD-L1-dependent manner leading to regulation of expansion of DCs and adaptive immunity. Cancer cells could also control NK cytotoxicity by providing inhibitory PD-L1-mediated signals to PD-1 expressing NK cells. This setting is particularly important in malignancies where therapeutic monoclonal antibodies, such as cetuximab that can both block EGFR and stimulate IFN γ secretion via activation of NK and CTLs, are broadly used for patient immunotherapy (100-102).

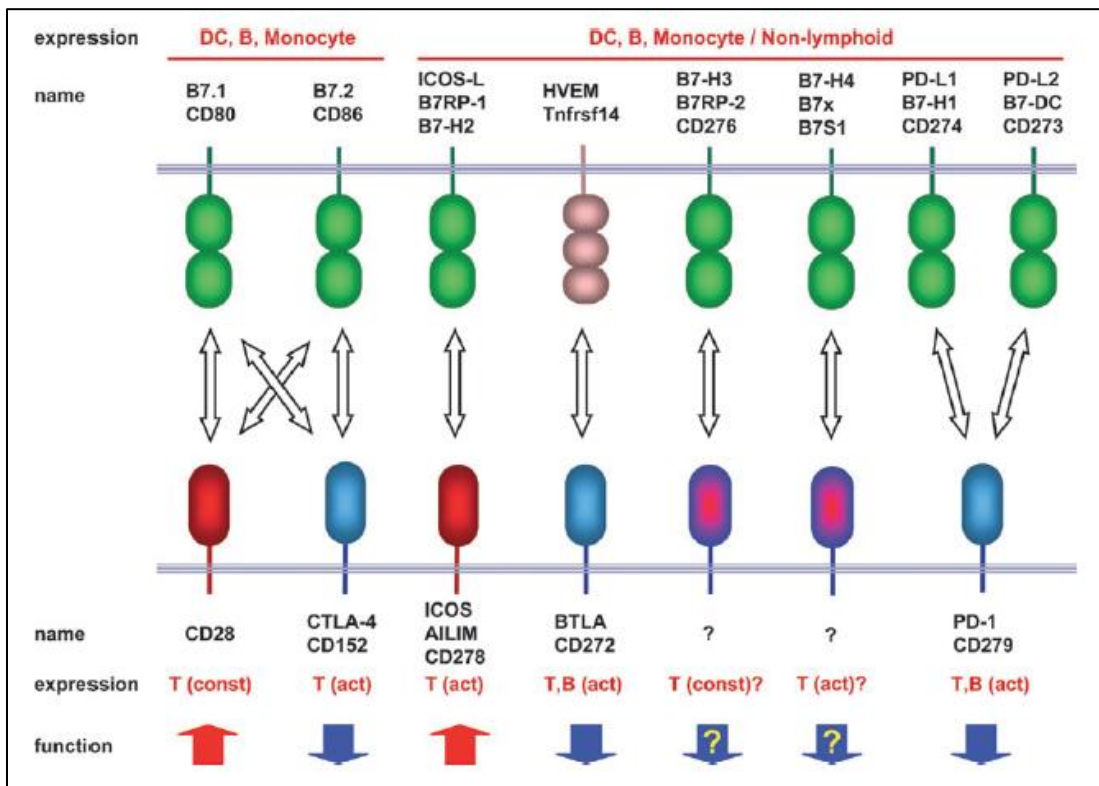


Figure 1.5.2 Superfamily of B7 and B7-H receptor/ligands: Nomenclature, expression pattern and function are indicated in the illustration. Act: expression upon activation, const: constitutive expression. [Adapted from Okazaki T, Honjo T. PD-1 and PD-1 ligands: from discovery to clinical application. *International immunology* (103)].

1.5.5 SIGNAL 3: tumor derived cytokines and chemokines

Inflammation is a beneficial response that restores tissue injury and activates the immune system to fight pathogenic agents. However, in malignant transformation, inflammation is unregulated and perpetuates in time becoming chronic. Indeed, more than a century ago, Rudolph Virchow described tumor infiltrating inflammatory cells and hypothesized that cancer could emerge as a consequence of inflammation (104). Recent work has proved Virchow's postulate with sufficient evidence supporting that various cancers are triggered by infection and chronic inflammatory

disease (105). In the first stages of inflammation, during the *elimination* phase of tumor immunoediting a tumor-rejecting cytokine milieu is characterized by cytokines such as IL-1beta, IL-2, IL-12, TNFalpha, IFNalpha and IFNgamma, which skew the immune response to a Th1/M1 pattern. These cytokines enhance B cell proliferation, increase antigen presentation and synergize with IL-2 to induce proliferation of helper T cells and cytotoxic T lymphocytes (CTL), which in turn stimulate differentiation of M1 myeloid cells via MyD88-mediated activation of NFkB signaling (106, 107). Importantly, TNFalpha and IFNgamma are crucial mediators for NK cell activation in cancer control positively correlating with good prognosis and survival of patients (108). However, tumor variants eventually become less immunogenic and secrete a set of signature immunosuppressive cytokines that prevent proper immune activation or induce differentiation and expansion of immunoregulatory cell subsets such as Tregs, M2 macrophages, myeloid derived suppressor cells (MDSC) and immature DCs. At the molecular level TGFβ, IL-4, IL-6, IL-10, IL-13 (Th2 cytokines) and VEGF and GM-CSF (Angiogenic cytokines) all play major roles in cancer immune escape.

Transforming growth factor beta (TGFβ): The role of TGFβ in cancer is complex and paradoxical, varying by cell type and stage of tumorigenesis. In early stages, TGFβ acts as a tumor suppressor, inhibiting cell cycle progression and promoting apoptosis, TGFβ exerts a tumor suppressor effect through p21 upregulation and c-Myc downregulation [L85]. However in later stages of cancer, enhances invasion and metastasis by inducing epithelial to mesenchymal transition (EMT) (109). Furthermore, TGFβ directly inhibits the cytolytic activity of NK cells, macrophages, and CTLs. Interestingly a previous report showed that CD8⁺ cells when exposed to

tumor-secreted IL-6 and TGF β *in vitro* or *in vivo*, began to express IL-17, which directly promoted tumor growth and survival (110).

Th2 cytokines: TGF β also favors the secretion of IL-4, IL- and, IL-10 from T cells, skewing the immune response to a Th2 profile (111). These cytokines seem to be important for proliferation and maintenance of MDSC and M2 macrophages. In turn, IL-6 plays a key role inhibiting apoptosis via gp130/JAK/STAT signaling pathway that ultimately leads to STAT3 activation (112). Moreover, IL-10, which is also secreted by tumor cells and M2 macrophages, induces sustained STAT3 phosphorylation in an autocrine-paracrine loop (113). IL-10 and IL-6 mediated STAT3 upregulation is further discussed in chapter 3.

Angiogenic cytokines: VEGF-A, an angiogenic cytokine also induces immunosuppression by inhibiting DC maturation (114), and serves as a chemoattractant for M2 macrophages. M2 macrophages in turn are a significant source of VEGF, MMPs, and M-CSF/CSF1, which increase expression of VEGF; thus, providing a positive feedback loop between inflammation/angiogenesis and immunosuppression (115).

IL-17: The role of IL-17 in cancer progression is controversial since it has been demonstrated anti- and pro-tumorigenic effects. Interestingly, a previous study in HNC patients showed elevated circulating Th17 cells that were further enriched in the tumor. A bead-based multiplex and ELISA revealed that Th17 cells in the tumor milieu secreted IL-1 β , IL-6, and IL-23. This study also noted that co-culturing HNC cells with Th17 cells resulted in a net increase in many pro-angiogenic cytokines (116). Most recently, the relationship between Th17 cells and angiogenesis has been strengthened by a report in which IL-17 and Th17 cells have been implicated in tumor resistance to anti-angiogenic therapy by inducing tumor associated

fibroblasts expressing granulocyte colony stimulating factor (G-CSF), a known cytokine involved in the recruitment and expansion of MDSCs (117).

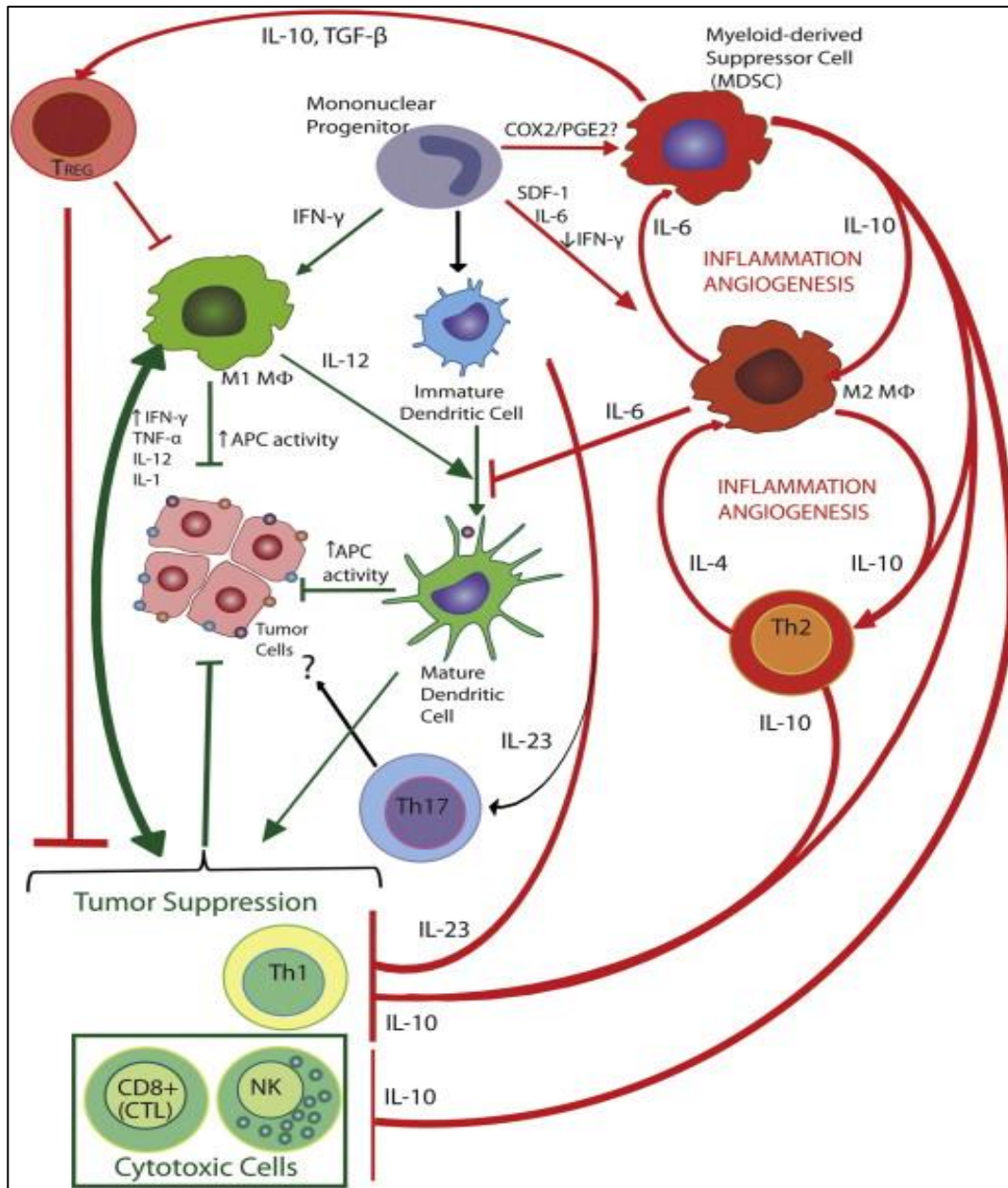


Figure 1.5.3 Immunosuppressive cytokine and cellular network in the tumor microenvironment: Illustration summarizes the interactions of principal suppressive cytokines in the tumor microenvironment. [Adapted from Burkholder et al. (118)].

1.6 HEAD AND NECK CANCER (HNC)

Head and neck cancer accounts for more than 90% of the malignancies that arise in the head and neck (119). Unfortunately, despite standard chemo and radiotherapy, 50% of the patients will succumb to this malignancy (120). The epidermal growth factor receptor (EGFR/ErbB1) is a tyrosine kinase receptor from the Erb/HER family that is overexpressed in approximately 90% of head and neck squamous cell carcinomas (121) and correlates with decreased survival (122). The EGFR activates many downstream signaling pathways including JAK/STAT, phosphatidylinositol 3-kinase (PI3K)/AKT and Ras/mitogen-activated protein (MAP) kinase pathways leading to cell proliferation, survival and invasion (123). Tumor cells overexpress both the receptor and the ligand, leading to an uncontrolled autocrine activation (124), which in turn induces the constitutive activation of signal transducer and activator of transcription 3 (STAT3), an oncogenic transcription factor (125-127).

1.6.1 The EGFR/JAK2/STAT3 pathway activation

The EGFR constitutively activates STAT3, which blocks apoptosis, induces proliferation, angiogenesis and immune escape (128, 129). STAT3 is considered an oncogene and its inhibition leads to apoptosis *in vitro* and reduced tumor growth in xenografted mouse models (130, 131). Interestingly, Janus Kinase 2 (JAK2) is a molecule downstream the EGFR that mediates STAT3 phosphorylation, and is upregulated in some HNC cell lines (132). JAK2 inhibition suppresses HNC proliferation and angiogenesis but even more interesting is the finding that selective JAK2 inhibitors favor tumor cell death (133) indicating that JAK2 plays a major role in HNC tumorigenesis. Currently, numerous pharmacologic JAK2 inhibitors are being tested in the clinic for treatment of myeloproliferative malignancies where STAT3 is overactive

(134). BMS-911543 is a selective JAK2 small molecule inhibitor that causes downregulation of pSTAT3 levels in a human megakaryoblastic cell line (135). However, its effect inhibiting the EGFR/JAK2/STAT3 pathway in HNC is still uncharacterized.

1.6.2 Cetuximab-mediated EGFR blockade

The oncogenic transformation induced by overexpressed wild type EGFR in HNC cells and the modest success of conventional chemo and radiotherapy in HNC patients led to the implementation of monoclonal antibody immunotherapy targeting the EGFR. Cetuximab, an EGFR-specific chimeric IgG1 mAb, not only blocks ligand binding but also induces EGFR internalization and degradation (136), further limiting EGFR signaling. Even though cetuximab interferes with growth signals, its not sufficient to induce cell death, most likely because of alternative survival pathways in cancer cells. Interestingly, cetuximab-induced tumor cell death occurs only when NK cells are added to *in vitro* co-cultures (137-139), providing evidence that the major cetuximab antitumor mechanisms are immune mediated.

1.6.3 Cetuximab-mediated NK cell activation

Cetuximab IgG1 framework allows its interaction with Fc gamma receptors (FcγR) expressed on immune cells, particularly FcγRIIIA (CD16) which is expressed on natural killer cells (NK). Binding of cetuximab to CD16 on NK cells triggers antibody-dependent cellular cytotoxicity (ADCC), NK cell activation and secretion of IFNγ. Moreover, IFNγ-secreted from cetuximab activated NK cells mediate NK-DC cross talk via enhancing IL-12/IFNγ production and enhances DC maturation and MHC class I antigen presentation, which in turn induces clonal expansion of EGFR-specific CD8⁺ T cells (100, 140-143). Clinically, cetuximab has shown to be

effective increasing survival of patients either when added to radiation or platinum-based chemotherapy (144, 145) or as monotherapy (146), however, effective in only 10-20% of the patients (147, 148). Consequently, understanding the immune mechanisms initiated by cetuximab and how tumor cells evade cetuximab-mediated immune activation will allow us to overcome resistance to cetuximab therapy in HNC patients.

1.6.4 EGFR-mediated immune escape

Head and neck cancer presents as an ideal model of tumor immune escape where EGFR overexpression induces oncogenic transformation as discussed in previous sections. However, more important is to understand the role that EGFR plays in tumor immunoescape. We present the notion that tumor immune evasion is characterized by distorting the three fundamental signals for efficient immune activation: Signals 1, 2 and 3. An aberrant Signal 1 is characterized by downregulation of APM components and HLA class I antigen presentation, mediated in part by EGFR-induced Src homology-2 domain containing phosphatase (SHP2) activation, leading to reduced levels of phosphorylated signal transducer and activator of transcription 1 (STAT1) (59, 66, 149). Interestingly, this phenomenon can be counteracted by IFN γ treatment or inhibition of SHP2, which is overexpressed in HNC (150). Furthermore, SHP2 depletion also resulted in phospho-STAT1 (pSTAT1) activation and restoration of APM components, leading to HLA class I restricted, TA-specific CTL recognition (150). In addition, SHP2-mediated pSTAT1 suppression reduced type 1 cytokine production by HNSCC cells, since its inhibition resulted in the secretion of Interleukin-12 (IL-12) p35/p40 and IFN γ -dependent CXCR3 and CCR5 binding chemokines (150). Paradoxically, IFN γ is also a major inducer of PD-L1 expression as shown in fibrosarcoma (151), glioblastoma (152) and multiple myeloma cells (153). In HNC, cetuximab

mediated NK activation and IFN γ secretion that is otherwise beneficial to enhance tumor immune recognition, could also upregulate PD-L1 expression through a tumor cell-extrinsic pathway. However, even more interesting is the speculation that the overactive EGFR/JAK2 pathway may constitute a cell-intrinsic stimulus for PD-L1 upregulation and provide an aberrant signal 2. Finally, EGFR-mediated STAT3 overactivation would also lead to increased secretion of signature immunosuppressive cytokines and chemokines providing an abnormal signal 3. Ultimately, these EGFR-dependent aberrant signals 1, 2 and 3 will induce evasion of immune effector cell recognition and lysis. Since, JAK2 is common to IFN γ and EGFR pathways, presents as a crucial target to inhibit in order to reverse the *extrinsic* (IFN γ mediated) and *intrinsic* (EGFR mediated) PD-L1 expression and immunosuppressive phenotype of HNC cells.

1.7 HYPOTHESIS

EGFR and JAK2 inhibition will reverse the immunosuppressive phenotype of head and neck cancer cells and subsequently enhance tumor immune detection and NK cell cytotoxicity.

1.8 SPECIFIC AIMS

1.8.1 SPECIFIC AIM 1

Determine the in vitro effect of EGFR and JAK2 inhibition to reverse PD-L1 upregulation and correlate with patient tumor expression data from The Cancer Genome Atlas (TCGA) and pre- and post- single agent cetuximab clinical trial UPCI 08-013.

1.8.2 SPECIFIC AIM 2

Determine the in vitro effect of EGFR and JAK2 inhibition downregulating STAT3 dependent tumor derived cytokines and correlate with TCGA tumor expression data and patient serum specimens from pre- and post- single agent cetuximab clinical trial UPCI 08-013.

1.8.3 SPECIFIC AIM 3

Determine the effect of EGFR and JAK2 inhibition in order to enhance NK cell mediated tumor lysis in vitro and correlate with patient tumor expression data from TCGA and pre- and post- single agent cetuximab clinical trial UPCI 08-013.

2.0 IDENTIFICATION OF THE CELL-INTRINSIC AND EXTRINSIC PATHWAYS DOWNSTREAM OF EGFR AND IFN γ THAT INDUCE PD-L1 EXPRESSION IN HEAD AND NECK CANCER

2.1 INTRODUCTION

The cancer immunoediting theory states that lymphocytes successfully suppress tumor growth (154). However, tumor cell immune escape can eventually occur, such as by downregulating HLA class I antigen processing (149) or by providing checkpoint inhibitory signals or suppressive cellular subsets (155) to disable effector immune cell infiltrates in the tumor microenvironment, preventing the generation and maintenance of an effective antitumor response (9). Cytotoxic T lymphocyte antigen-4 (CTLA-4) and programmed death-1 (PD-1) are two relevant immune checkpoint receptors expressed by tumor infiltrating lymphocytes that are being actively targeted in the clinic. PD-1 limits the function of activated T cells and other lymphocytes (155, 156). Moreover, its cognate binding partner programmed death ligand-1 (PD-L1) is expressed in many types of cancers including melanoma, ovarian, renal and lung cancer (156). Given the frequent expression of PD-L1 in tumors (157), trials targeting the PD-L1/PD-1 pathway with blocking antibodies have been carried out with encouraging results in patients with renal cell carcinoma, non-small cell lung cancer and melanoma where tumor cell surface PD-L1 expression was associated with objective response to anti-PD-1 therapy (18, 19, 158, 159). Recent data support a similar enrichment of clinical responders in PD-L1⁺ HNC patients (160).

HPV associated HNC is increasing worldwide with prevalence reaching 50% of all oropharyngeal cancers (161). Interestingly, HPV positive tumors are more responsive to oncologic therapy, which may be in part immune mediated (162-164).

A previous report suggested that PD-L1 expression contributed to immune resistance in HPV positive HNC tumors (157), relating PD-1⁺ CD8⁺ tumor infiltrating lymphocytes (TIL) with an anergic phenotype. In contrast, Badoual et al. relates PD-1⁺ CD8⁺ T cells with an activated phenotype, which constitutes a favorable prognostic biomarker in HPV positive HNC (165). Given the importance of PD-L1 expression in HNC, the stimuli and signaling pathways that induce PD-L1 expression in HPV⁺ and HPV⁻ HNC cells are clinically important. A more precise understanding of PD-L1 regulation would permit the development of more effective approaches to anti PD-L1/PD-1 therapy in order to improve clinical outcomes.

We hypothesized that targeting signaling molecules involved in PD-L1 expression in HNC cells might synergize with current anti-EGFR antibody targeted immunotherapies such as cetuximab, that are known to activate natural killer (NK) cells and cytotoxic T lymphocytes (CTL) (100). However, because activated NK and T cells secrete IFN γ , a known stimulus for PD-L1 expression, understanding the complex signaling pathway regulating this immunosuppressive ligand is crucial.

PD-L1 expression in tumor cells may be regulated by two major mechanisms. First, an “extrinsic” mechanism where an antitumor cellular immune response driven by NK and CD8⁺ tumor infiltrating T lymphocytes (TIL) produce inflammatory cytokines such as IFN γ , which in turn may induce PD-L1 expression on tumor cells. Indeed, a previous study showed that IFN γ and CD8 expression were increased in a small number of PD-L1 positive tumors (157). Second, an “intrinsic” mechanism may exist in which constitutive oncogenic signaling pathways within the tumor cell itself lead to PD-L1 overexpression. In glioblastoma, PTEN deletion promotes PI3K-AKT mediated PD-L1 overexpression (166), while EGFR mutant lung cancer cells have

been associated with PD-L1 overexpression (167, 168). In contrast to lung cancer, in the setting of HNC, EGFR mutations are extremely rare, whereas, wild type EGFR is overexpressed in approximately 80-90% of tumors (169). Since an extrinsic (IFN γ -mediated) and intrinsic (EGFR-mediated) mechanism may cooperate to promote PD-L1 upregulation, we investigated signaling pathways that mediate both IFN γ and EGFR induced PD-L1 upregulation in tumor cells. These findings have particular relevance given the clinical utility of EGFR-specific FDA-approved monoclonal antibody cetuximab, which can both block EGFR signaling and stimulate IFN γ secretion via activation of NK and CTL (100-102).

2.2 MATERIALS AND METHODS

2.2.1 Tumor cell lines

HPV negative HNC cell lines used in this report (JHU020, JHU022, JHU029, PCI13) and HPV positive (SCC2, SCC47, SCC90 and 93VU) were cultured in IMDM (Invitrogen, Carlsbad, CA) supplemented with 10% FBS (Mediatech, Herndon, VA), 2% L-glutamine and 1% penicillin/streptomycin (Invitrogen Corp, Carlsbad, CA). JHU020, JHU022 and JHU029 were a kind gift from Dr. James Rocco (Ohio state university, Columbus, OH) in January of 2006. SCC90 and PCI13 were isolated from patients treated at the University of Pittsburgh Cancer Institute (Pittsburgh, PA) through the explant/culture method, authenticated, and validated as unique using STTR profiling and HLA genotyping every 6 months (170, 171). UD-SCC2 and UM-SCC47 (called SCC2 and SCC47 in this report) were a kind gift from Dr. Thomas Carey (University of Michigan, Ann Arbor, MI) in December of 2005. 93-VU-147 T (called 93VU in this report) was a kind gift from Dr. Henning Bier (Technische Universitat Munchen, Munich, Germany) in October of 2013. All cell lines were routinely tested every 6 months and found to

be free of *Mycoplasma* infection. For all treatments involving the IFN γ and EGFR pathways cell lines were cultured overnight in serum free AIM-V media (Invitrogen, Carlsbad, CA) and treatments (IFN γ , EGF and inhibitors) were started when cells reached at least 20% confluence. Adherent tumor cells were detached by warm trypsin–EDTA (.25%) solution (Invitrogen, Carlsbad, CA) incubated for 5 min at 37°C. We previously determined that Trypsin treatment did not cleave surface PD-L1 by comparing with a non-enzymatic detachment method. Surface protein PD-L1 expression was determined by flow cytometry and pSTAT1 or total STAT1 was determined by intracellular flow cytometry (IFC).

2.2.2 Antibodies and treatments

PE conjugated PD-L1 monoclonal antibody (mAb) was purchased from BD Pharmingen (San Jose, CA). The anti-PD-L1 monoclonal antibody (mAb) clone 405.9A11 used for IHC was previously validated (172) and kindly provided by Dr. Gordon J. Freeman (Dana-Farber Cancer Institute, Boston, MA). The rabbit monoclonal anti-pJAK2 (Y1007 and Y1008) antibody used for IHC staining in this report was purchased from Abcam (Cambridge, United Kingdom), the FITC conjugated anti-HLA-ABC mAb (clone w6/32) was purchased from E-biosciences (San Diego, CA) and was used in the flow cytometry determinations in this report. The intracellular phosphorylated and total STAT staining was performed using PE-conjugated irrelevant IgG1 mAb isotype control, PE conjugated anti phosphorylated tyrosine 701 STAT1 mAb (pSTAT1 Tyr701), PE conjugated total STAT1 and PE conjugated total STAT3 were purchased from BD Biosciences (San Jose, CA), PE conjugated rabbit anti human phospho-AKT (Thre308) was purchased from Cell Signaling (Danvers, MA), primary anti-p44/42 MAPK (Erk1/2) and phospho-p44/42 MAPK (Erk1/2) (Thr202/Tyr204) antibodies were purchased from Cell Signaling (Danvers, MA), secondary PE conjugated anti-rabbit secondary antibody was

purchased from Cell Signaling as well. Western blotting antibodies include rabbit anti-human total JAK2, pJAK2 (y1007/1008), total AKT, pAKT, pERK and mouse anti-human β -actin that were all purchased from Cell signaling (Danvers, MA).

Human recombinant interferon gamma (IFN γ) was purchased from R&D systems (Minneapolis, MN) reconstituted according manufacturer instructions and kept at -80 Celsius in 20 microliter aliquots, for all experiments in this report IFN γ was used at 10 IU/mL. Human recombinant interferon alpha 2a (IFN α 2a) was purchased from PBL Interferon Source (Piscataway, NJ), reconstituted and kept at -20 Celsius, for all experiments in this report IFN α 2a was used at 1000 IU/mL. The specific JAK2 inhibitor BMS-911543 (N,N-dicyclopropyl-4-((1,5-dimethyl-1H-pyrazol-3-yl)amino)-6-ethyl-1-methyl-1,6-dihydroimidazo[4,5-d]pyrrolo[2,3b]pyridine-7-carboxamide) was characterized previously (171) and kindly provided by Bristol-Myers Squibb. The JAK2 inhibitor was reconstituted in dimethylsulfoxide (DMSO) as a 10mM stock solution, stored in aliquots at -20C and was used at 10uM final concentration in all the *in vitro* experiments in this report. The selective JAK1/3 inhibitor (ZM39923) was characterized previously (152, 173) and purchased from Tocris bioscience (Bristol, United Kingdom) reconstituted in DMSO, stored at -80 Celsius, and was used at 10uM final concentration. The pan-PI3K inhibitor wortmannin was purchased from Cell Signaling (Danvers, MA) and resuspended at a concentration of 10uM and used at a final concentration 1uM. The specific PI3K α 110 subunit inhibitor (BYL-719) was used at a 1uM final concentration and the MEK1/2 inhibitor (PD0325901) was used at a 5uM final concentration; both inhibitors were purchased from Tocris Bioscience (Bristol, United Kingdom).

2.2.3 Flow cytometry analysis

Surface flow cytometry was performed as follows, cells were harvested and resuspended in PBS containing a 1:50 dilution of a previously validated viability dye Zombie Aqua (174), following the manufacturer's protocol (Biolegend, San Diego, CA), then resuspended in 50uL of fluorescence-activated cell sorting (FACS) buffer and fluorophore conjugated antibodies were added at 1:10 dilution, incubated for 15 minutes at 4 Celsius, then antibodies were washed away twice by sequential centrifugation at 1400 RPM with FACS buffer and resuspended in 2% PFA solution until analyzed in the flow cytometer. Intracellular flow cytometry was performed as described (175). Briefly, cells were fixed using 1.5% for 15 min at room temperature (RT) and permeabilized with ice cold 100% methanol for 10 minutes at 4 Celsius and kept for 18h at -20 Celsius. Cells were then washed in FACS buffer and stained either with a fluorophore-conjugated primary pSTAT1, STAT1 or pSTAT3 mAb, cells were then incubated for 45 min at RT, washed and resuspended in FACS buffer. When using an unconjugated primary antibody cells were stained with a secondary PE-conjugated antibody for additional 45 minutes and then washed as previously described. Flow cytometry analysis was performed on the same day as staining. Isotype control antibody staining was added for each condition and each mAb used for targeted markers (STAT1, pSTAT1 and pSTAT3) samples were collected and analyzed in an LSR Fortessa cytometer (BD Biosciences). A minimum of 10,000 cells was collected per test. Data analysis was performed using FlowJo version 10 (FlowJo, Ashland, OR). All surface and intracellular markers in this study were calculated as median fluorescence intensity (MFI) fold change and normalized with either untreated or vehicle control after subtracting the isotype control (MFI) of each sample. Each experiment was repeated at least three times and mean and

standard error of the mean (SEM) was calculated and plotted using GraphPad PRISM software version 6.

2.2.4 Western Blotting

Cells were lysed in 10 mM Tris HCl, 5 mM EDTA, 50 mM NaCl, 30 mM Na₂P₂O₇, 50 mM NaF, 1 mM NaVO₄, 1% Triton X-100, 1 mM PMSF and vortexed for at least 1 h at 4°C, and centrifuged at 4°C, 16,100 g for 15 min. The supernatant protein was quantified and normalized, and 40–60 µg of protein were loaded and size fractionated through a 4–12% SDS–PAGE gel (Lonza, Rockand, ME), transferred to a PVDF membrane (Millipore, Billerica, MA) and immunoblotted with the indicated antibodies for βactin, pJAK2, JAK2, pERK, pAKT and total AKT.

2.2.5 siRNA knockdown

HNC cell lines were transfected at 30% confluence with STAT1-targeting siRNA, STAT3-targeting siRNA or a non-targeting siRNA control (Ambion, Austin, TX), Lipofectamine RNAi max (Invitrogen Corp) and Optimem I (Invitrogen Corp) according to the Lipofectamine RNAi max instructions. 48 hours after the transfection, cells were washed with PBS and incubated with or without INF γ (10IU/mL) or EGF (10ng/mL) for 48 h at 37°C. Then, cells were harvested and analyzed by flow cytometry for STAT1, STAT3 and PD-L1 expression. siRNA STAT1: 5-CUACGAACAUGACCCUAUTT-3(s) and 5-AUAGGGUCAUGUUCGUAGGTG-3(as) siRNA STAT3: 5-GCCUCAAGAUUGACCUAGATT-3(s) and 5-UCUAGGUCAAUCUUGAGGCCT-3(as) and siRNA non-targeting 5-AGUACAGCAAACGAUACG Gtt-3 control: (s) and 5-CCGUAUCGUUUGCUGUACUtt-3(as).

2.2.6 Quantitative PCR (qPCR)

Total RNA was extracted using Trizol reagent (Invitrogen, Grand Island, NY) and purified using RNA cleanup (Qiagen), followed by Purelink on-column DNase digestion (Invitrogen, Grand Island, NY) according to manufacturer's instructions. The concentration and purity of RNA was determined by measuring absorbance at 260 and 280 nm. 2000 ng of RNA was used for first strand cDNA synthesis using random hexamers and MultiScribe reverse transcriptase (Applied Biosystems, Foster City, CA) according to manufacturer's instructions. PCR probes for PD-L1 (Hs01125301_m1) and GUSB (Hs99999908_m1) were purchased from Applied Biosystems for TaqMan® Gene Expression Assay. Real-time PCR cycling was performed using StepOne™ Real-Time PCR Systems (Applied Biosystems, Carlsbad, CA). GUSB was amplified as an internal control. All of the experiments were performed in triplicates. Relative expression of the target genes to endogenous control gene (GUSB) was calculated using the Δ CT method: relative expression = $2^{-\Delta CT}$, where $\Delta CT = CT(\text{target gene}) - CT(\text{GUSB})$.

2.2.7 Chromatin immunoprecipitation (ChIP) assay

Cells were serum starved for 18 h at 37°C in AIM V medium (Invitrogen Corp, Carlsbad, CA) prior to incubation with, IFN- γ (10 IU/ml) for 30 min at 37°C, or sequentially with cetuximab (10 ug/ml) for 30 min at 37°C. At the end of the incubation, cells were fixed with formaldehyde (1% final concentration) (Sigma–Aldrich Inc.) for 10 min at RT. Cells were then quenched with glycine (0.125 M final concentration) (Sigma–Aldrich Inc.) for 5 min, washed twice with ice-cold PBS and harvested. After centrifugation at 16,100 g for 12 min at 4°C, cells were lysed in SDS lysis buffer (Millipore) containing protease inhibitors. Chromatin was sheared by sonication for 5 cycles of 9s at 40% of the maximum potency (Cole Palmer Instrument) to generate fragmented DNA with an average length between 400 and 1,000 base pairs. pSTAT1, pSTAT3

and IgG control mAbs were used to immunoprecipitate pSTAT1- or pSTAT3-bound chromatin (5 µg of antibody) rotating overnight at 4°C. Protein A agarose beads were added to each IP (60 µl) and incubated for 1 h rotating at 4°C. The subsequent washes and elution steps were performed using the Ez-ChIP™ kit (Millipore) and according to the manufacturer's instructions. Protein–DNA crosslinks were reversed at 65°C overnight. After RNase (10 µg, 30 min at 37°C) (Sigma–Aldrich Inc.) and sequential proteinase K (10 µg, 2 h at 45°C) (Sigma–Aldrich Inc.) digestion, DNA was purified using the QIAquick PCR purification kit (Qiagen). Purified DNA was used in each quantitative RT-PCR using the EpiTect ChIP qPCR (Qiagen) SYBR-green Master Mix method (at 94°C for 10 min, and 50 cycles at 94°C for 20 s, 60°C for 1 min) using the primer for the PD-L1 promoter NM_014143.2 (-)16Kb. qPCR amplification data were normalized and analyzed as percent input as described previously (176) and expressed as relative enrichment to % input.

2.2.8 Immunohistochemistry (IHC) protocol

The use of clinical tumor samples from HNC patients was approved by the Institutional Review Board (IRB approval #99-069) at the University of Pittsburgh, and written informed consent was obtained from all participants. Slides were deparaffinized and rehydrated using a standard histology protocol. Antigen retrieval was performed using Diva Retrieval solution (Biocare Medical, Concord, CA) and a Decloaking chamber at 124°C, 3 minutes, and cooled for 10 minutes on the counter. The slides were placed on an Autostainer Plus (Dako, Carpinteria, CA) using a TBST rinse buffer (Dako) and stained using the following protocol. 3% H₂O₂ (ThermoFisher Scientific, Pittsburgh, PA) for 5 minutes, CAS Block (Invitrogen, Grand Island, NY) for 10 minutes.

The primary antibody for PD-L1 (clone 405.9A11) was previously characterized (177) and the pJAK2 (Y1007-1008) (clone E132) used according to manufacturer instructions. The secondary consisted of Envision Dual Link + (Dako) polymer for 30 minutes, rinsed, then a TBST holding rinse was applied for 5 minutes. The substrate used was 3,3, Diaminobenzidine + (Dako) for 7 minutes and counterstained with hematoxylin. PD-L1 and pJAK2 staining were quantified by positive pixel count v9 algorithm (Aperio). The protein expression level is represented by the score of intensity of staining multiplied by the positive area percentage. Tumor sections stained with PD-L1 and pJAK2 were examined by a head and neck pathologist (RRS) who was blinded to the clinical patient data. Scoring was determined by tumor percentage stained positive for PD-L1 or pJAK2, respectively. Tumors with less than a 5% tumor cells positive cut-off staining were considered as negative.

2.2.9 Cellular cytotoxicity assays

Cytotoxicity was determined using a ^{51}Cr release assay. Briefly, target cells were incubated in 100 μL of media with 25 μCi of $\text{Na}^{251}\text{CrO}_4$ (Perkin Elmer, Boston MA) for 60 min at 37°C and resuspended in RPMI 1640 medium supplemented with 25 mM HEPES. Cells were thoroughly washed and plated at various effector: target (E:T) ratios in 96-well plates. Cetuximab or human IgG1 was added (10 $\mu\text{g}/\text{mL}$) then freshly purified NK cells were added at the specified effector:target (E:T) ratios. The supernatants were collected and analyzed with a Perkin Elmer 96-well plate gamma counter. Specific lysis = $(\text{experimental lysis} - \text{spontaneous lysis}) / (\text{experimental lysis} - \text{maximal lysis}) \times 100$. Results are representative of 4 different donors and were plotted in bar graphs.

2.2.10 The Cancer Genome Atlas (TCGA) data retrieval and analysis

TCGA data for HNC gene expression by RNAseq were downloaded from the UCSC cancer genomics browser (<https://genome-cancer.ucsc.edu>). The HNC gene expression profile from 500 head and neck tumor specimens was measured experimentally using the Illumina HiSeq 2000 RNA Sequencing platform by the University of North Carolina TCGA genome characterization center as described previously (178). Level 3 interpreted data was downloaded from TCGA data coordination center. This dataset shows the gene-level transcription estimates, as in RSEM normalized count, percentile ranked within each sample. Genes are mapped onto the human genome coordinates using UCSC cgData HUGO probeMap. The RSEM units to quantitate RNAseq expression data were described and validated previously (179). Correlations from TCGA data were calculated using Pearson r test (Two or One tailed) and linear regression curve fits were graphed using GraphPad PRISM software version 6 and values were plotted into either graphs or tables.

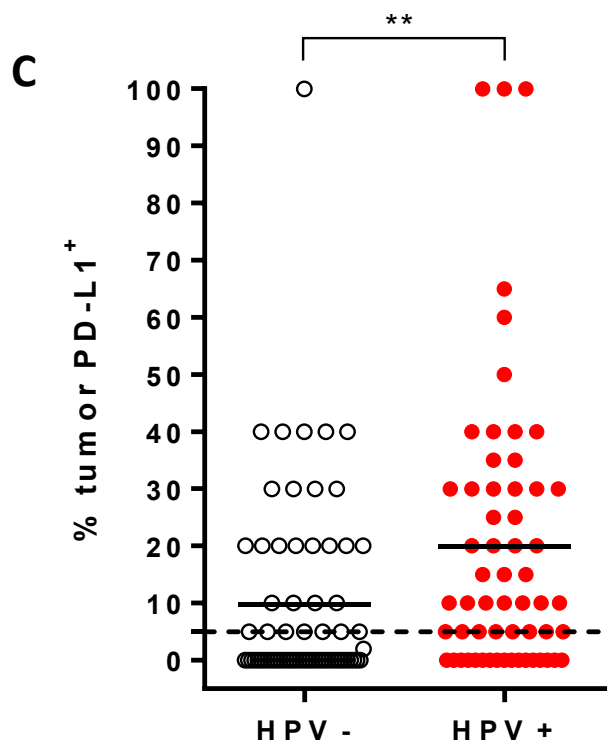
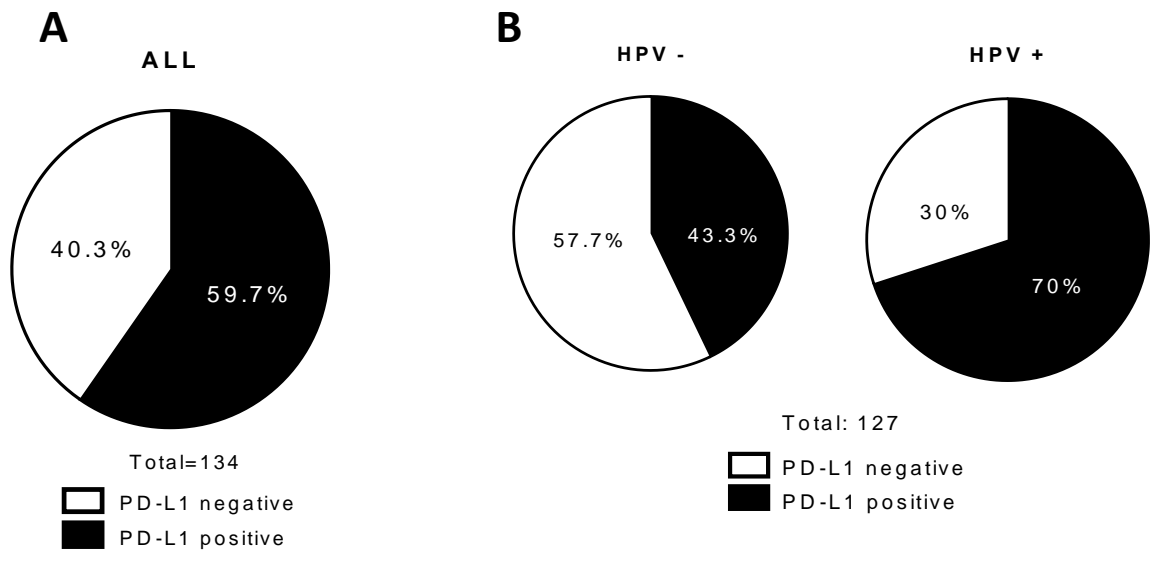
2.2.11 IPA Ingenuity pathway software analysis

Software was accessed via the University of Pittsburgh health sciences library system (HSL) license. Path Explorer tool available in IPA Ingenuity was utilized for exploration of EGFR and IFN γ pathways for any association with PD-L1 expression. Pathway matching relationships for PD-L1, EGFR and IFN γ were selected specifically in the human species. As stated in the Results section, software-generated possible matches were STAT1, STAT3, AKT, Jun and Myc.

2.3 RESULTS

2.3.1 PD-L1 protein expression is higher in HPV positive HNC tumor specimens

Immunohistochemistry staining of tumor specimens (n=134) revealed that 59.7% of HNC patients express detectable PD-L1 on the tumor cell surface, as determined by a threshold of >5% positive tumor cells (Figure 2.3.1A). Furthermore, when segregated by HPV status (n=127, 63 HPV⁻ and 64 HPV⁺), we noted that PD-L1 expression was more frequent in HPV⁺ specimens (70% vs. 43.3%, respectively, Figure 2.3.1B) and the % PD-L1 expression was also significantly higher in HPV⁺ tumors (Figure 2.3.1C). Interestingly, PD-L1 expression was more intense on the cell membrane than in the cytoplasm and was heterogeneously expressed within the microenvironment, generally forming clusters of PD-L1⁺ tumor cells with a higher intensity at the cluster periphery (Figure 2.3.1D and 2.3.1E). To study the stimuli and pathways by which PD-L1 is upregulated *in vitro*, we analyzed a panel of HPV⁺ and HPV⁻ HNC lines for PD-L1 expression, which was expressed variably (Figure 2.3.1F) similar to patient tumors by IHC.



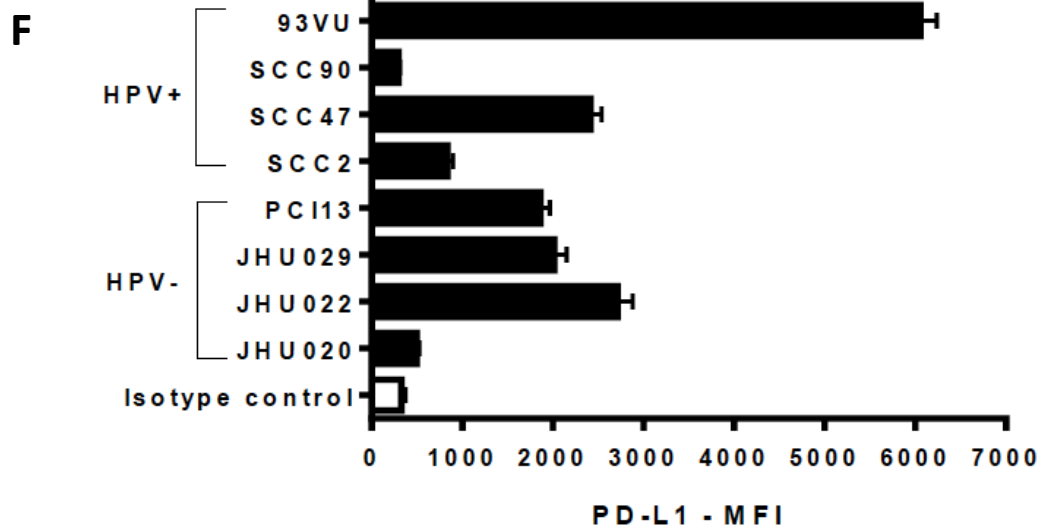
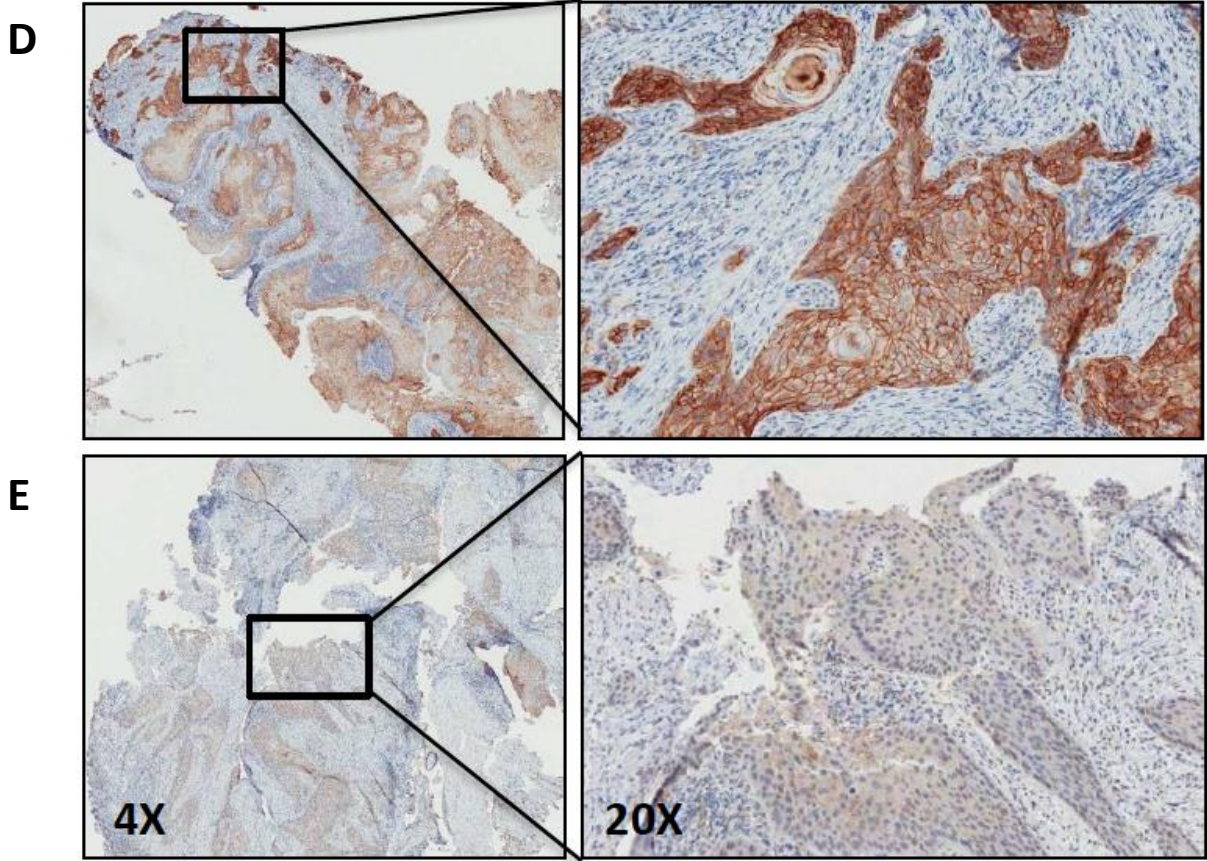


Figure 2.3.1 PD-L1 protein expression is higher in HPV⁺ tumor specimens: **A.** PD-L1 protein expression in HNC tumor specimens (IHC, n=134). Tumors were considered positive for PD-L1 when higher than 5% tumor staining threshold. 59.7% of tumors were PD-L1⁺. **B.** PD-L1 expression in HPV⁻ and HPV⁺ tumor specimens using the same criteria as in A. 70% HPV⁺ vs. 43.3% HPV⁻ specimens were PD-L1⁺. **C.** percent PD-L1⁺ tumor area in HPV⁻ and HPV⁺ specimens. Dotted line represents the 5% tumor positive cut-off, solid lines represent the median value. (Mann-Whitney test, ** P<0.001). **D.** Representative image of a high intensity, 100% PD-L1⁺ tumor of a HPV⁺ specimen. **E.** Representative image of a low intensity, 50% PD-L1⁺ tumor of a HPV⁻ specimen. Insets on the left represent the magnification (20X) on the right. **F.** HNC tumor cell lines expressed heterogeneous levels of PD-L1, which resembled those seen in vivo by IHC.

2.3.2 HPV positive tumor specimens show higher Th1 type expression profile

We then analyzed PD-L1 expression in a large cohort of HNC specimens for which gene expression TCGA repository data were available (178). Since PD-L1 expression has been linked with that of CD8 and IFN γ (102, 157), we investigated the Th1 mRNA expression profile of HPV⁺ versus HPV⁻ specimens. Pooled data from 88 HNC specimens were plotted using a heat map, segregated by HPV status (Figure 2.3.2A, red boxes depict higher expression in HPV⁺ tumors). A Th1 type expression profile (PD-1, CD8A, CD8B, IFNG and JAK2) was significantly higher in HPV⁺ than HPV⁻ tumors (Figure 2.3.2B) suggesting that activated immune effector cells readily infiltrate HPV⁺ tumors, which may be important for PD-L1 induction due to this source of IFN γ . Importantly, JAK2 expression (but not JAK1) was also higher in HPV⁺ tumors (Figure 2.3.2B). Therefore, JAK2 was associated with a Th1 profile and with PD-L1 expression, particularly in HPV⁺ tumors.

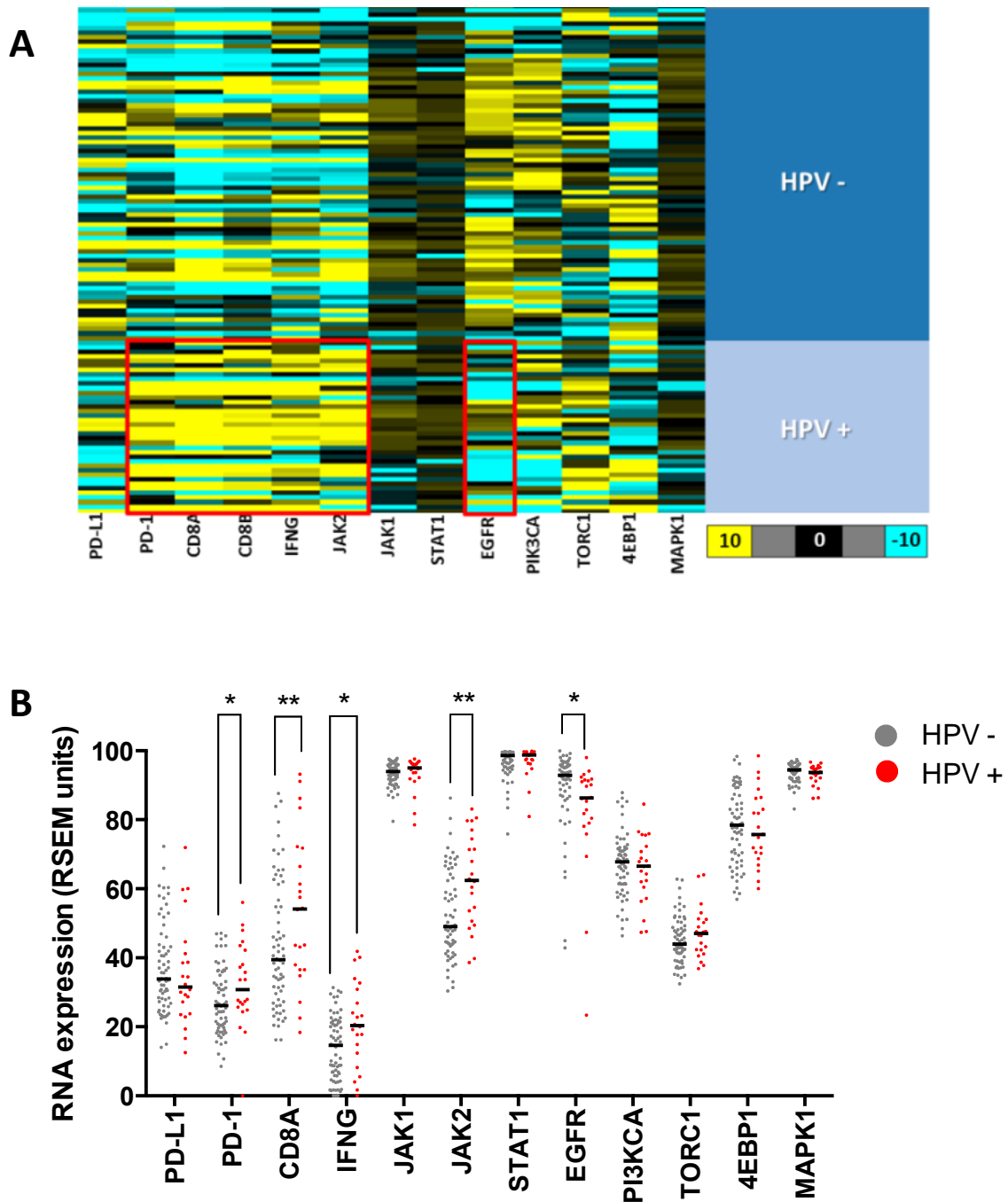
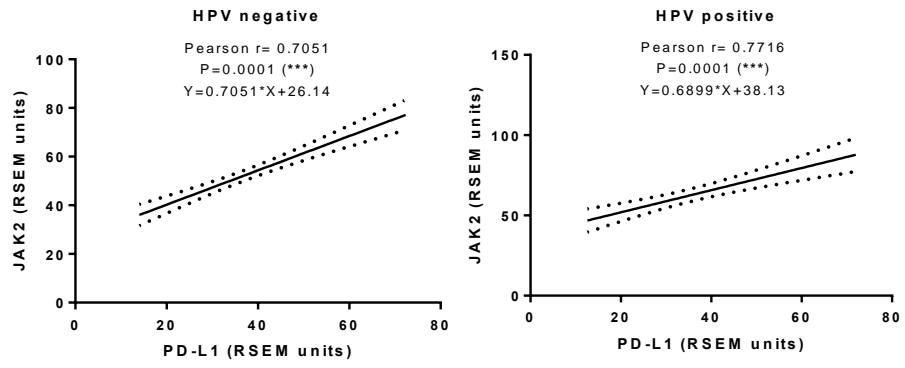
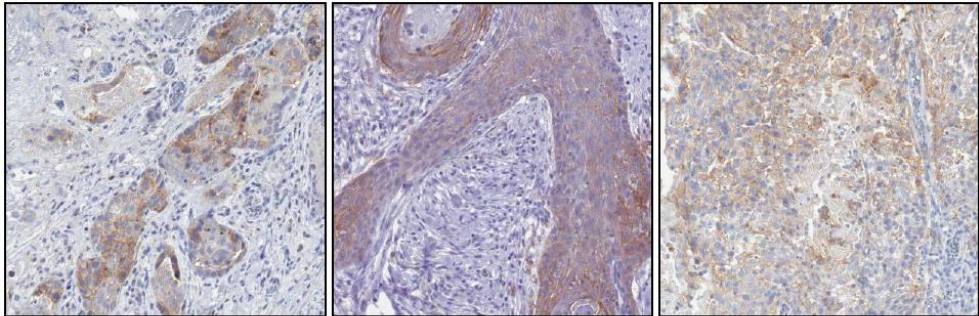
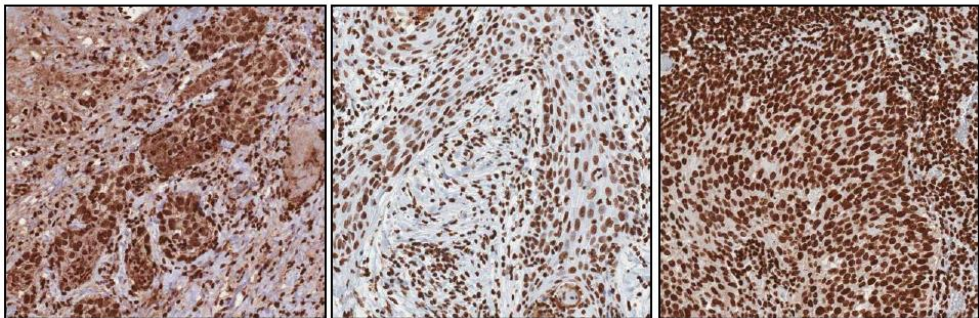


Figure 2.3.2 HPV⁺ specimens show higher expression of a Th1 type RNA expression profile:
 A. Heat map of RNAseq expression level expressed as RSEM units (as described in Materials and Methods) of PD-L1, PD-1, CD8A, CD8B, IFN γ , JAK2, JAK1, STAT1, EGFR, PIK3CA, TORC1, 4EBP1 and MAPK1 (66 HPV⁻ and 22 HPV⁺) TCGA database (178), red boxes emphasize a higher expression of a Th1 profile in HPV⁺ specimens and higher EGFR expression

in HPV⁻ counterparts (color code, yellow 10 fold higher, turquoise 10 fold lower relative expression change over black). **B.** HPV⁺ tumor specimens show significantly higher expression of a Th1 type expression profile: PD-1, CD8A, IFN γ and JAK2. EGFR expression is significantly higher in HPV⁻ tumor specimens (Mann-Whitney * P<0.05, ** P<0.001).

2.3.3 PD-L1 expression correlates with that of JAK2, EGFR, IFN γ and a Th1 profile regardless HPV status

Given that JAK2 is a common signaling molecule downstream of the EGFR and IFN γ pathways, we found that PD-L1 and JAK2 mRNA expression were highly correlated (n=500) and persisted when the cohort was segregated by HPV status (Figure 2.3.3A). In order to further assess the relationship between JAK2 and PD-L1 *in vivo* at the protein level, we determined phospho-JAK2 and PD-L1 using IHC from adjacent sections of HNC specimens (n=23). Corroborating our previous findings, PD-L1 was predominantly expressed on the tumor cell membrane while phospho-JAK2 exhibited strong nuclear staining, with occasional weak-moderate cytoplasmic staining. PD-L1 positive tumor islands were found to be strongly positive for phospho-JAK2 (Figure 2.3.3B). Furthermore, we also found a significant correlation between EGFR and PD-L1 expression, which was somewhat weaker in HPV⁻ tumors (Figure 2.3.3C). Likewise, PD-L1 expression was highly correlated with a Th1 type expression profile (IFN γ , CD8A and PD-1) regardless of HPV status (Figure 2.3.3D and Table 2.3.3.1). In addition, correlation of EGFR and CD8 or JAK2 was only significant in HPV⁺ tumors, given that their expression level was higher than in HPV⁻ tumors. However, this finding did not preclude the fact that JAK2 could also be important for PD-L1 expression in HPV⁻ tumors given that they were strongly correlated regardless of HPV status.

A**B****1****2****3****PD-L1****pJAK2**

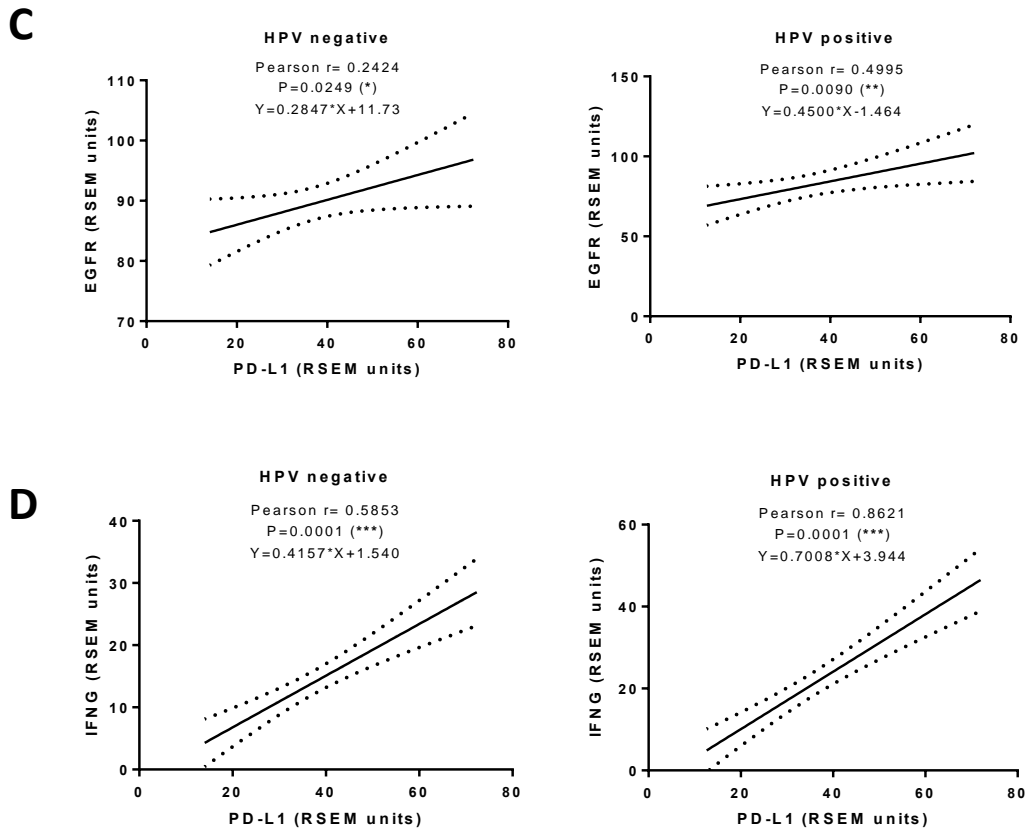


Figure 2.3.3 PD-L1 expression correlates with that of JAK2, EGFR and IFN γ regardless HPV status: **A.** PD-L1 expression significantly correlated with that of JAK2 in both HPV⁻ and HPV⁺ specimens (Pearson r and linear regression curve fit, *** $p < 0.0001$). **B.** PD-L1 and pJAK2 IHC staining in adjacent sections and matching areas of HNC specimens. PD-L1 (top panel) was predominantly expressed on the tumor cell membrane. Phospho-JAK2 (bottom panel) exhibits a strong nuclear staining with occasional weak to moderate cytoplasmic staining. PD-L1 positive tumor islands are also diffusely strongly positive for phospho-JAK2 (3 representative specimens out of 23) **C.** PD-L1 mRNA expression significantly correlated with that of EGFR in both HPV⁻ and HPV⁺ specimens (Pearson r and linear regression curve fit * $P < 0.05$ ** $P < 0.001$). **D.** PD-L1 mRNA expression significantly correlated with that of IFN γ regardless HPV status (Pearson r and linear regression curve fit *** $P < 0.0001$). 66 HPV⁻ and 22 HPV⁺ tumor specimens collected from TCGA database.

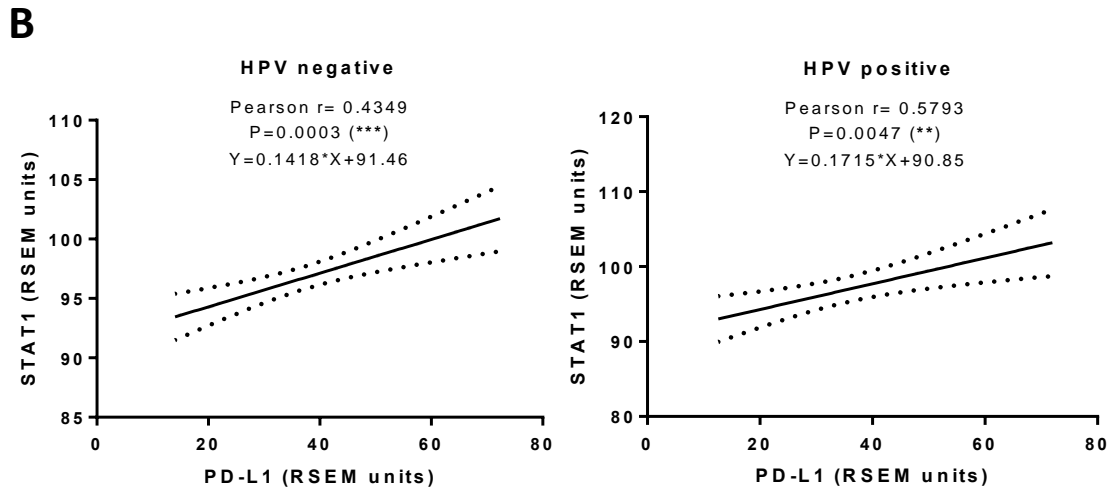
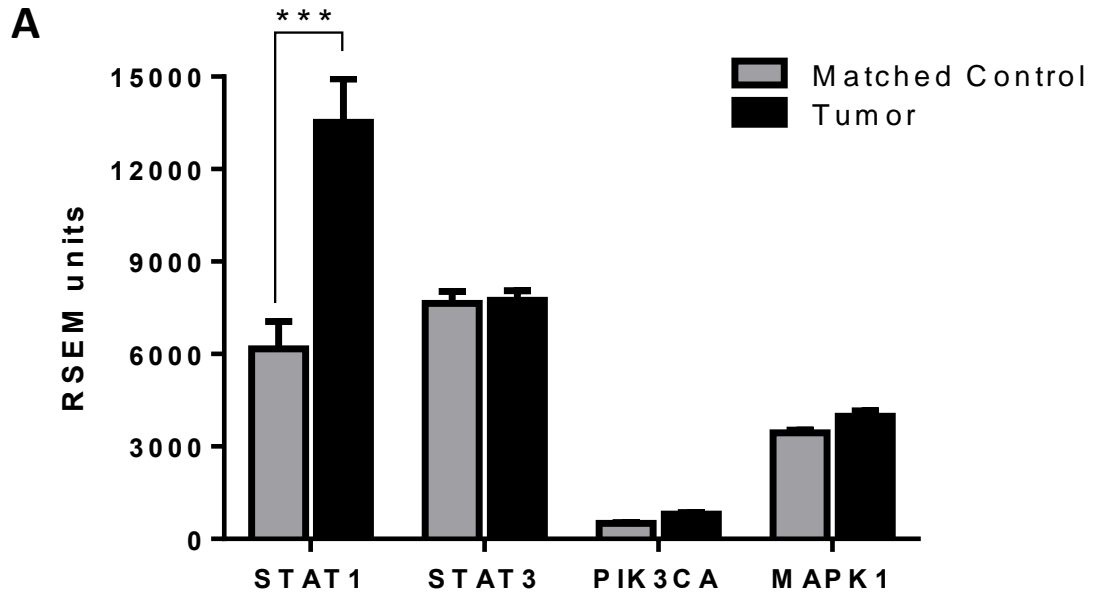
Correlation (XY)	HPV Negative		HPV Positive	
	Pearson r	P value	Pearson r	P value
PD-L1 vs. PD-1	0.5937	< 0.0001 (***)	0.7538	< 0.0001 (***)
PD-L1 vs. CD8A	0.5157	< 0.0001 (***)	0.8363	< 0.0001 (***)
EGFR vs. CD8A	-0.01368	0.4566 (ns)	0.4705	0.0136 (*)
EGFR vs. JAK2	0.1853	0.0681 (ns)	0.438	0.0207 (*)
IFNγ vs. CD8A	0.7747	< 0.0001 (***)	0.9396	< 0.0001 (***)
IFNγ vs. JAK2	0.7264	< 0.0001 (***)	0.7391	< 0.0001 (***)

Table 2.3.3.1 Correlation of PD-L1, EGFR and IFNG with a Th1 profile in HPV negative and HPV positive tumors: PD-L1 mRNA expression highly correlated with that of PD-1 and CD8A regardless HPV status. In addition, EGFR expression correlated with that of CD8A or JAK2 in HPV⁺ but not HPV⁻ tumors. As expected, IFN γ shows a strong correlation with that of CD8A and JAK2 regardless HPV status

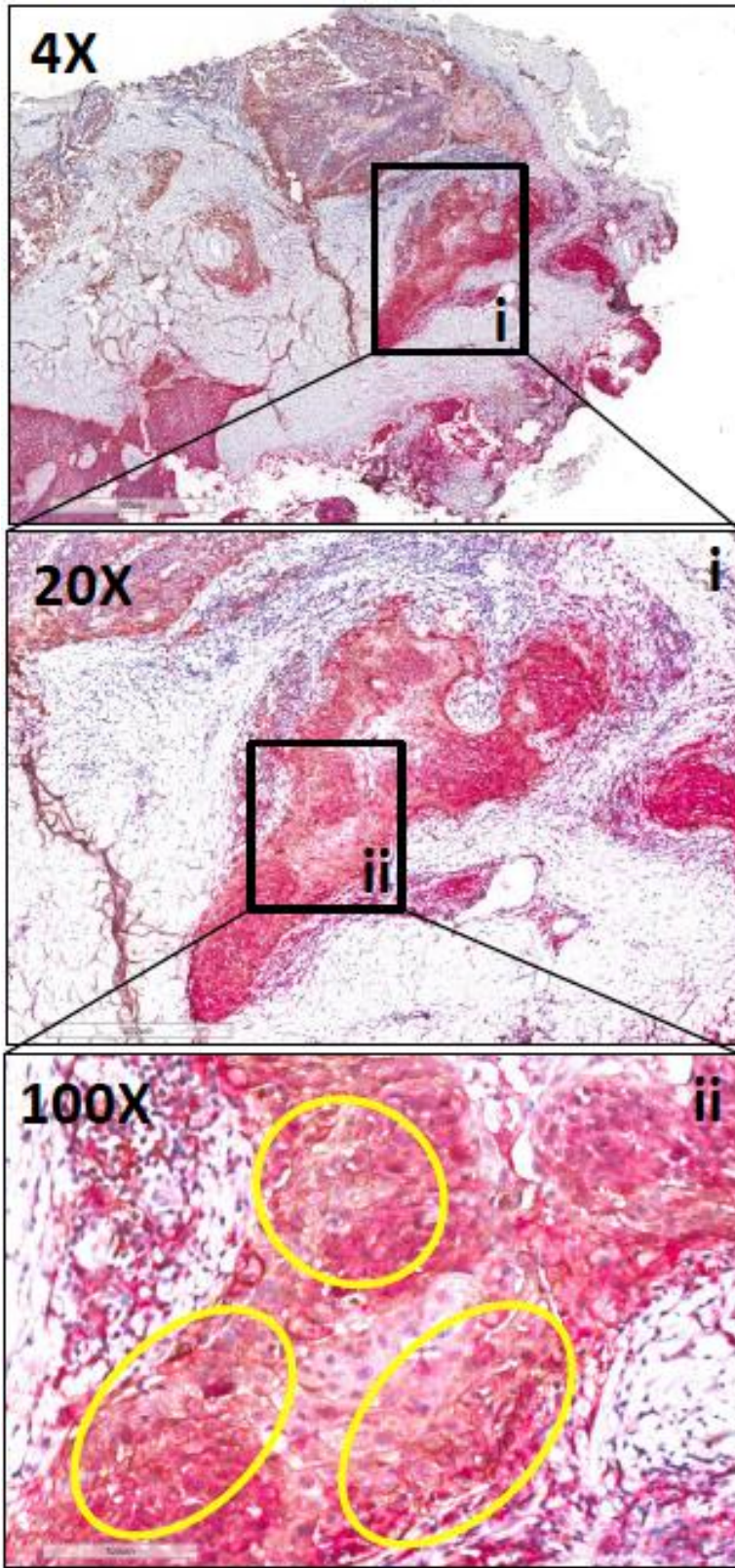
2.3.4 STAT1 but not STAT3, PIK3CA or MAPK1 expression is higher in tumor tissue and strongly correlates with PD-L1, EGFR and IFN γ regardless of HPV status

Since PD-L1 expression strongly correlated with a Th1 type expression profile in the tumor microenvironment, we hypothesized that PD-L1 may depend on STAT1 activation, a known Th1 type transcription factor. Indeed, STAT1 emerged as one of the highly predicted transcription factors binding to PD-L1 promoter region and common to EGFR and IFN γ pathways when utilizing previously validated software for transcription factor binding prediction (MATCH) and pathway exploration (Ingenuity IPA) (180). Given that previous reports presented STAT3, PI3K and MAPK as possibly involved in PD-L1 expression in other tumor types, we included these in our investigation. We pooled RNAseq data collected from 46 paired specimens of tumor vs. matched normal mucosa and found that STAT1 (but not STAT3, PIK3CA or MAPK1) was

significantly upregulated in tumor tissue (Figure 2.3.4A). Furthermore, STAT1 expression highly correlated with that of PD-L1 in TCGA (n=500), which was preserved when segregated by HPV status (Figure 2.3.4B). Concordant with TCGA data, we found that STAT1 protein was widely expressed in HNC tumor tissues, and that PD-L1 positive tumor islands were also strongly positive for total STAT1 staining (Figure 2.3.4C, circled areas highlight co-localization, 100X inset). Interestingly, STAT1 expression also showed strong correlation with that of EGFR (Figure 2.3.4D). As expected, STAT1 tumor expression also was strongly correlated with that of IFN γ (Figure 2.3.4E). Notably, STAT3 and PI3K pathway components (AKT1, TORC1 or 4EBP1) showed no correlation with PD-L1 in HPV⁺ tumors and only weakly in the HPV⁻ HNC. Likewise, MAPK1 was not correlated with PD-L1 expression in either cohort (Table 2.3.4.1). Overall, our findings suggest that the JAK2/STAT1 pathway may serve as an important common mediator for both EGFR- and IFN γ -mediated PD-L1 expression in HNC tumors, regardless of HPV status.



C



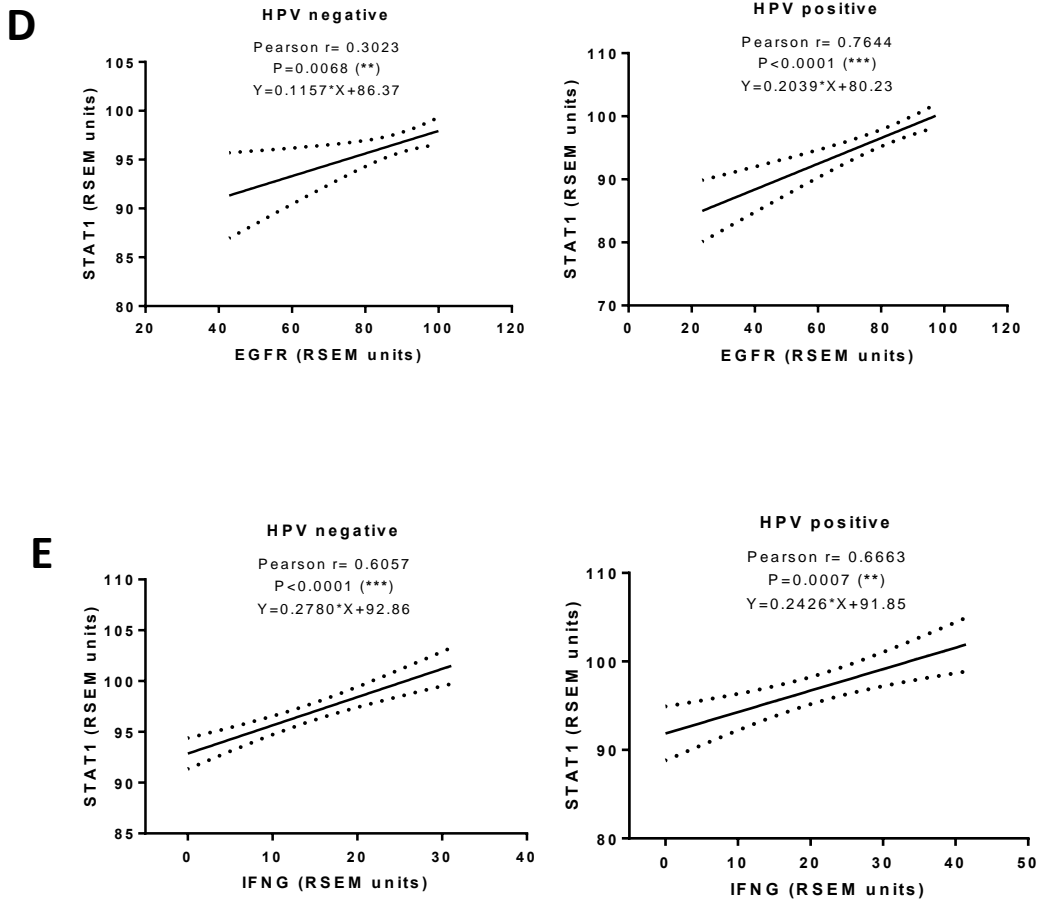


Figure 2.3.4 STAT1, but not STAT3, PI3KCA or MAPK1 expression is higher in tumor tissue and strongly correlates with that of PD-L1, EGFR and IFN γ regardless HPV status:

A. Expression of STAT1 but not STAT3, PIK3CA or MAPK1 was significantly higher in tumor specimens when compared with matched control mucosa (TCGA, 46 HNC tumor specimens and matched controls, Mann-Whitney test, *** $P < 0.0001$). **B.** STAT1 expression is strongly correlated with that of PD-L1 regardless HPV status (Pearson r and linear regression curve fit, ** $P < 0.001$ *** $P < 0.0001$) **C.** PD-L1⁺ tumor islands are also strongly positive for STAT1 protein in HNC specimens. Representative section of a HNC specimen co-stained for PD-L1 (brown chromogen) and STAT1 (red chromogen). Insets represent magnification of the tumor area, yellow circles indicate co-localization. **D-E.** STAT1 expression correlated with that of EGFR and IFN γ regardless HPV status. (Pearson r and linear regression curve fit, ** $P < 0.001$ *** $P < 0.0001$).

Correlation (XY)	HPV Negative		HPV Positive	
	Pearson r	P value	Pearson r	P value
PD-L1 vs STAT3	0.2503	0.0427 (*)	0.3867	0.0754 (ns)
PD-L1 vs AKT1	-0.2048	0.099 (ns)	0.00568	0.98 (ns)
PD-L1 vs TORC1	-0.2743	0.0258 (*)	-0.1973	0.3787 (ns)
PD-L1 vs 4EBP1	-0.2488	0.044 (*)	-0.2206	0.3238 (ns)
PD-L1 vs MAPK1	-0.1659	0.1832 (ns)	0.07862	0.728 (ns)

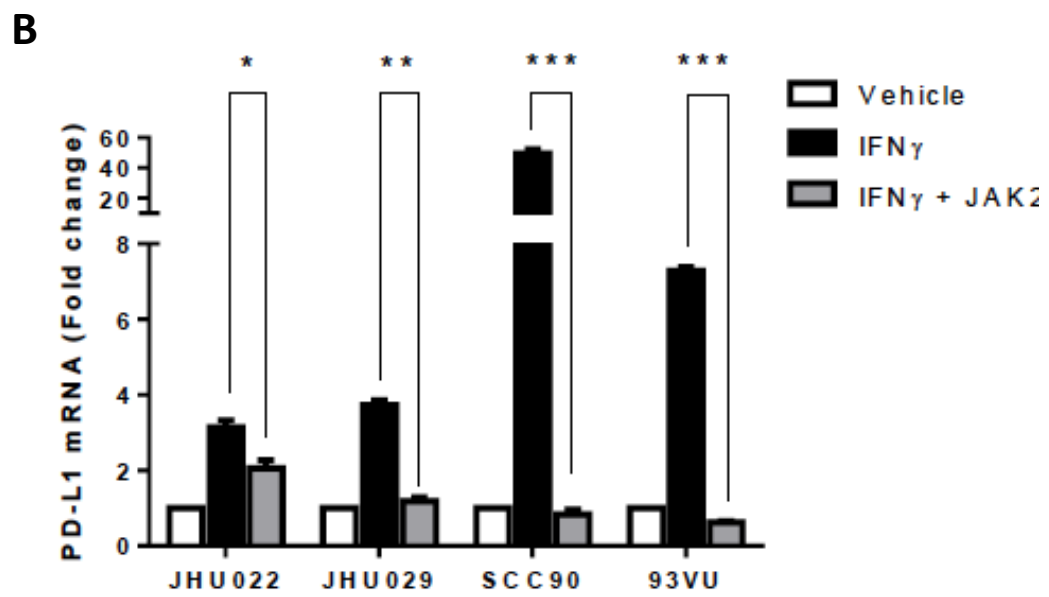
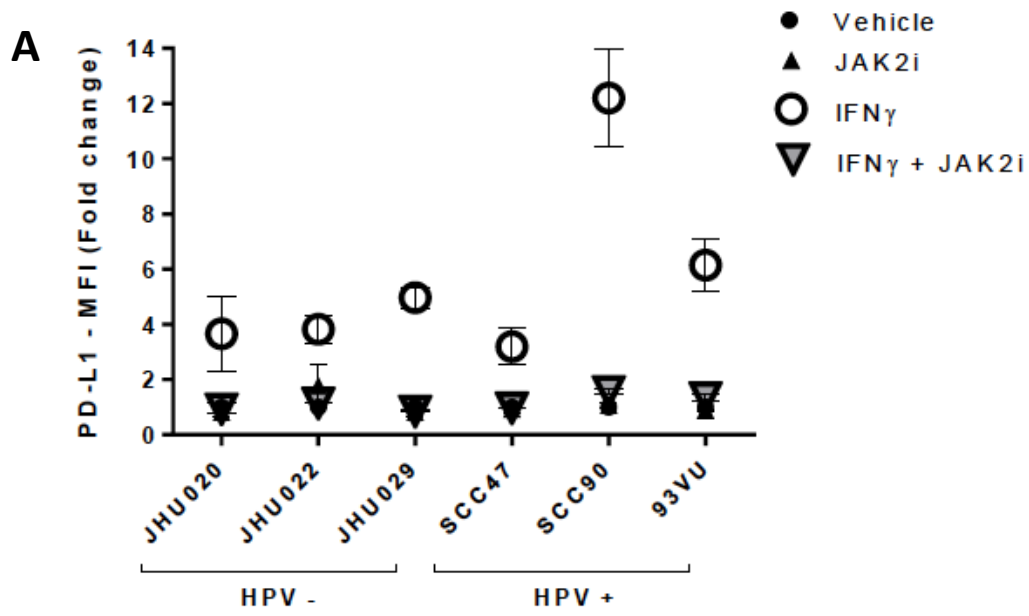
Table 2.3.4.1 Correlation of PD-L1 and STAT3, PI3K and MAPK pathway components in HPV negative and HPV positive tumors: PD-L1 mRNA expression did not show a strong correlation with STAT3, PI3K and MAPK pathways regardless HPV status. (TCGA, 66 HPV⁻ and 22 HPV⁺ tumor specimens).

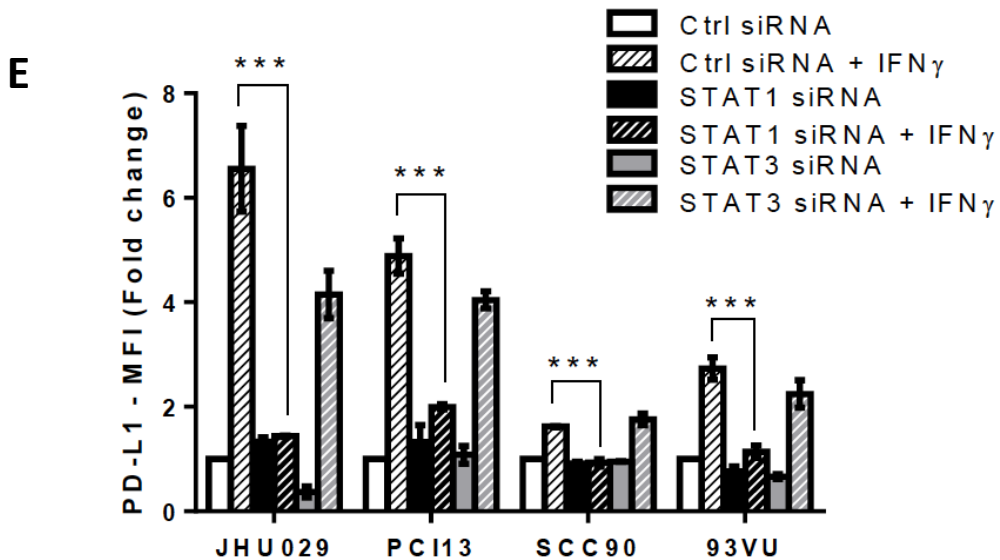
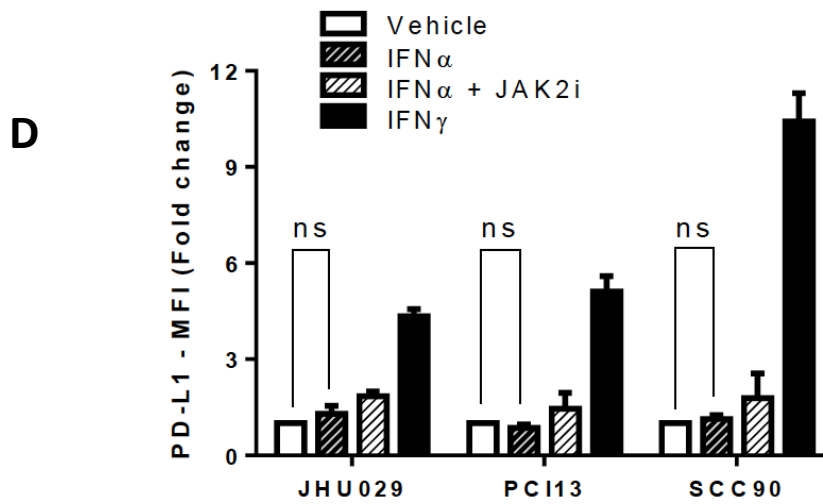
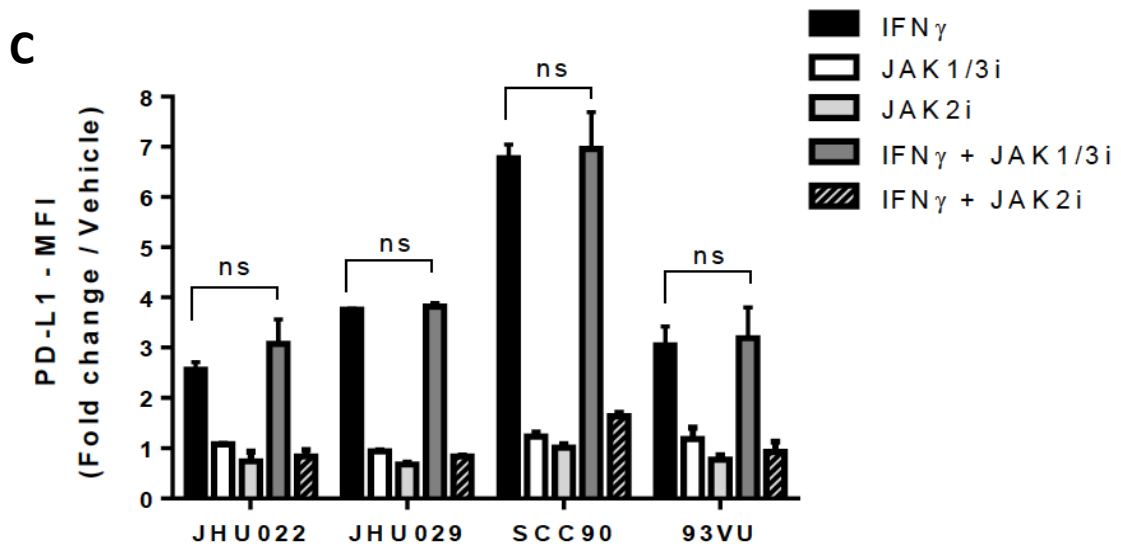
2.3.5 IFN γ -mediated PD-L1 upregulation is JAK2/STAT1 dependent

Based on our TCGA analysis and previous reports linking IFN with PD-L1 expression at the mRNA level, we investigated the signaling pathway by which IFN γ upregulates PD-L1 expression in vitro. Indeed, a panel of HPV+ and HPV- HNC cell lines upregulated PD-L1 expression after IFN γ treatment (Figure 2.3.5A). Given that IFN γ -mediated PD-L1 upregulation was linked with PI3K pathway activation (166), we tested whether wortmannin (pan-PI3K inhibitor) or BYL-719 (PI3K α 110 subunit specific inhibitor) could prevent IFN γ -mediated PD-L1 upregulation. PI3K pathway inhibition did not induce PD-L1 downregulation, under conditions in which these inhibitors effectively prevented AKT phosphorylation (Supplementary Figure 2.5.1-4). Since IFN γ signals via JAK1 and JAK2, we utilized a clinical grade, selective JAK2 inhibitor BMS-911345 (JAK2i) which was previously characterized (181), finding an abrogation of IFN γ -mediated PD-L1 upregulation in all cell lines tested, both at the mRNA and

protein level (Figure 2.3.5A and 2.3.5B, Supplementary Figure 2.5.5). Interestingly, specific JAK1/3 inhibition (JAK1/3i) did not show a significant downregulation of IFN γ -mediated PD-L1 protein expression (Figure 2.3.5C). We then used IFN α , which signals via JAK1 and TYK2, but not JAK2. IFN α treatment did not upregulate PD-L1 expression (Figure 2.3.5D) but still induced pSTAT1 upregulation, although to a lesser extent than IFN γ , in all cell lines tested. Moreover, JAK2 inhibition did not affect HLA-ABC upregulation (Supplementary Figure 2.5.6-7), which suggests that the kinetics of IFN α -induced pSTAT1 binding to the PD-L1 promoter differ for HLA-ABC.

In order to determine whether the IFN γ -mediated PD-L1 upregulation was solely STAT1 dependent, we silenced each transcription factor using siRNA technology (80-90% knockdown efficiency, supplementary Figure 2.5.8). STAT1 but not STAT3 knockdown potentially impaired IFN γ -mediated upregulation of PD-L1 (Figure 2.3.5E). Moreover, chromatin immunoprecipitation (ChIP) assays documented that pSTAT1 but not pSTAT3 binds to the promoter region of PD-L1 after IFN γ treatment (Figure 2.3.5F). Interestingly, cetuximab mediated EGFR blockade downregulated IFN γ induced pSTAT1 binding to the PD-L1 promoter and significantly downregulated the IFN γ -mediated PD-L1 upregulation at the mRNA and protein level, respectively. (Figure 2.3.5G-H and Supplementary Figure 2.5.9).





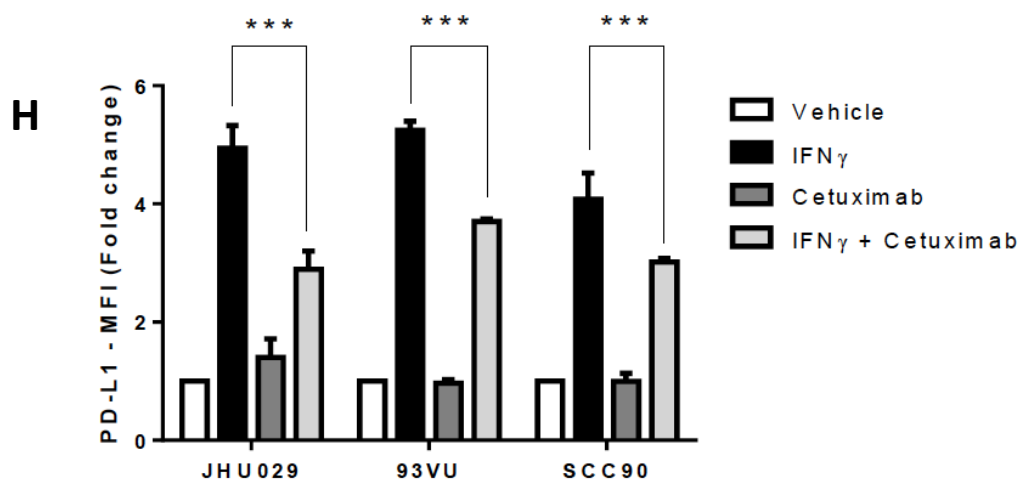
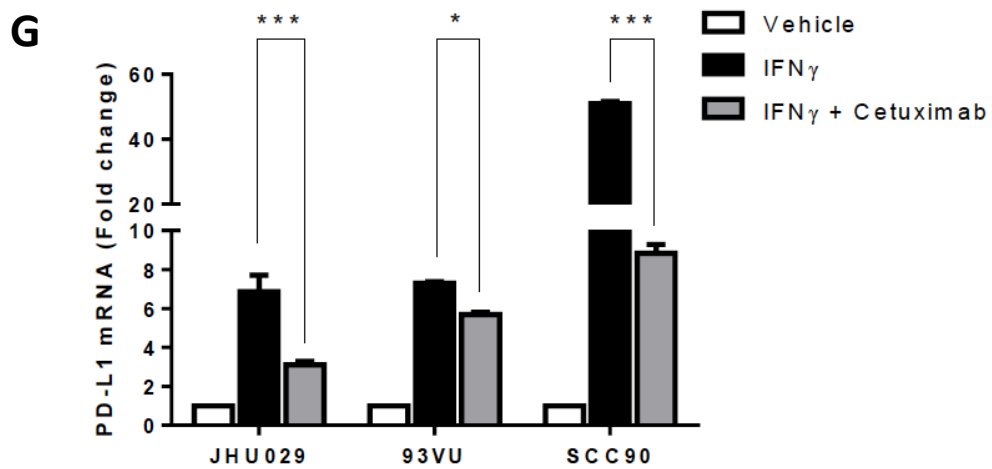
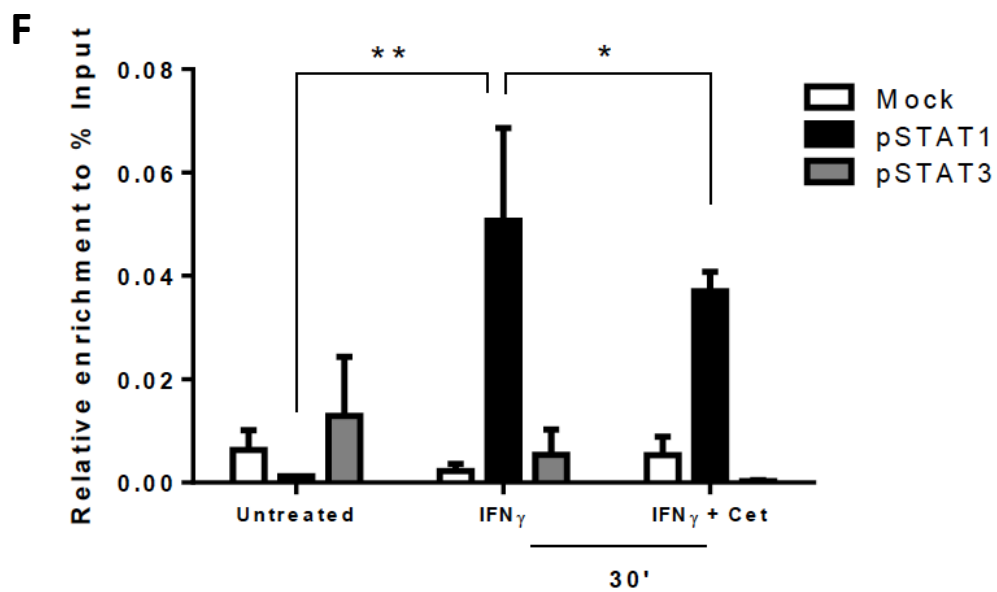


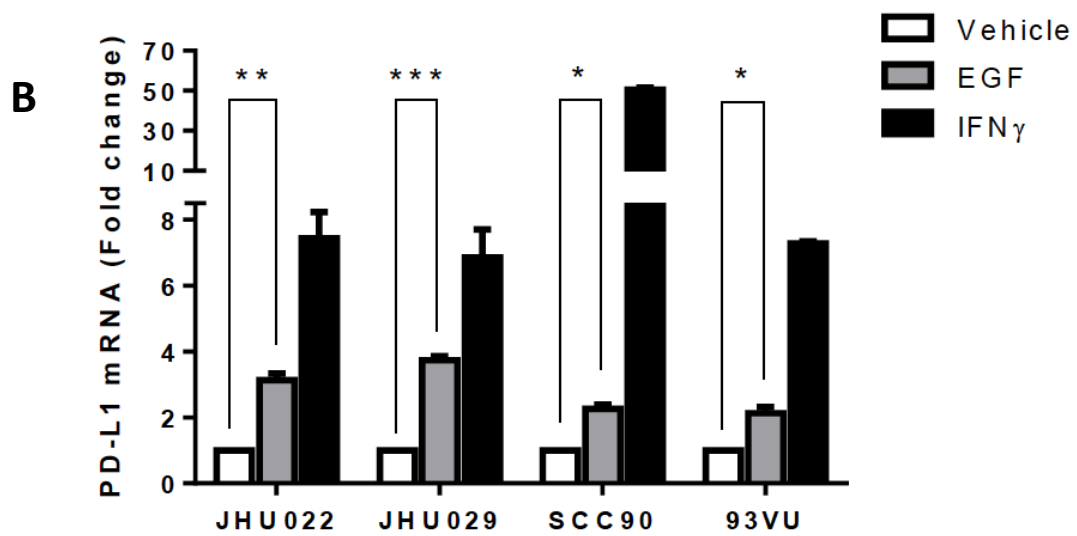
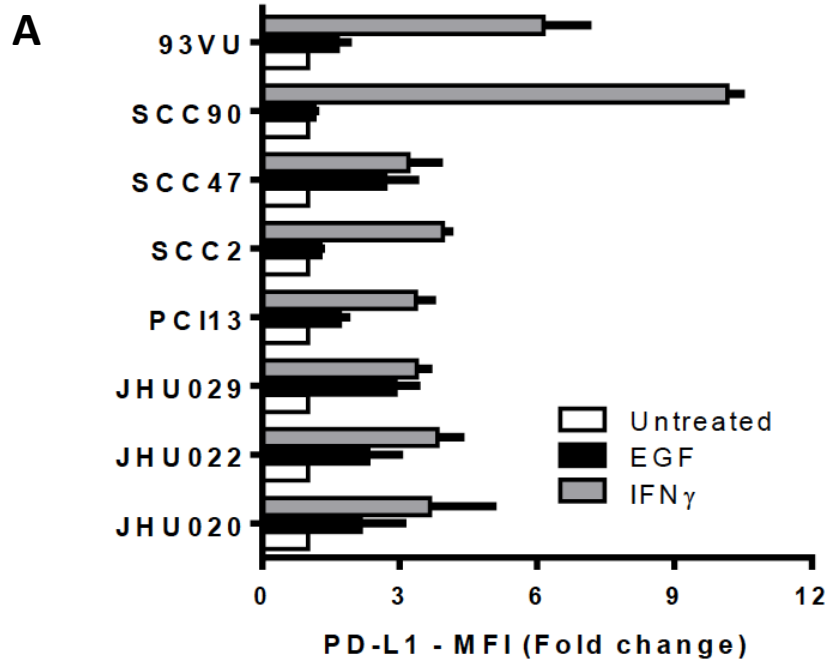
Figure 2.3.5 IFN γ mediated PD-L1 upregulation is JAK2/STAT1 dependent: **A.** Specific JAK2 inhibitor BMS-911345 (JAK2i) abrogates IFN γ -mediated PD-L1 protein upregulation in all cell lines tested regardless HPV status. Cell lines were either treated with vehicle control, JAK2i (10uM), IFN γ (10IU/mL) or the combination for 48h, harvested and PD-L1 expression was determined by flow cytometry (FC) **B.** JAK2i abrogates IFN γ -mediated PD-L1 mRNA upregulation. Cell lines were either treated with vehicle control, IFN γ (10IU/mL) or JAK2i (10uM) or the combination for 24h; PD-L1 mRNA was determined by qPCR and expressed as fold change over vehicle control **C.** Specific JAK1/3 inhibition did not prevent IFN γ -mediated PD-L1 upregulation in HNC cell lines. Cell lines were either treated with vehicle control, JAK1/3i (10uM), JAK2i (10uM), IFN γ (10IU/mL) or the combination for 48h, harvested and PD-L1 expression was determined by FC (ANOVA, ns= not significant) **D.** IFN α did not upregulate PD-L1 expression. Cells were incubated with IFN α (1000 IU/mL), JAK2i (10uM) and the combination for 48 h. IFN γ (10IU/mL) was used as a positive control. PD-L1 expression was determined by FC (ANOVA, ns= not significant). **E.** IFN γ -mediated PD-L1 upregulation is abrogated when STAT1, but not STAT3, is silenced. Cells were incubated with STAT1 siRNA, STAT3 siRNA or control siRNA (10nM) for 48h then were either left untreated or treated with IFN γ (10IU/mL) for additional 48h, harvested and PD-L1 expression was determined by FC. **F.** pSTAT1 but not pSTAT3 binds to the PD-L1 promoter region after IFN γ treatment as determined by CHIP assay. Cells were either left untreated or treated with IFN γ (10IU/mL) or IFN γ +cetuximab for 30 minutes, CHIP assay showed enrichment of pSTAT1 in the PD-L1 promoter (black bars). PD-L1 enrichment calculated as % input DNA (refer to Materials and Methods) (ANOVA * P<0.05, ** P<0.01). **G.** Cetuximab-mediated EGFR blockade downregulated IFN γ -mediated PD-L1 mRNA upregulation. Cell lines were either treated with vehicle control, IFN γ (10IU/mL), cetuximab (10ug/mL) or IFN γ +cetuximab for 24 h. harvested and mRNA was quantified by qPCR and expressed as fold change over vehicle control (ANOVA, * P<0.05, *** P<0.0001) **H.** Cetuximab-mediated EGFR blockade downregulated the IFN γ -mediated PD-L1 protein upregulation. Cell lines were either treated as in G for 48h harvested and PD-L1 protein expression was determined by FC (ANOVA, *** P<0.0001)

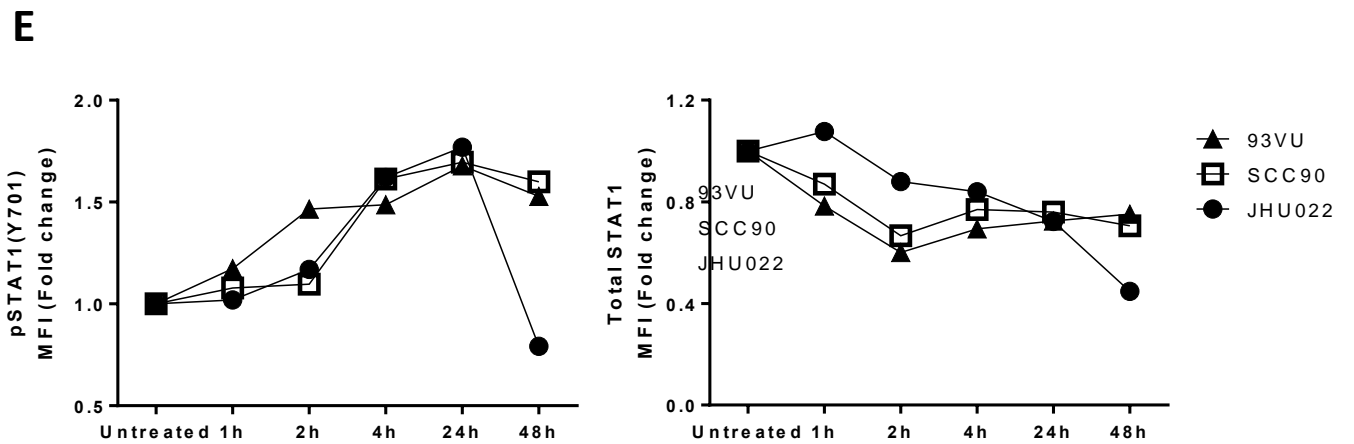
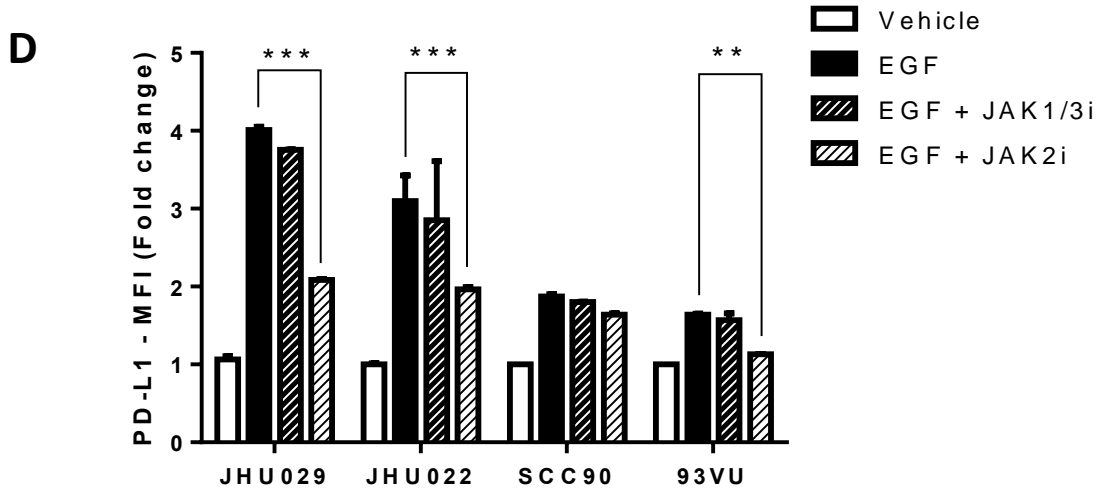
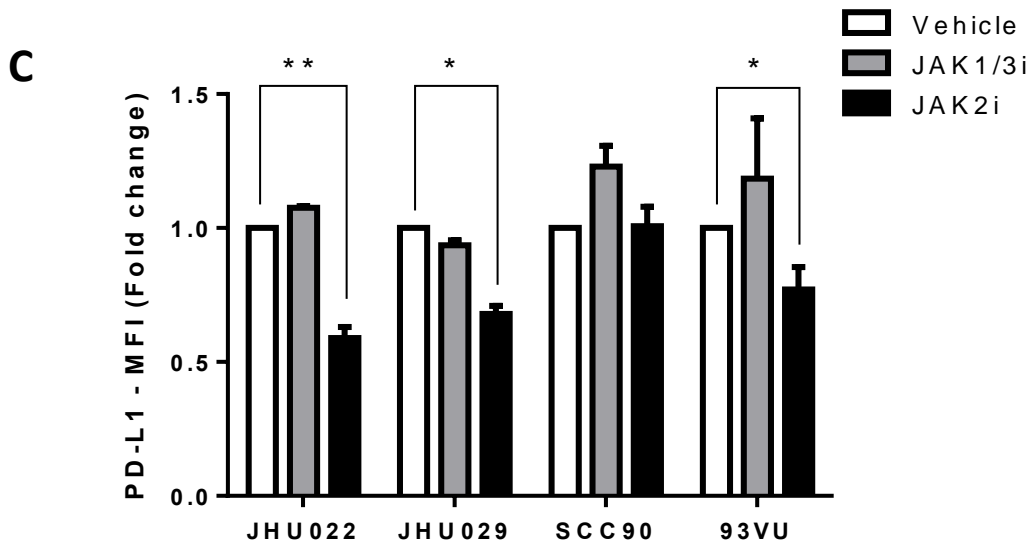
2.3.6 EGFR-mediated PD-L1 upregulation is JAK2/STAT1 dependent

Since EGFR strongly correlated with PD-L1 expression in TCGA specimens and a previous report showed that EGFR activating mutations induce PD-L1 in lung cancers (167), we hypothesized that wild type EGFR, overexpressed in 80-90% of HNC, may promote PD-L1 upregulation. EGF treatment induced upregulation of PD-L1 protein in 7 of 8 HNC lines studied, though to a lesser extent than that induced by IFN γ (Figure 2.3.6A). This effect was also seen at the mRNA level (Figure 2.3.6B). Although EGFR activates multiple downstream pathways, including PI3K, MAPK and JAK/STAT pathway, TCGA analysis yielded weak if any correlation between PD-L1 and PIK3CA or MAPK1 (Table 2.3.1.1). However, a strong correlation was observed with that of JAK2 and STAT1 (Figure 2.3.3A and 2.3.4B respectively). Given that JAK2 serves as a common signaling molecule for both IFN γ and EGFR pathways, we investigated whether EGF-mediated PD-L1 upregulation was JAK2 and/or STAT1 dependent. Indeed, basal expression of PD-L1 in HNC cell lines was downregulated by JAK2 but not JAK1/3 inhibition (Figure 2.3.6C). Furthermore, EGF induced JAK2 phosphorylation (Supplementary Figure 2.5.10) and upregulation of basal PD-L1 expression (Figure 2.3.6D). Additionally, specific JAK2, but not JAK1/3, inhibition prevented EGF induced PD-L1 upregulation (Figure 2.3.6D and Supplementary Figure 2.5.11). Interestingly, the EGF-mediated PD-L1 upregulation was higher in cell lines with a higher EGFR expression (JHU029 and JHU022 vs 93VU and SCC90). Likewise, JAK2 inhibition more strongly downregulated basal and EGF-mediated PD-L1 expression in the EGFR^{high} cell lines (Figure 2.3.6D, JHU022 and JHU029).

Since EGFR activates PI3K and MAPK pathways, we tested whether these mediated PD-L1 upregulation after EGFR stimulation. We found that neither wortmannin-mediated PI3K

inhibition nor MEK1/2-mediated MAPK inhibition prevented EGF-induced PD-L1 upregulation (Supplementary Figures 2.5.12 and 2.5.13). However, these inhibitors effectively suppressed AKT and ERK phosphorylation, respectively (Supplementary Figures 2.5.14 and 2.5.15). In light of this result and the positive correlation found between EGFR and STAT1, we hypothesized that EGF may be activating STAT1 phosphorylation, mediated by JAK2. Indeed, EGF induced STAT1 (tyrosine701) phosphorylation reaching its maximum peak at 24 hours, while total STAT1 levels remained stable (Figure 2.3.6E). Furthermore, siRNA-targeted STAT1 knockdown efficiently suppressed total STAT1 levels, (Supplementary Figure 2.5.16) as well as significantly abrogating EGF induced PD-L1 upregulation (Figure 2.3.6F).





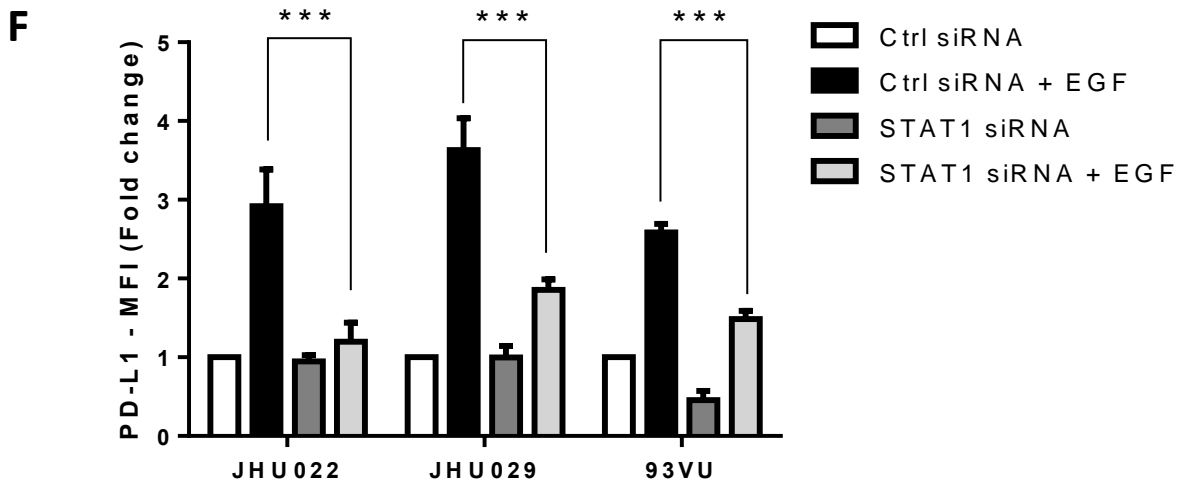


Figure 2.3.6 EGFR-mediated PD-L1 upregulation is JAK2/STAT1 dependent: **A.** EGF upregulates PD-L1 protein expression. Cells were either left untreated or treated with EGF (10ng/mL) for 48h, IFN γ (10IU/mL) was used as a positive control. Cells were harvested and PD-L1 surface expression was determined by FC **B.** EGF treatment upregulates PD-L1 mRNA expression. Cells were treated as in **A** for 24h, harvested and PD-L1 mRNA expression was determined by qPCR and expressed as fold change over vehicle control (ANOVA, * $P < 0.05$, ** $P < 0.01$, *** $P < 0.001$). **C.** JAK2 but not JAK1/3 inhibition downregulates baseline expression of PD-L1. Cells were treated with JAK1/3 inhibitor (JAK1/3i, 10uM) or JAK2i (10uM) for 48h and PD-L1 expression level was determined by FC (ANOVA, * $P < 0.05$, ** $P < 0.001$). **D.** JAK2 but not JAK1/3 inhibition prevents EGF-mediated PD-L1 upregulation. Cells were treated with JAK1/3i (10uM) or JAK2i (10uM) for 48h and PD-L1 expression level was determined by FC (ANOVA, ns= non-significant ** $P < 0.001$ *** $P < 0.0001$). **E.** EGF induces pSTAT1y701 upregulation. Cells were either left untreated or treated with EGF (10ng/mL) for 1, 2, 4, 24 and 48 hours, harvested, fixed and permeabilized and pSTAT1y701 or total STAT1 expression were determined by ICF. **F.** STAT1 silencing prevents EGF induced PD-L1 upregulation. Cells were treated with either control siRNA or STAT1 siRNA (10nM) and EGF (10ng/mL) for 48h, harvested and PD-L1 expression was determined by FC (ANOVA, *** $P < 0.001$).

2.4 DISCUSSION

Previous studies showed that PD-L1 is expressed in many types of malignancies including HNC. Given the known importance of HPV infection in the etiology of HNC, several studies have sought to correlate expression of PD-L1 with HPV status. Indeed, recent reports have shown higher PD-L1 expression in HPV positive compared to HPV negative tumors (157, 165, 182, 183). Interestingly, Lyford-Pike et al. (157) only noted 29% PD-L1 positivity among a small cohort (n=9) of HPV negative HNC patients while Malm et al. reported 80% (183) making the association of PD-L1 expression with HPV positivity controversial. In our large series of 134 patients, we found that the majority of HNC tumor specimens analyzed (approximately 60% of n=134) were positive for PD-L1 (using a 5% cutoff threshold). Most importantly, we found HPV positive tumors to be more frequently PD-L1 positive (70%, n=64) and have a significant higher percent area and intensity of PD-L1 expression in contrast to their HPV negative counterparts (figure 2.3.1C-D). Importantly, a previous study showed that PD-L1 co-localized with CD3 in 56% of tumors while 44% showed a diffuse pattern with no co-localization noted (183), raising the question of how PD-L1 is regulated in those tumors. These findings support the view that PD-L1 expression could be “extrinsically” induced by IFN γ secreting CD8⁺ TILs (where co-localization was found), particularly in HPV positive tumors and “intrinsically” induced via endogenous EGFR signaling (where no co-localization was found), particularly in HPV negative tumors.

In light of the finding that HPV positive tumors show higher PD-L1 protein expression *in vivo* and to extend findings reported previously, we took advantage of the large HNC cohort in TCGA repository, containing RNAseq expression data for 500 HNC tumor specimens, from which 88 have data available regarding HPV status assessed by p16 expression. Here we show

that HPV positive tumor specimens have significantly higher expression of a Th1 type profile including CD8A, PD-1, IFNG and JAK2 (Figure 2.3.2A-B). Our findings are concordant with those of a previous report where HPV positive HNC tumors showed more PD-1⁺ CD8⁺ T cell infiltration and that PD-1 expression was a marker of activated T cells and correlated with favorable clinical outcome (165). These data suggest that PD-1 expressing cells are biologically relevant and may play a crucial role in HPV positive disease and PD-L1 induction. Importantly, we report that PD-L1 expression highly correlated with that of JAK2 at the mRNA level. Furthermore, pJAK2 protein expression was strongly associated with that of PD-L1 *in vivo* as determined by IHC from HNC tumor specimens (Figure 2.3.3B, n=23). Additionally, we found that pJAK2 staining was significantly higher in HPV positive than HPV negative specimens (data not shown). Interestingly, PD-L1 was also strongly correlated with a Th1 type profile regardless of HPV status (Figure 2.3.3C-D and Table 2.3.3.1), suggesting that the PD-L1/PD-1 axis represents an important mechanism of immune evasion in both HPV negative and positive tumors, such that HPV negative tumors may rely more on a tumor intrinsic oncogenic (EGFR-driven) PD-L1 expression, while HPV positive tumors rely more on a tumor extrinsic IFN γ -mediated Th1 like response.

The tumor microenvironment contains effector cell infiltrates but also a complex network of immune cells such as dendritic cells (DC), myeloid derived suppressor cells (MDSC) or tumor-associated macrophages (TAM) that could also express PD-L1, ligate PD-1 expressing lymphocytes, and play a pivotal role affecting antigen presentation and CTL generation. Indeed, PD-L1 expressing DCs infiltrating ovarian tumors are higher when compared with normal lymph nodes, and blockade of PD-L1 increases infiltrates of CD8⁺ cells and tumor rejection in a mouse model (172). Interestingly, Chikamatsu et al. found a higher frequency of MDSC, defined as

CD14⁺ HLA-DR⁻ cells, in peripheral blood of HNC patients when compared to normal controls, and treatment with anti-PD-L1 antibody restored T cell proliferation and IFN γ production *in vitro* (173). However, further investigation may be needed to define the specific role of antigen presenting cells in HNC and whether there is a different pattern of infiltration and PD-L1 expression in HPV negative versus positive tumors. In our study we focus principally on PD-L1 expression on tumor cells given that EGFR expression is mainly limited to tumor cells rather than immune cells and its activation leads to PD-L1 upregulation having JAK2/STAT1 as a common mediator with the IFN γ pathway.

We found that STAT1 was a predominant transcription factor upregulated in HNC tumors when compared with paired autologous normal mucosa (Figure 2.3.4A, n=46) and that PD-L1 was significantly correlated with STAT1 expression regardless of HPV status (Figure 2.3.4B). Moreover, we corroborated these TCGA findings *in vivo* as STAT1 and PD-L1 protein showed co-localization in tumor islands as determined by IHC (Figure 2.3.4C). Notably, components of other signaling pathways such as PI3K and MAPK, which have been previously associated with PD-L1 expression in other types of cancer and tissues, such as glioma or non-small cell lung cancer (NSCLC) (152, 166) did not show significant correlation with PD-L1 expression in HPV positive tumors or induce PD-L1 in our cell lines. Indeed, the unique biology, mutational landscape and predominant signaling pathways in HNC may explain the differences with those of glioblastoma and NSCLC regarding PD-L1 expression. Indeed, it has been recently reported that PTEN loss-of-function mutations are frequent in glioblastoma (31.9% of specimens, TCGA data) (184). Furthermore, Parsa et al. showed that PD-L1 was upregulated after PTEN loss/PI3K activation in glioblastoma cell lines, suggesting that gliomas may rely more on this signaling pathway. Likewise, in the setting of NSCLC, PD-L1 protein is

upregulated after EGFR/RAS/MAPK pathway activating mutations. Indeed, HRAS and EGFR mutations in NSCLC are far more frequent than in HNC (2-5%) (185, 186). Therefore, we speculate that mutant EGFR may induce a stronger MAPK pathway activation than wild type EGFR. On the other hand, PTEN or PIK3CA mutations are rather infrequent in HNC, 7% and 8% respectively (186). Hence, in the setting of HNC the intrinsic oncogenic signaling mostly depends on overexpressed wild type EGFR stimulation and presents as a unique feature of this type of cancer, in which the JAK/STAT3 oncogenic pathway is best characterized (187). Importantly, in our series, STAT3 showed no significant correlation with PD-L1 expression in HPV positive tumors and only a weak correlation in HPV negative tumors, most likely because of higher EGFR expression in these tumors versus HPV positive ones.

Concordant with other types of cancer, IFN γ induced PD-L1 upregulation in all of the HNC cell lines tested in our study (Figure 2.3.5A), however its upregulation was not PI3K dependent as reported for glioma, lymphoma or lung cancer (152, 188, 189). We are the first to report that specific JAK2 inhibition completely abrogated the IFN γ -mediated PD-L1 upregulation at the mRNA and protein level (Figure 2.3.5A-C). Interestingly, IFN α , which does not signal via JAK2, did not upregulate PD-L1 expression, confirming the specific role of JAK2 upregulating PD-L1. However, IFN α did upregulate pSTAT1(Y701) although not to the extent of IFN γ (Supplementary Figure 2.5.5). These findings suggest that the binding kinetics of pSTAT1(Y701) to the PD-L1 promoter may have differences in the amount of pSTAT1 molecules required to initiate gene transcription, a threshold that IFN γ may reach. Likewise, we should emphasize the fact that IFN α not only induces STAT1 phosphorylation but also STAT2, and complexes with IRF9 in the transcription factor assembly cascade, forming the ISGF3 transcription complex, where IRF9 is the main DNA binding domain (190). In contrast IFN γ

mainly induces the formation of pSTAT1 dimers that directly bind to the DNA's promoter region of the target gene, which explains why IFN α may not upregulate PD-L1 although it still upregulates pSTAT1. In addition, and corroborating our TCGA findings, *in vitro* knockdown experiments show that STAT1 but not STAT3 mediates IFN γ induced PD-L1 upregulation (Figure 2.3.5E), further supported by a ChIP assay, providing additional evidence that pSTAT1 but not pSTAT3 binds to the PD-L1 promoter region as early as 30 minutes after IFN γ treatment (Figure 2.3.5F). Our findings complement that of a previous report performed in AG490 cells (lung cancer) that shows IRF-1 binding to the PD-L1 promoter after IFN γ treatment (191). However, we used a 10-fold lower dose of IFN γ (10 IU/mL) constituting a more physiologic dose as previously determined in tumor supernatants (data not shown). Interestingly, we are the first to report that cetuximab-mediated EGFR blockade significantly downregulates IFN γ -induced PD-L1 expression (Figure 2.3.5G-H), suggesting cross-talk between the IFN γ and EGFR pathways in regulating PD-L1 expression mediated through STAT1 modulation.

PD-L1 overexpression was associated with mutant EGFR in a murine lung cancer model as well as in surgically resected human NSCLC specimens (167, 168, 189), but studies associating wild type overexpressed EGFR signaling and PD-L1 expression have not been reported. Our TCGA database analysis showed higher EGFR expression in HPV negative tumors concurring with a previous report (192). EGFR mRNA expression significantly correlated with that of PD-L1 although to a lesser extent than that seen for IFN γ (Figure 2.3.3C-D). Moreover, EGFR and PD-L1 showed a higher correlation in HPV positive tumors that corresponds to the higher correlation seen with CD8A, JAK2 and STAT1 as well. These otherwise counter intuitive results may be explained by the fact that PD-L1 expression might be more dependent on the strength of EGFR/JAK2 pathway activation rather than EGFR higher expression in HPV

negative tumors that may induce an increased STAT1 activation and induction of PD-L1 expression. Alternatively, other immune cells infiltrating the tumor microenvironment may also express PD-L1, such as dendritic cells, macrophages, monocytes, B cells as well as non-immune cells like tumor associated fibroblasts and stromal cells (172, 193). PD-L1 expression on these cells may confound the strength of correlation with that of EGFR given that the expression of the latter is mostly on tumor cells, given that the TCGA RNAseq values represent whole tumor and are not cell specific. Therefore, protein levels maybe a better readout for EGFR-JAK2-PD-L1 correlations.

In light of our findings we hypothesized that JAK2/STAT1 signaling is a major common regulator for PD-L1 transcription driven by IFN γ and EGFR pathways. Since EGFR mutations are very rare in HNC (2% of tumors) (185), we hypothesized that EGFR pathway overactivation, rather than activating mutations, are more important for PD-L1 upregulation in this type of cancer. We are the first to report that wild type EGFR pathway induces PD-L1 upregulation at the mRNA and protein level (Figure 2.3.6A-B), and that specific JAK2 inhibition significantly downregulated baseline and EGF-induced PD-L1 upregulation (Figure 2.3.6C-D). Though the latter not completely, which suggests other alternative pathways not dependent on JAK2 may also contribute to PD-L1 expression in HNC. It is noteworthy that JAK2 inhibition was more effective at downregulating basal and EGF-mediated PD-L1 expression on those cell lines with higher EGFR surface expression (Figure 2.3.6C-D. JHU029, JHU022 vs. 93VU, SCC90). In addition, we are the first to report that EGFR stimulation induces phosphorylation of STAT1 (Figure 2.3.6E), which in turn mediates PD-L1 upregulation, since its silencing completely abrogated the EGF induced PD-L1 expression (Figure 2.3.6F). Indeed, EGFR and JAK2 inhibition may synergize downregulating the “intrinsic” PD-L1 expression. Most importantly,

however, is the speculation of potential added benefit of JAK2 inhibition with the simultaneous blockade of the “extrinsic” IFN γ -mediated PD-L1 upregulation, which seems to be more important in HPV positive tumors. Notably, anti-PD-1 immunotherapies in the clinic aim to restore the antitumor capabilities of the CD8⁺ PD-1⁺ TILs by releasing the PD-1-mediated inhibition of TCR downstream activation signaling. If that is achieved, TIL will re-acquire an effector phenotype that will involve secretion of a Th1 cytokine profile including IFN γ that paradoxically will lead to tumor cell PD-L1 overexpression and immune escape. This strategy most likely will benefit patients with HPV positive tumors. Additionally, we think that blocking PD-L1 expression rather than PD-1 would be a more effective approach for restoring an effector T cell phenotype and favor tumor cell lysis given that PD-1 expression on a subset of TIL may represent their activated status rather than true exhaustion.

In conclusion, our study shows that HPV positive tumors have higher PD-L1 protein expression, which correlates with a Th1 expression profile driving PD-L1 expression, most likely by an “extrinsic” (IFN γ -mediated) pathway. In addition we present JAK2 as a central mediator also driving “intrinsic” PD-L1 tumor cell expression, downstream of wild type EGFR. Consequently, JAK2 specific inhibition may constitute a logical therapeutic strategy to prevent PD-L1 upregulation and enhance CTL and NK cell mediated tumor lysis that is otherwise impaired by PD-L1/PD-1 axis interaction. Further investigation is necessary in order to elucidate whether JAK2 inhibition may synergize with anti-EGFR blockade to more potently abrogate EGF-induced PD-L1 upregulation, as well as to understand heterogeneity in EGFR⁺ cells which nonetheless are PD-L1 negative. This discordance appears to represent a minority of HNC given the high rate (>60-70%) of PD-L1⁺ HNC tumors.

2.5. SUPPLEMENTARY DATA

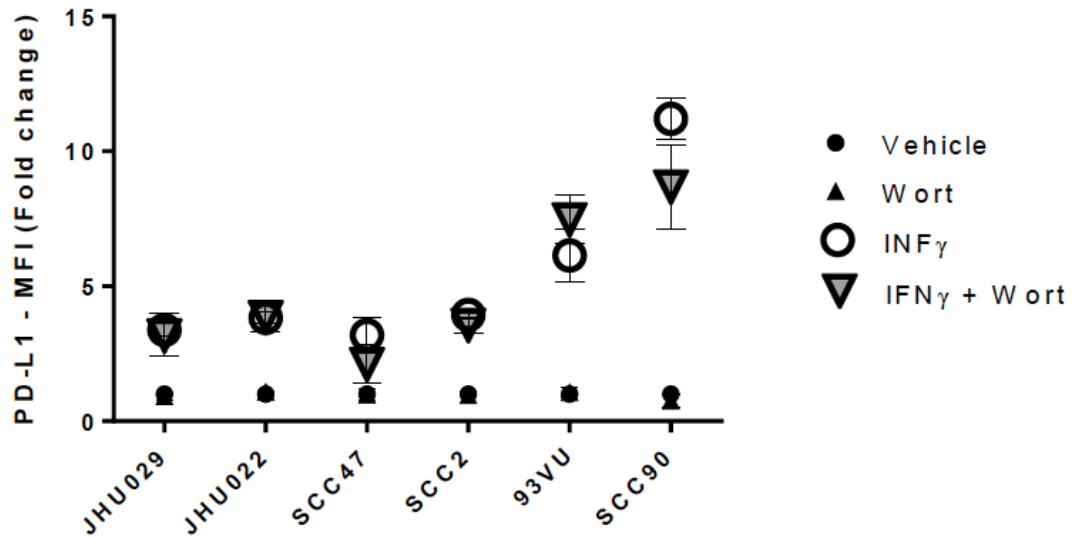


Figure 2.5.1 IFN γ -induced PD-L1 upregulation is not PI3K dependent: Wortmannin (Wort) a pan-PI3K inhibitor did not prevent IFN γ -mediated PD-L1 upregulation in all cell lines tested regardless HPV status. Cells were either treated with vehicle control; wortmannin (1 μ M), IFN γ (10IU/mL) or the combination for 48h harvested and PD-L1 was determined by FC.

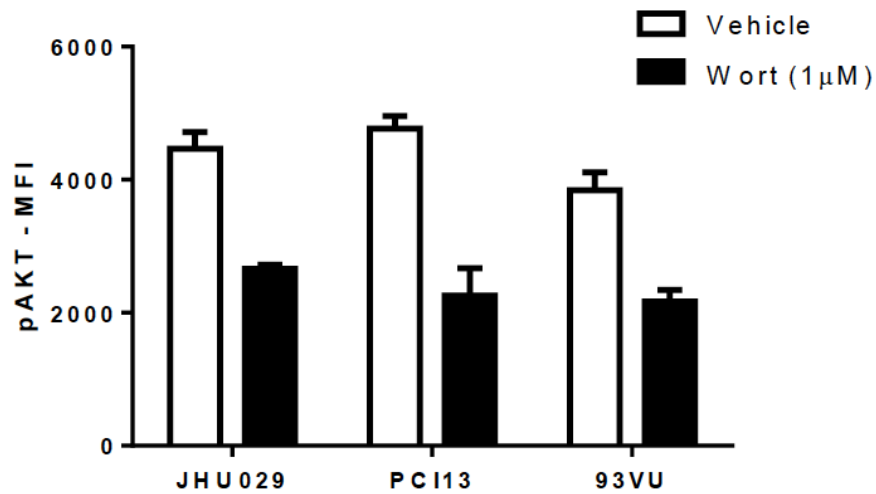


Figure 2.5.2 Wortmannin (Wort) effectively downregulated phosphorylation of AKT: Cells were either treated with vehicle control or wortmannin (1uM) for 30 min, harvested and pAKT was determined by intracellular flow cytometry (ICF).

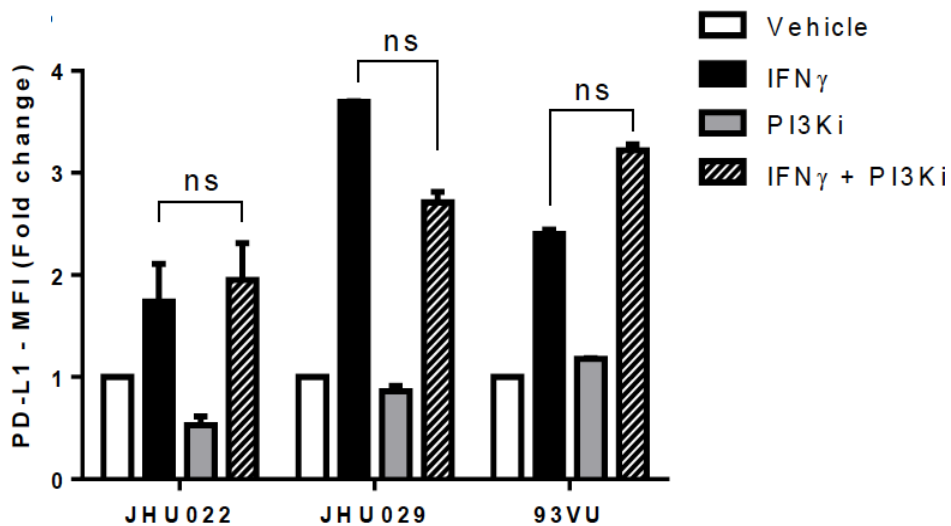


Figure 2.5.3 Specific PI3Kα110 subunit inhibitor BYL-719 (PI3Ki) did not prevent IFNγ induced PD-L1 upregulation: Cells were either treated with vehicle control, PI3Ki (5uM), IFNγ (10IU/mL) or the combination for 48h harvested and PD-L1 was determined by FC.

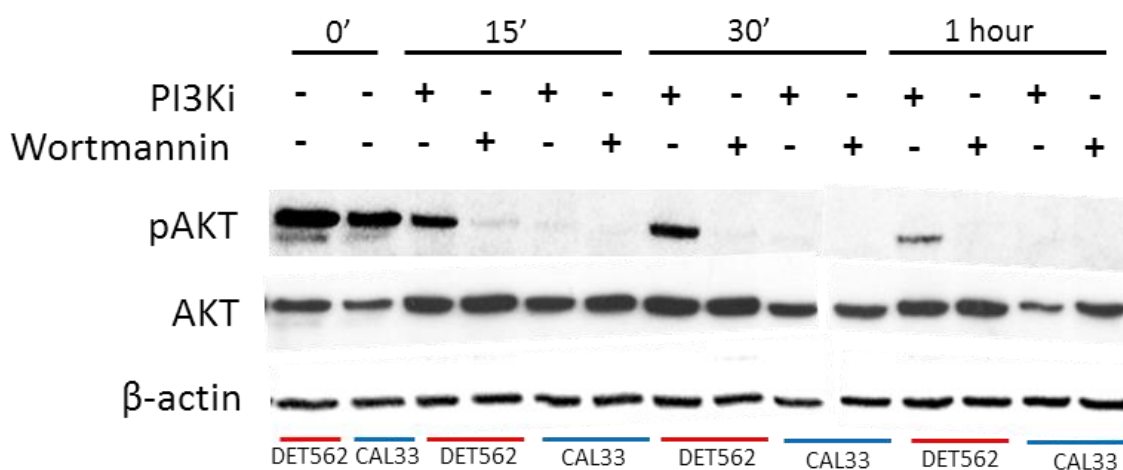


Figure 2.5.4 Wortmannin and PI3Ki (BYL-719) effectively inhibit AKT phosphorylation: DET652 and CAL33 cell lines were either left untreated or treated with Wortmannin (1uM) or PI3Ki (5uM) for 15, 30 minutes and 1 hour. Cells were harvested and pAKT, total AKT and beta actin were determined by WB. Note that Wortmannin and PI3Ki effectively inhibit AKT phosphorylation in both HNC cell lines.

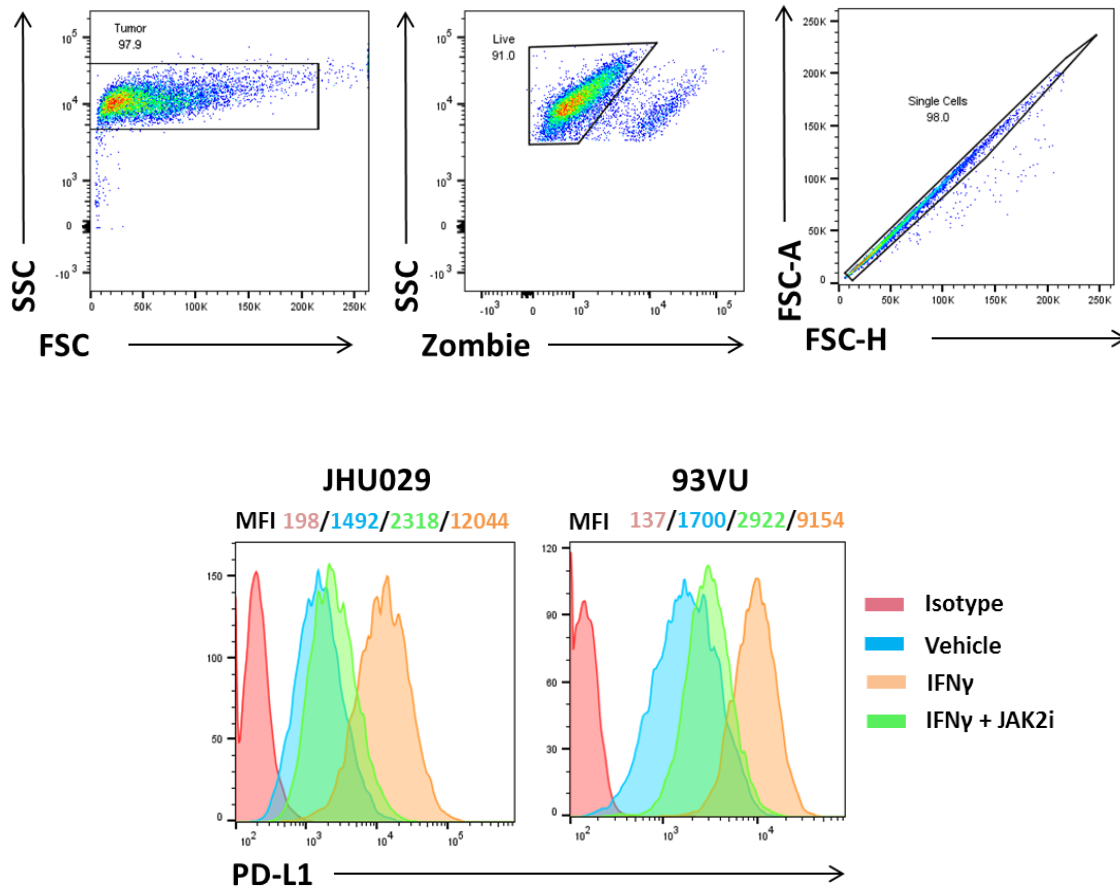


Figure 2.5.5 Flow cytometry gating strategy and representative histograms: Top. Flow cytometry gating strategy used in all PD-L1 determinations in this report. Tumor cells were collected according to size and granularity (FSC vs. SSC), then Zombie aqua negative cells were gated in (as described in Material and Methods) and finally duplets were gated out. **Bottom.** Representative histograms of HNC cell lines showing color-coded MFI values of PD-L1 expression after IFN γ and JAK2i treatments.

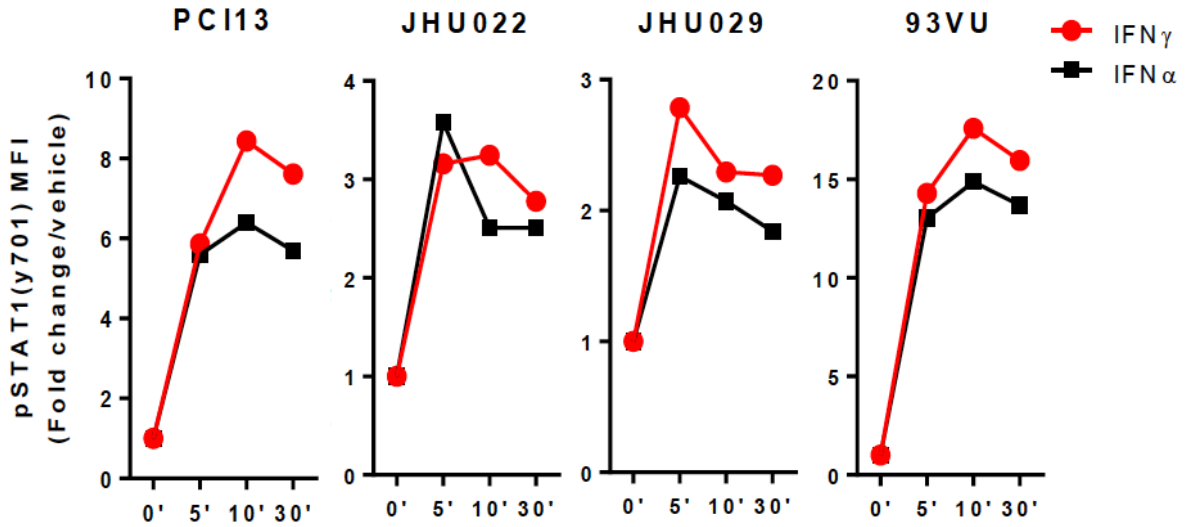


Figure 2.5.6 IFN α induces pSTAT1 upregulation: IFN α induced pSTAT1 upregulation although to a lower extent than IFN γ . HNC cells lines were treated with IFN α (1000IU/mL) or IFN γ (10IU/mL) for 0, 5, 10 or 30 minutes and pSTAT1 (Y701) was determined by intracellular flow cytometry.

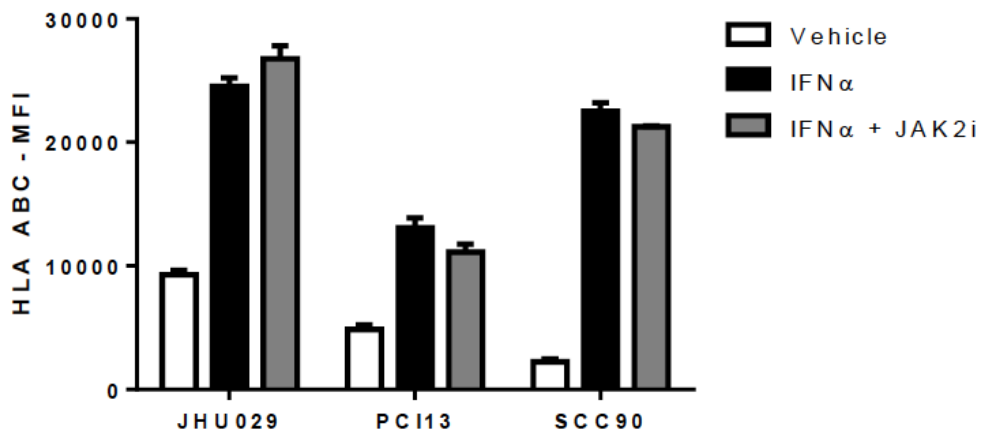


Figure 2.5.7 IFN α induces HLA-ABC upregulation, which is not downregulated by JAK2 inhibition: HNC cells were treated with IFN α 2a (1000IU/mL) or IFN α 2a (1000IU/mL) + JAK2i (10uM) for 48h and HLA-ABC was determined by FC.

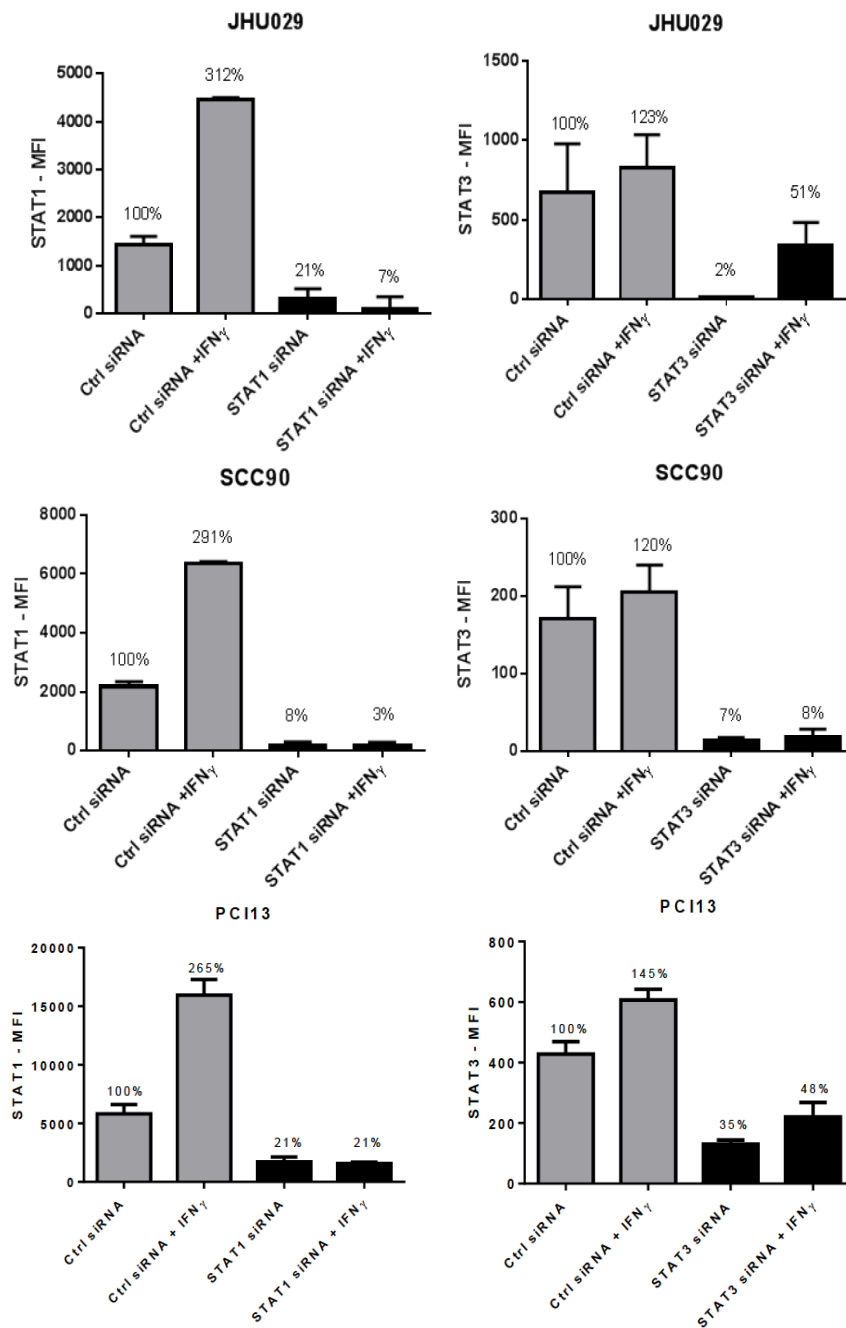


Figure 2.5.8 STAT1 and STAT3 siRNA knockdown efficiency: HNC cell lines were either treated with control siRNA, STAT1 or STAT3 siRNA (as indicated in Materials and Methods section). Cells were harvested, fixed and permeabilized and total STAT1 and STAT3 were determined by ICF (3 independent experiments). Percentages on top of bars represent percent of remaining STAT1/3 after knockdown compared to control siRNA (100%).

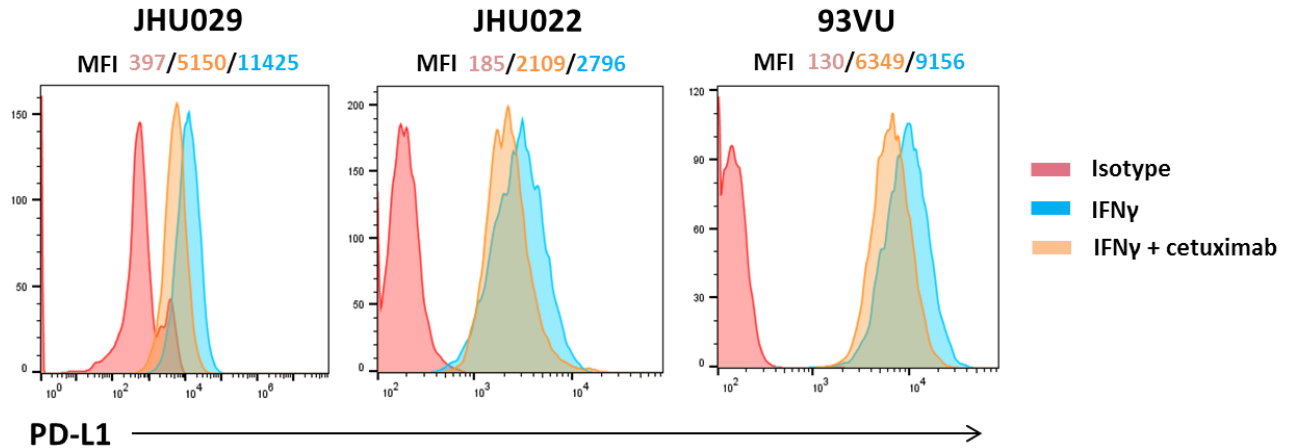


Figure 2.5.9 Cetuximab downregulates IFN γ mediated PD-L1 upregulation, representative histograms: Representative histograms of HNC cell lines showing color-coded MFI values of PD-L1 expression after IFN γ and cetuximab treatments.

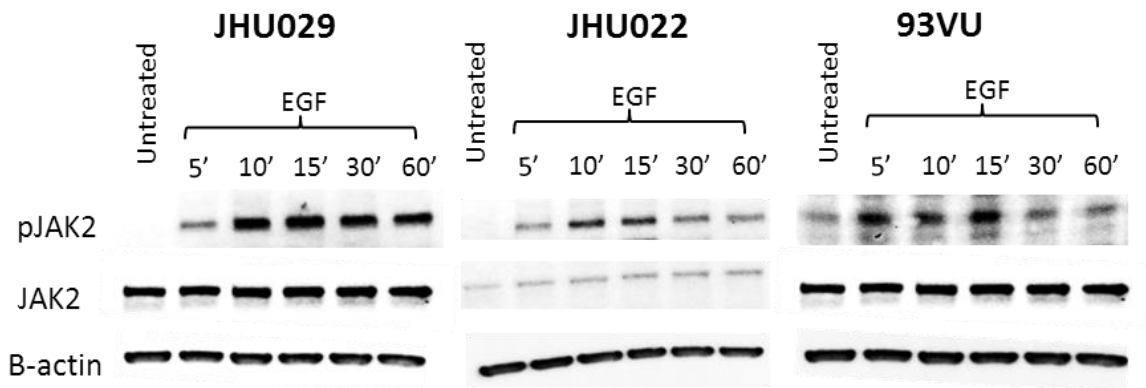


Figure 2.5.10 EGF induces JAK2 phosphorylation: EGF treatment (10ng/mL) induced upregulation of phospho-JAK2. HNC cell lines were serum starved for 18h and either left untreated or treated with EGF (10ng/mL) at different time points, harvested and pJAK2 (y1007/1008), total JAK2 and β -actin were determined by WB.

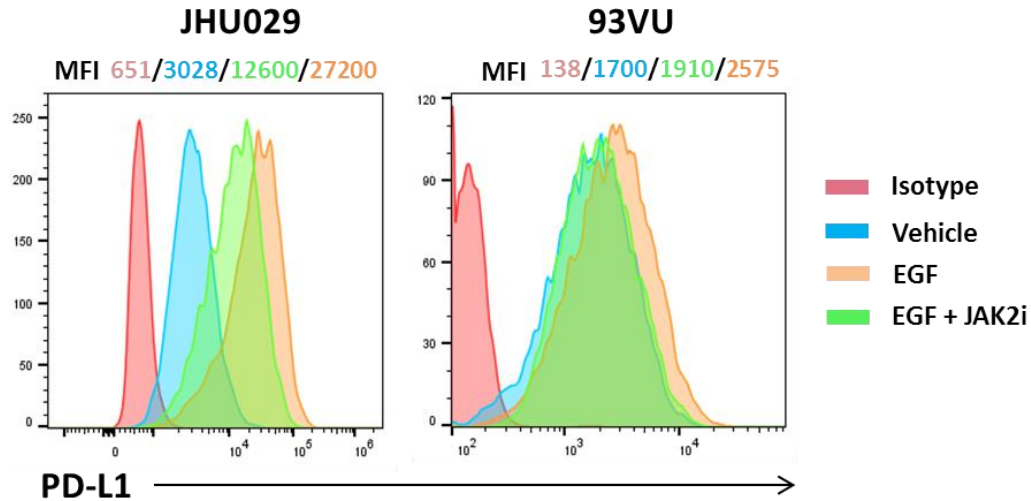


Figure 2.5.11 JAK2 inhibition prevents EGF mediated PD-L1 upregulation, representative histograms: Representative histograms of HNC cell lines showing color-coded MFI values of PD-L1 expression after EGF and JAK2i treatments.

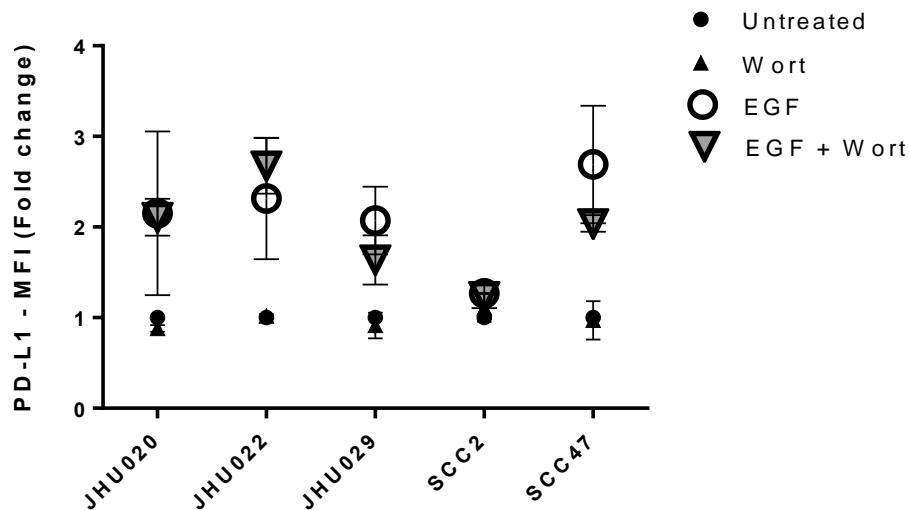


Figure 2.5.12 EGF-induced PD-L1 upregulation is not PI3K or MAPK dependent: Wortmannin (Wort), a pan PI3K inhibitor did not prevent EGF-mediated PD-L1 upregulation in all cell lines tested regardless HPV status. Cells were either treated with vehicle control, wortmannin (1uM), EGF (10ng/mL) or the combination for 48h, harvested and PD-L1 was determined by FC.

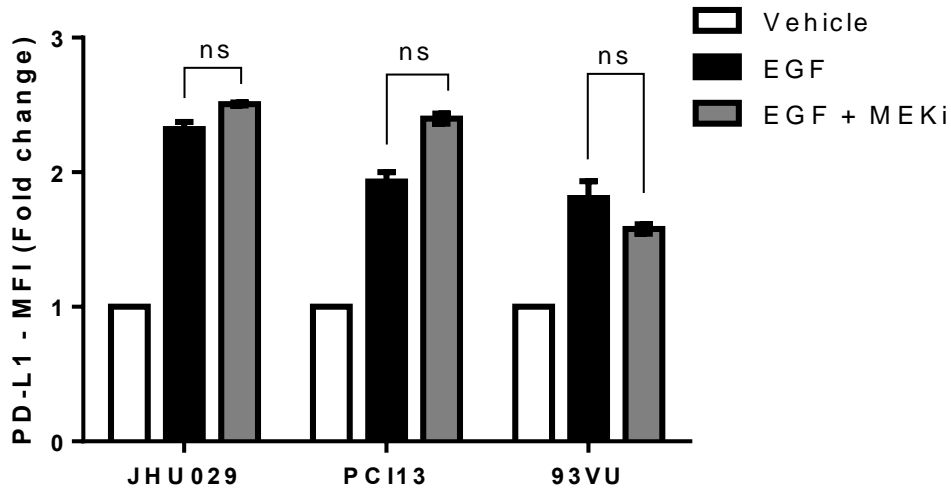


Figure 2.5.13 MEK1/2 inhibitor PD0325901 (MEKi) did not prevent EGF induced PD-L1 upregulation: MEK1/2 inhibitor PD0325901 (MEKi) did not prevent EGF induced PD-L1 upregulation. Cells were either treated with vehicle control, EGF (10ng/mL), MEKi (10nM) or the combination for 48h, harvested and PD-L1 was determined by FC.

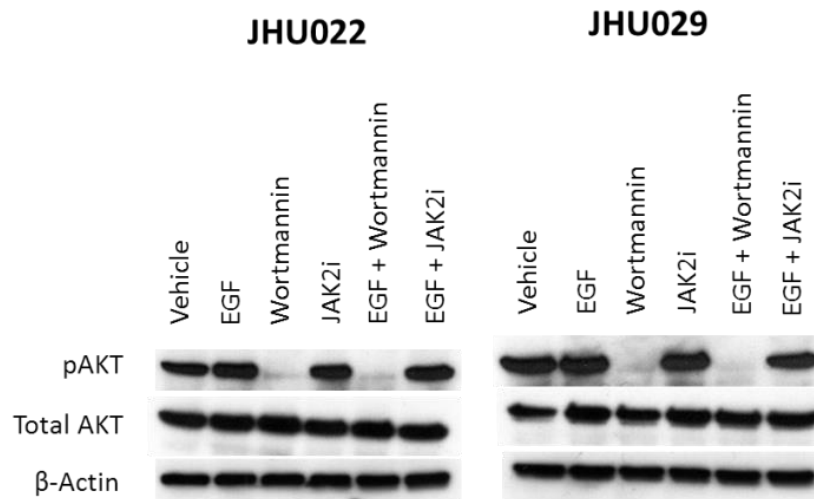


Figure 2.5.14 Wortmannin effectively prevented EGF mediated phosphorylation of AKT: Wortmannin effectively prevented EGF mediated phosphorylation of AKT. Cells were both treated with vehicle control, EGF (10ng/mL), wortmannin (1uM), JAK2i (10uM) or the respective combinations for 1 hour, harvested and pAKT, total AKT and β -actin were determined by WB.

3.0 EGFR AND JAK2 MEDIATED DOWNREGULATION OF IMMUNOSUPPRESSIVE CYTOKINE SECRETION IN HEAD AND NECK CANCER

3.1 INTRODUCTION

Head and neck cancer (HNC) accounts for more than 90% of the malignancies that arise in the head and neck (119). Unfortunately, despite standard chemo and radiotherapy, 50% of patients will succumb to this malignancy (120). EGFR is overexpressed in 92% of head and neck squamous cell carcinomas (121) and corresponds to a decrease in patient survival (122). EGFR activates many downstream signaling cascades including JAK/STAT, phosphatidylinositol 3-kinase (PI3K)/AKT and Ras/mitogen-activated protein (MAP) kinase pathways leading to cell proliferation, survival and invasion (123). Tumor cells overexpress both the receptor and ligand, leading to an uncontrolled autocrine activation of EGFR oncogenic signaling pathways (124). Importantly, EGFR activation in turn induces the constitutive activation of signal transducer and activator of transcription 3 (STAT3), a known oncogenic transcription factor (125-127). STAT3 plays a major role in promoting tumor immune evasion, previous work showed that it not only inhibits production of inflammatory signals from tumor cells but also production of immunosuppressive mediators, thus inducing a tolerant tumor microenvironment (194, 195).

HNC exhibits a constitutively active STAT3 that blocks apoptosis, favors proliferation, angiogenesis and immune evasion (128, 129). STAT3 is considered an oncogene, its inhibition leads to apoptosis *in vitro* and to impairment of tumor growth in xenografted mouse models (130, 131). Previous studies showed that STAT3 mediates the expression of vascular endothelial growth factor (VEGF), IL-6 and IL-10 in many cancer types. IL-6, IL-10 and VEGF are known to activate STAT3 in tumor-associated suppressive immune cells, providing a feed forward

mechanism to ensure a STAT3-dominated microenvironment. Tumor-secreted VEGF and IL-10 induce T cell tolerance through inhibition of DC differentiation and maturation (196, 197). Moreover, blocking STAT3 in macrophages restored T cell responsiveness by inducing secretion of IL-12 and CCL5. Likewise, IL-10 induces immunosuppression by protecting tumor cells from CTL lysis by downregulation of APM components (TAP1, TAP2) and surface HLA class I (198, 199). Transforming growth factor beta (TGF β), a known immunosuppressive cytokine, is found to be present at high concentrations in plasma of cancer patients and is associated with disease progression and poor response to immunotherapy. TGF β is produced by many tumor types including melanoma, breast and colon cancer and its known to prevent proper CTL generation and function (200), however its production by HNC cells is still not well characterized. Interestingly, TGF β and IL-10 are involved in the generation of regulatory T cells (Treg) that are known to inhibit CD8⁺ T cell activation, IFN γ production and proliferation (201). Additionally, Tregs can secrete TGF β and IL-10 in a STAT3-dependent fashion, further propagating the immunosuppressive signals (202, 203). The intricate tumor microenvironment cellular network also includes tumor-associated macrophages (TAM), which are induced by monocyte exposure to tumor-secreted IL-6, IL-10 and VEGF (204). TAMs suppress DC maturation in an IL-10 dependent manner that in turn inhibits CD8⁺ T cell proliferation and function (205, 206). TAM-derived IL-10 can also induce differentiation of naive T cells into Tregs (203).

Cetuximab, an EGFR-specific mAb, not only interferes with ligand binding and receptor dimerization, limiting EGFR signaling and STAT3 activation (136). However, resistance to cetuximab has been observed, this phenomenon most likely occurs via EGFR-independent STAT3 activation. Notably, the IL-6 receptor (IL-6R)/CD130 signaling complex has been shown to be a major pathway involved in EGFR-independent STAT3 activation and tumorigenesis

(207-209) and is further correlated with poor survival in HNC patients (210). Therefore, the expected cetuximab-mediated growth inhibition of HNC implemented by blocking EGFR-dependent signals would be negated by STAT3 constitutive activation through alternative pathways, particularly the IL-6R. Given that JAK2 is common signaling molecule to both EGFR and IL-6R pathways we hypothesized that combined EGFR and JAK2 inhibition may downregulate STAT3-dependent production of immunosuppressive cytokines revising signal 3 mediated tumor immunoescape.

3.2 MATERIALS AND METHODS

3.2.1 Patient plasma specimens collection and storage

All patients signed an informed consent approved by the Institutional Review Board (IRB #99-06). Peripheral venous blood samples were obtained from HNC patients with stage III/IVA disease, receiving neoadjuvant cetuximab on a prospective phase II clinical trial (UPCI 08-013, NCT 01218048), plasma was isolated and stored in -80C the same day the blood specimen was drawn. Tumors were biopsied immediately before, and again after 4 weeks of cetuximab therapy. Clinical response was analyzed by comparing paired CT scans pre/post-cetuximab, and quantifying tumor measurement by a dedicated head and neck radiologist blinded to patient status. Anatomic tumor measurements were recorded in two dimensions and the cohort segregated into clinical “responders,” who showed a reduction in tumor volume, or “nonresponders,” whose tumors grew during this therapy. Tumor biopsies (pre-treatment) or surgical tumor specimens (post-treatment) were preserved for a maximum of 12 hours in complete media until tumor infiltrating lymphocytes were isolated.

3.2.2 Tumor cells and treatments

HNC cell lines used in this report: JHU022, JHU029, SCC90 and 93VU. JHU022, JHU029 were a kind gift from Dr. James Rocco (Harvard Medical School, Boston, MA) in January of 2006. SCC90 were isolated from patients treated at the University of Pittsburgh Cancer Institute (Pittsburgh, PA) through the explant/culture method, authenticated, and validated as unique using STTR profiling and HLA genotyping every 6 months. 93-VU-147 T (called 93VU in this report) was a kind gift from Dr. Henning Bier (Technische Universitat Munchen, Munich, Germany) in October of 2013. All cell lines were routinely tested every 6 months and found to be free of *Mycoplasma* infection and were cultured in IMDM (Invitrogen, Carlsbad, CA) supplemented with 10% FBS (Mediatech, Herndon, VA), 2% L-glutamine and 1% penicillin/streptomycin (Invitrogen Corp, Carlsbad, CA). For treatment with rhEGF or JAK2 inhibitor, cells were cultured overnight in serum free AIM-V media (Invitrogen, Carlsbad, CA) and rhEGF (10ng/mL) or JAK2 inhibitor (10uM) treatment was started when cells reached at least 20% confluence. Adherent tumor cells were detached by warm trypsin–EDTA (0.25%) solution (Invitrogen, Carlsbad, CA) incubated for 5 min at 37. Surface or intracellular protein expression was determined by flow cytometry.

3.2.3 Antibodies and other reagents

Total STAT3 and phosphorylated STAT3 antibodies were purchased from BD Biosciences (San Jose, CA). APC conjugated TGFbeta-LAP antibody was purchased from Biolegend. rhEGF was purchased from R&D systems, reconstituted in PBS containing 0.1% BSA and used at a final concentration of 10ng/mL. The specific JAK2 inhibitor BMS-911543 (was characterized previously (171) and kindly provided by Bristol-Myers Squibb.

3.2.4 ELISA

Human TGF beta and soluble PD-L1 ELISA kits were purchased from R&D systems (Minneapolis, MN) and used according manufacturer protocol. Samples of frozen tumor cell culture supernatants or human plasma were thawed at room temperature for 15 minutes before starting the protocol. Results were normalized to cell counts on each experimental condition and expressed as pg per 500 000 cells.

3.2.5 Flow cytometry analysis

Surface flow cytometry was performed as follows, cells were harvested and resuspended in PBS containing a 1:50 dilution of a previously validated viability dye Zombie Aqua (174), following the manufacturer's protocol (Biolegend, San Diego, CA), then resuspended in 50uL of fluorescence-activated cell sorting (FACS) buffer and fluorophore conjugated antibodies were added at 1:10 dilution, incubated for 15 minutes at 4 Celsius, then antibodies were washed away twice by sequential centrifugation at 1400 RPM with FACS buffer and resuspended in 2% PFA solution until analyzed in the flow cytometer. Intracellular flow cytometry was performed as described (175). Briefly, cells were fixed using 1.5% for 15 min at room temperature (RT) and permeabilized with ice cold 100% methanol for 10 minutes at 4 Celsius and kept for 18h at -20 Celsius. Cells were then washed in FACS buffer and stained either with a fluorophore-conjugated primary STAT3 pSTAT3 or pJAK2 mAb, cells were then incubated for 45 min at RT, washed and resuspended in FACS buffer. When using an unconjugated primary antibody cells were stained with a secondary PE-conjugated antibody for additional 45 minutes and then washed as previously described.

Isotype control antibody staining was added for each condition and each mAb used for targeted markers, samples were collected and analyzed in an LSR Fortessa cytometer (BD Biosciences). A minimum of 10,000 cells was collected per test. Data analysis was performed using FlowJo version 10 (FlowJo, Ashland, OR). All surface and intracellular markers in this study were calculated as median fluorescence intensity (MFI) fold change and normalized with either untreated or vehicle control after subtracting the isotype control (MFI) of each sample. Each experiment was repeated at least three times and mean and standard error of the mean (SEM) was calculated and plotted using GraphPad PRISM software version 6.

3.2.6 Luminex assay

Human plasma samples and frozen tumor cell culture supernatants were assayed for cytokines by fluorescent bead Luminex assay 29-plex (Millipore) following the manufacturer protocol and as previously validated (211) by the Luminex core facility at the University of Pittsburgh Cancer Institute.

3.2.7 TCGA database analysis

TCGA data for HNC gene expression by RNAseq were downloaded from the UCSC cancer genomics browser (<https://genome-cancer.ucsc.edu>). The HNC gene expression profile was measured experimentally using the Illumina HiSeq 2000 RNA Sequencing platform. This dataset shows the gene-level transcription estimates, as in RSEM normalized count, percentile ranked within each sample. The RSEM units to quantitate RNAseq expression data were described and validated previously (179).

3.3 RESULTS

3.3.1 HNC tumors have higher expression of signature immunosuppressive cytokines than control tissues

In order to investigate whether HNC tumors expressed higher immunosuppressive cytokines, we took advantage of the large curated database of The Cancer Genome Atlas (TCGA) (178) and compared mRNA expression of the signature immunosuppressive cytokines TGF β , VEGFA, IL-10 and IDO from HNC tumor specimens (n=500) and normal mucosa. Likewise, we analyzed interferon- γ (IFNG) expression in both cohorts and considered including it as part of immunosuppressive cytokine group since we previously demonstrated that it induces PD-L1 upregulation, a known checkpoint inhibitor ligand that induces immune escape of HNC tumors (Chapter 2) (212). We observed that tumors from HNC patients had higher expression of signature immunosuppressive cytokines such as TGF β , VEGFA, IL-10 and IDO (Figure 3.3.1A-D). We also found that interferon- γ expression was upregulated in tumor tissues when compared with healthy mucosa (Figure 3.3.1E) corroborating our previous observations and providing more evidence supporting the IFN γ -PD-L1 immunosuppressive axis inducing tumor immunoescape. Overall, these results indicate that the tumor microenvironment of HNC patients is highly immunosuppressive and may induce and fuel the tolerant tumor cellular immune infiltrate preventing the onset of an efficient effector cell activation and antitumor immune response.

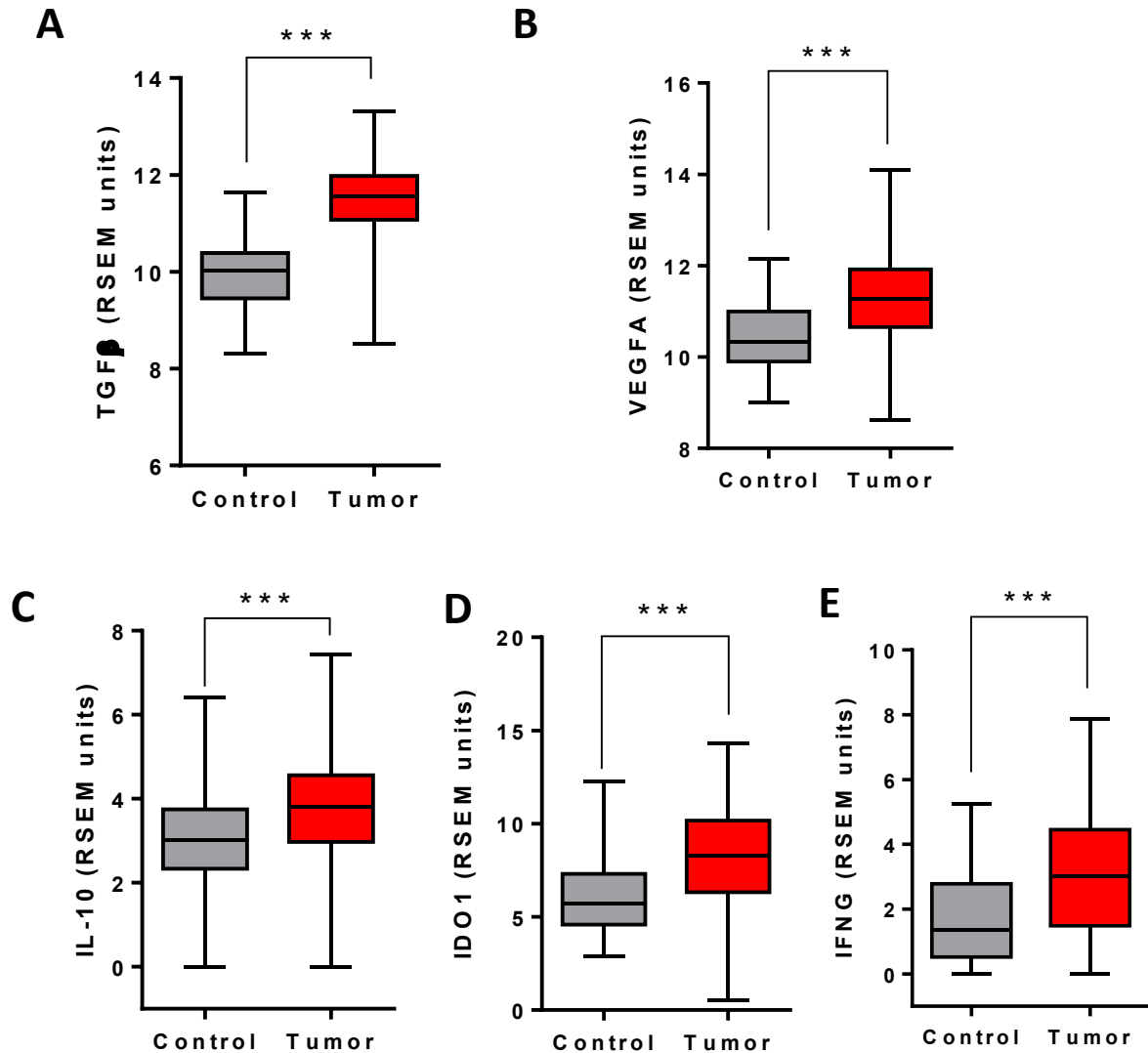


Figure 3.3.1 HNC tumor specimens have significantly higher expression of immunosuppressive cytokines than control tissues: A. TGFβ. B. VEGFA. C. IL-10. D. IDO. E. IFNγ. Cytokine mRNA expression (RSEM units, TCGA) is significantly higher in HNC tumor specimens than in normal control tissues. TCGA mRNA expression data from 500 HNC specimens and 43 control specimens. (Box and whiskers plots, bars represent maximum and minimum values, Kruskal-Wallis test *** P<0.001).

3.3.2 HNC tumors have lower expression of immunostimulatory cytokines than control mucosa

In order to further characterize the immunosuppressive milieu of the tumor microenvironment we analyzed the expression level of known immunostimulatory cytokines such as IL-12, IL-17 and IL-23 taking advantage of TCGA mRNA database. Herein we show that HNC specimens had significantly lower expression of IL-12A and IL-17A –but not IL-23A- when compared to healthy control mucosa (Figure 3.3.2A-B, n=500, Kruskal-Wallis test * $P < 0.05$, *** $P < 0.001$). Further supporting our view that HNC tumors are not only highly expressers of signature immunosuppressive cytokines but also lacking the expression of immunostimulatory ones, reflecting the tolerant milieu to which effector immune infiltrates are exposed to when reaching the tumor bed.

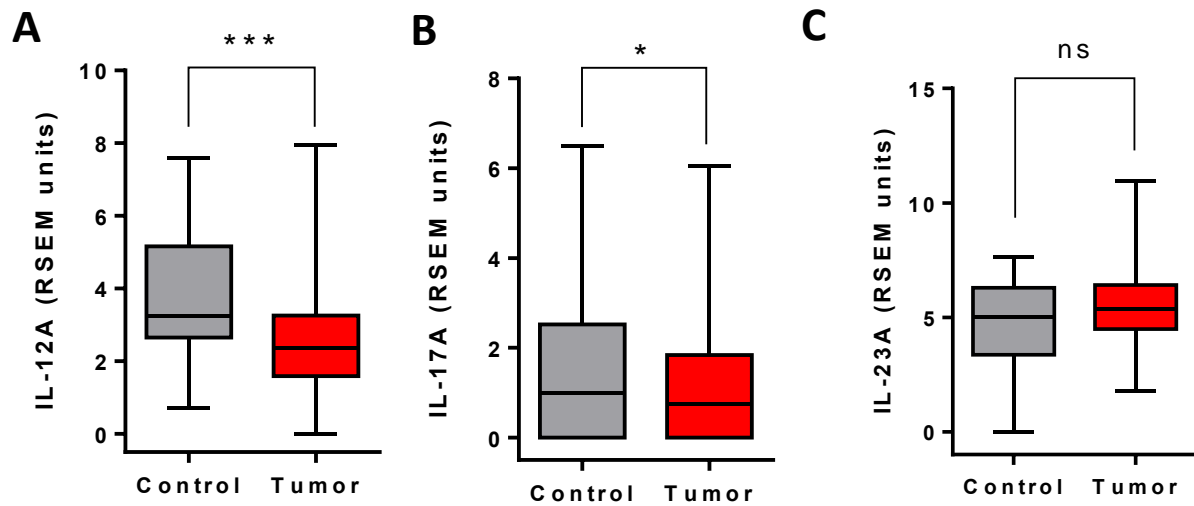


Figure 3.3.2 HNC tumor specimens have significantly lower expression of immunostimulatory cytokines than control tissues: A. IL-12A. B. IL-17A. C. IL-23A Cytokine mRNA expression (RSEM units, TCGA) is significantly lower in HNC tumor specimens than in normal control tissues. TCGA mRNA expression data from 43 HNC specimens. (Box and whiskers plots, bars represent maximum and minimum values, Kruskal-Wallis test * $P < 0.05$, *** $P < 0.001$, ns: non-significant).

3.3.3 EGFR and JAK2 inhibition downregulate STAT3 activation in tumor cells

Previous reports showed that EGFR signaling activates STAT3 and oncogenic transformation of HNC cells (126). In addition to the EGFR pathway some other STAT3 activating EGFR-independent pathways may exist. In fact a previous report showed that IL-6R is widely expressed in HNC cells and constitutes a strong stimulus for STAT3 activation via JAK2 activation (207). Therefore, inhibiting STAT3 activation not only targeting EGFR but also other STAT3 activating pathways such as the IL-6R, which shares JAK2 in their signaling pathway, may reverse the immunosuppressive phenotype of cancer cells. We found that specific EGFR and JAK2 inhibition effectively downregulated JAK2 phosphorylation and STAT3 phosphorylation in HNC cells (Figure 3.3.3A-C, ANOVA ** $P < 0.01$).

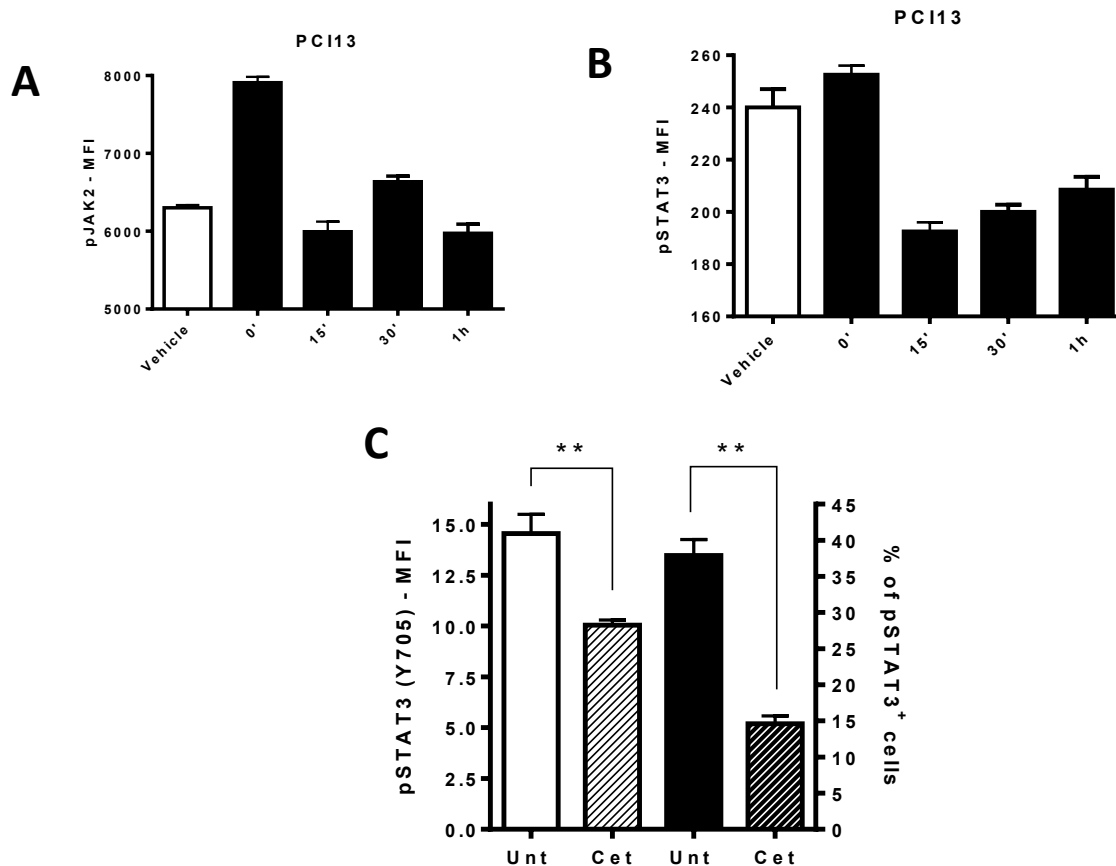
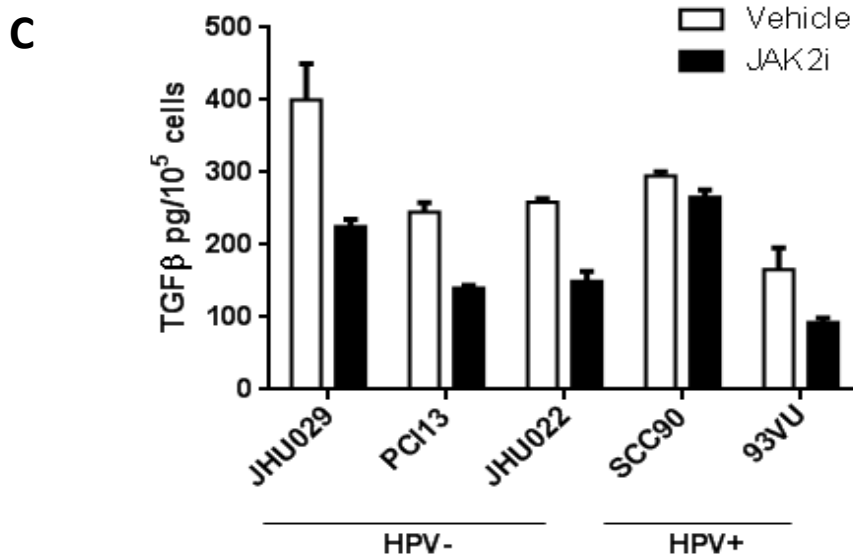
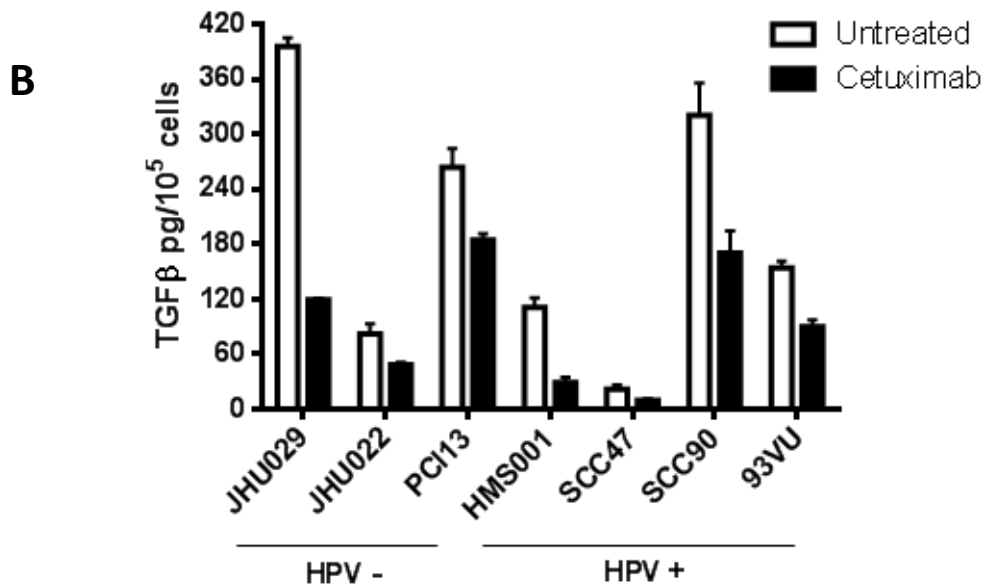
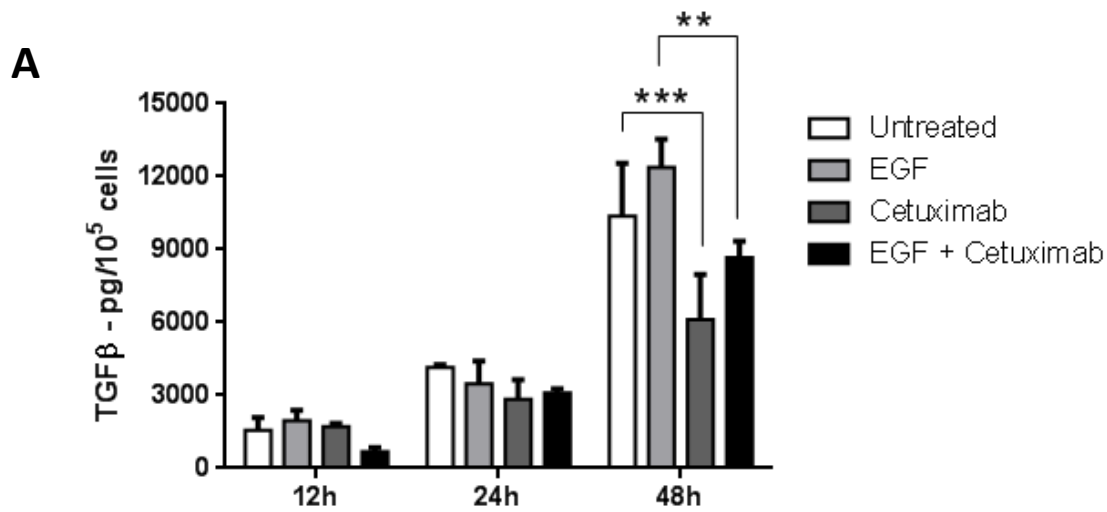


Figure 3.3.3 EGFR and JAK2 inhibition downregulate STAT3 activation in HNC cells: Tumor cells were cultured with JAK2i for different time points or vehicle control for 1 hour, harvested and **A.** pJAK2 and **B.** pSTAT3 were detected by intracellular flow cytometry. **C.** Cells were treated with cetuximab (10ug/mL) for 24h and pSTAT3(Y705) MFI and % of positive cells were detected by intracellular flow cytometry. (ANOVA ** P <0.01).

3.3.4 EGFR and JAK2 inhibition downregulate production of TGFβ and other signature immunosuppressive cytokines in tumor cells

Since EGFR and JAK2 inhibition downregulated STAT3 activation, we next investigated whether they could also downregulate production of STAT3-dependent immunosuppressive cytokines in HNC cells. We found that cetuximab downregulated TGFβ production, having its maximum inhibitory effect at 48h (Figure 3.3.4A, ANOVA ** P <0.01, *** P<0.001).

Moreover, cetuximab mediated TGF β downregulation was seen in all cell lines tested regardless HPV status (Figure 3.3.4B). Likewise, JAK2 inhibition downregulated TGF β production in HNC cell lines regardless HPV status under the conditions tested (10uM, 48h) (Figure 3.3.4C). Additionally, we observed that both EGFR and JAK2 inhibition downregulated other signature immunosuppressive cytokines such as VEGF, IL-6 and chemokines CCL22 and CCL2. Interestingly, EGFR and JAK2 inhibition showed an additive effect downregulating IL-6 secretion, not seen for other cytokines tested (Figure 3.3.4D, ANOVA ** P <0.01, *** P<0.001). Overall, these results indicate that EGFR and JAK2 inhibition significantly diminish tumor cell secretion of signature immunosuppressive cytokines and chemokines *in vitro*.



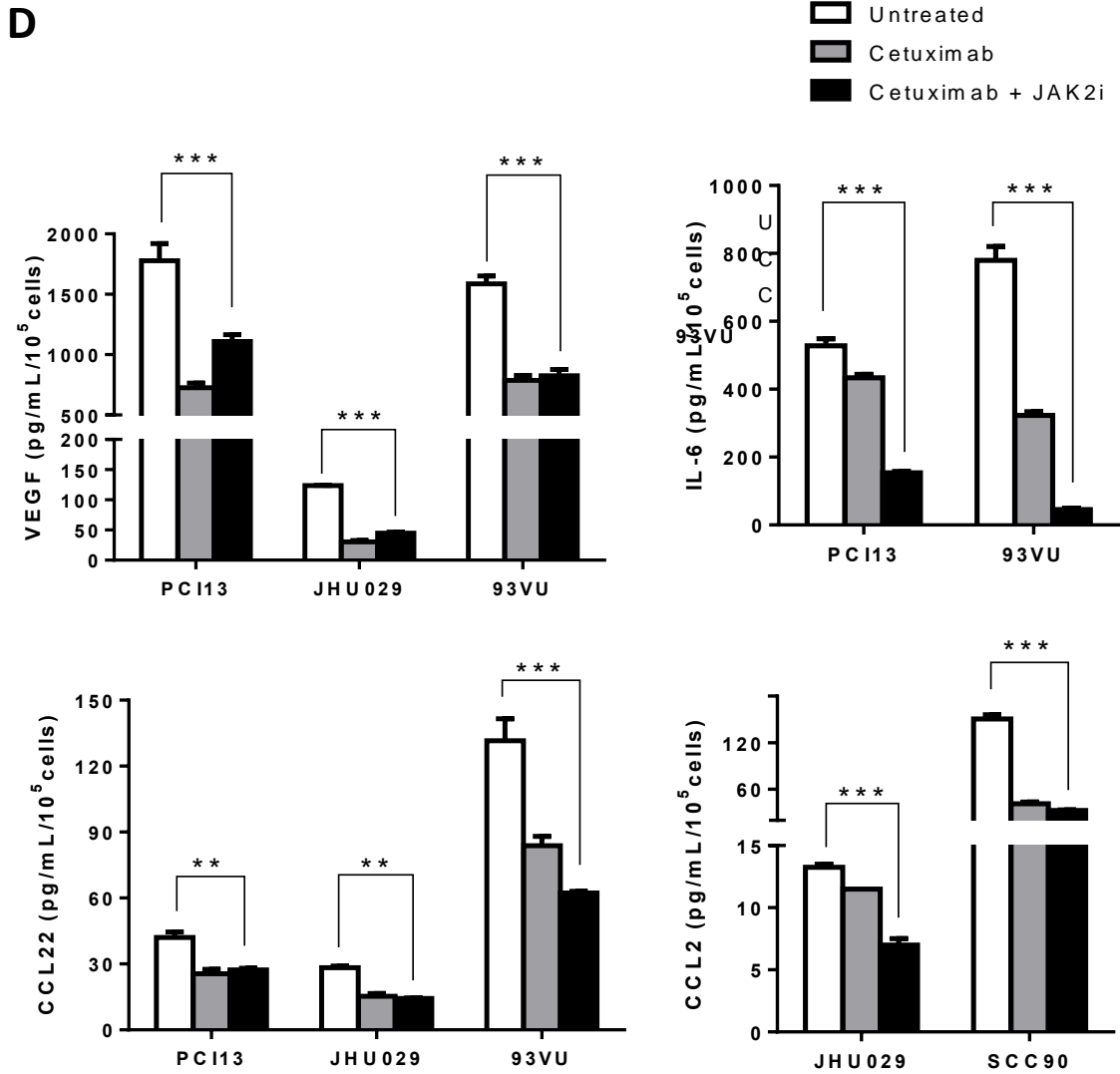


Figure 3.3.4 EGFR and JAK2 inhibition downregulate production of TGFβ and other signature immunosuppressive cytokines in tumor cells: **A.** Tumor cells were cultured with cetuximab (10ug/mL) for 24h, Golgi stop was added in the last 6h of culture and TGFβ-LAP expression was determined by intracellular flow cytometry. **B.** Cells were either left untreated or cultured for 12, 24 or 48h with EGF (10ng/mL), cetuximab (10ug/mL) or the combination, supernatants were harvested and TGFβ was determined by ELISA. Likewise cells were either left untreated or incubated with **C.** cetuximab (10ug/mL) or **D.** JAK2i (10uM) for 48h, supernatants were harvested and assayed for TGFβ by ELISA. **E.** Cells were either untreated or cultured for 48h with cetuximab (10ug/mL), JAK2i (10uM) or the combination, then supernatants were harvested and VEGF, IL-6, CCL22 and CCL2 were determined by Luminex.

3.3.5 EGFR and JAK2 inhibition diminish secretion of soluble PD-L1

As described in chapter 2, EGFR and JAK2 inhibition downregulated membrane bound PD-L1 expression in tumor cells. However, many studies have recently reported a soluble form of PD-L1 (sPD-L1). Circulating sPD-L1 was found in peripheral blood from gastric, lung and lymphoma patients (213-215). Furthermore, a previous study also showed that supernatants of lung cancer cells had detectable concentrations of sPD-L1 and it mediated inactivation of tumor-antigen specific T cells (213). We found that sPD-L1 is present in supernatants of HNC cells and its concentration was downregulated by EGFR and JAK2 inhibition in all cell lines tested (Figure 3.3.5A, ANOVA * $P < 0.05$, ** $P < 0.01$, *** $P < 0.001$). Thus, these results show that the EGFR/JAK2 pathway may mediate not only expression of membrane bound PD-L1 but also soluble PD-L1.

A

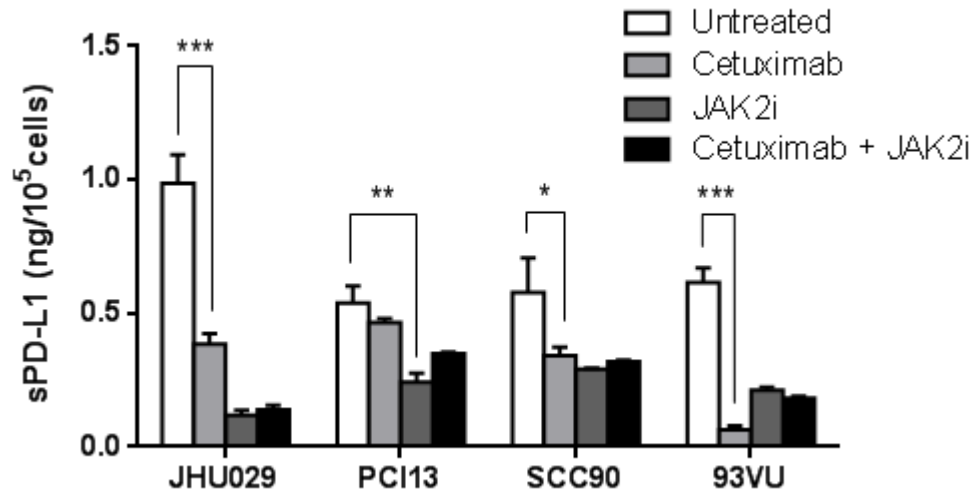


Figure 3.3.5 EGFR and JAK2 inhibition downregulate soluble PD-L1: A. Cells were either left untreated or cultured with cetuximab (10ug/mL) JAK2i (10uM) or the combination for 48h, supernatants were harvested and soluble PD-L1 was determined by ELISA.

3.3.6 Cetuximab resistant HNC patients have significantly lower concentrations of Th1 cytokines in plasma

In order to corroborate our TCGA and *in vitro* findings we determined the concentration of signature immunostimulatory cytokines in plasma obtained from advanced HNC patients that were treated with cetuximab on a prospective neoadjuvant trial (UPCI #08-013, NCT #01218048), peripheral blood was collected prior to and after 4 weeks of cetuximab therapy, plasma was isolated from samples from these patients pre- and post-cetuximab single agent treatment and analyzed by Luminex (see materials and methods). Response to cetuximab therapy was evaluated radiologically pre and post 4 weeks of treatment and response criteria were categorized as follows: Complete Response: disappearance of all targets, PR: Partial Response: greater than 30% decrease, LPR: Less than Partial Response: 10-30% decrease, PD: Progressive

Disease: 20% increase, Stable: Response between 10% decrease and 20% increase. Interestingly, we found that patients who responded to cetuximab therapy (CR, PR and LPR) had higher concentrations of immunostimulatory cytokines such as IL-12p70, IL-17A and IFN γ . While, patients who were resistant to cetuximab therapy (S or PD) had significantly lower concentrations of IL-12p70, IL-17A and IFN α 2, the same trend was noted for IFN γ however sample size was not sufficient to reach significance (P=0.055). (Figure 3.3.6A, Mann-Whitney test * P<0.05, ** P<0.01). In addition to the cytokines mentioned, we also determined the concentration of other inflammatory cytokines such as IL-1 β and TNF α , however no difference between responders or non-responders was noted (data not shown).

A

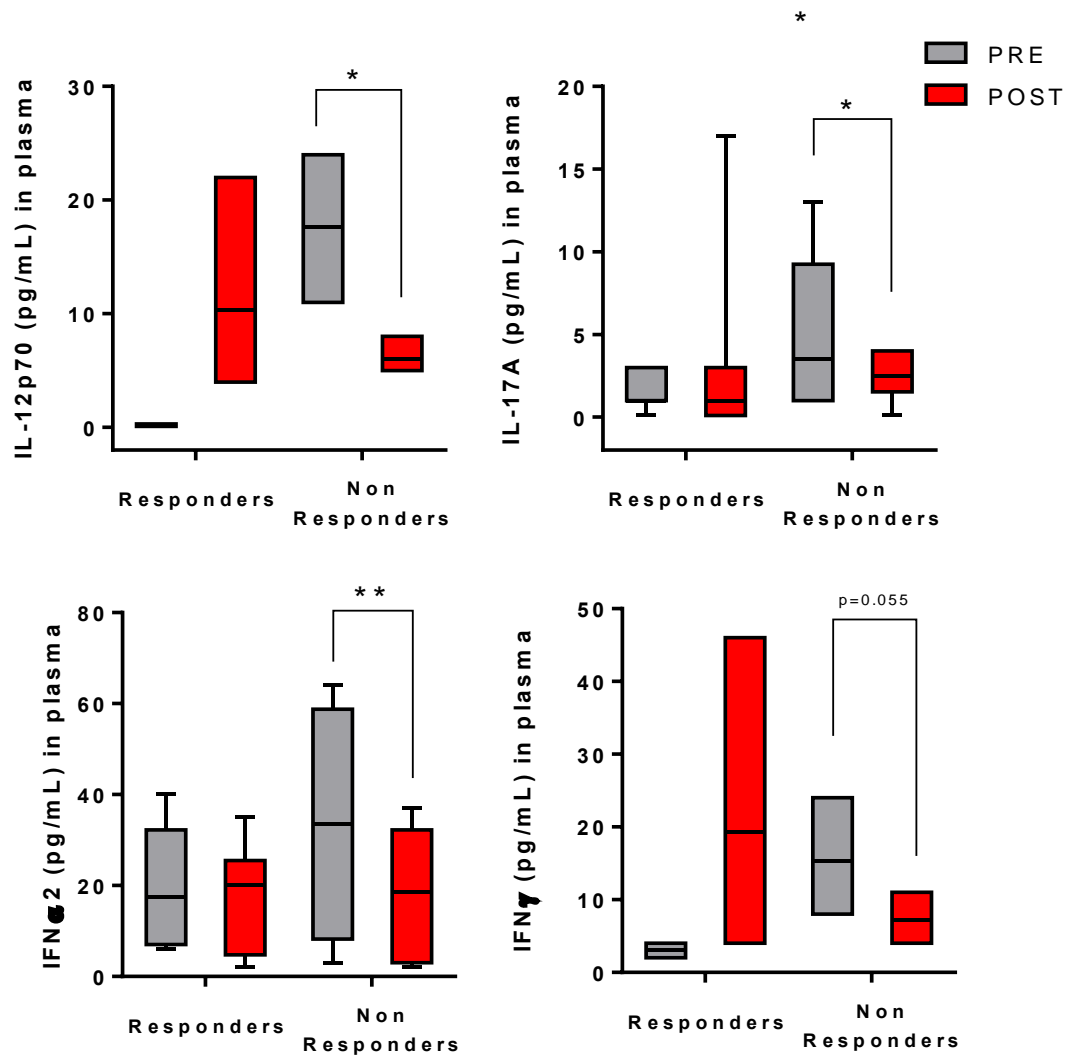


Figure 3.3.6 Cetuximab resistant HNC patients have significantly lower concentrations of Th1 cytokines in plasma than responders: A. Patient plasma specimens from cetuximab single agent clinical trial UPCI 08-013 were collected pre- and post- cetuximab administration and assayed for cytokine concentration by Luminex (Mann-Whitney * $P < 0.05$, ** $P < 0.01$). Response criteria: Complete Response: disappearance of all targets, PR: Partial Response: greater than 30% decrease, LPR: Less than Partial Response: 10-30% decrease, PD: Progressive Disease: 20% increase, Stable: Response between 10% decrease and 20% increase.

3.3.7 Cetuximab resistant patients have higher concentration of TGFβ in plasma

Likewise we determined TGFβ concentration in plasma from the same cohort of patients as in section 3.3.6. We found that patients who responded to cetuximab therapy showed no significant upregulation of TGFβ in plasma while those who were resistant to cetuximab therapy showed a significant increase (Figure 3.3.7A, Mann-Whitney test ns, non-significant, ** P<0.01).

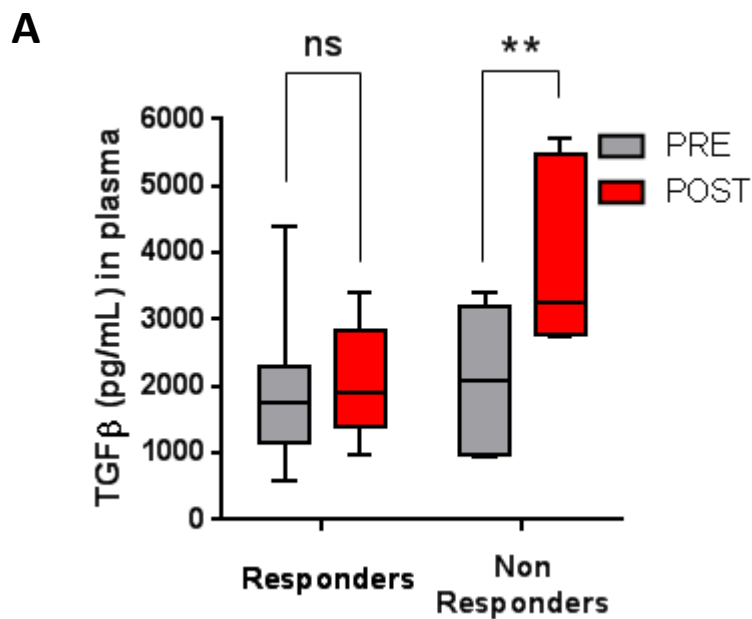


Figure 3.3.7 Cetuximab resistant HNC patients have significantly higher concentration of TGFβ in plasma: A. Patient plasma specimens from cetuximab single agent clinical trial UPCI 08-013 were collected pre- and post- cetuximab treatment and TGFβ was determined by ELISA. (Mann-Whitney ns; non-significant, ** P<0.01) Response criteria: Complete Response: disappearance of all targets, PR: Partial Response: greater than 30% decrease, LPR: Less than Partial Response: 10-30% decrease, PD: Progressive Disease: 20% increase, Stable: Response between 10% decrease and 20% increase.

3.4 DISCUSSION

Tumor cells evade immune recognition not only by providing an aberrant signal 1, represented by downregulation of APM components and HLA class I antigen presentation, or aberrant signal 2, characterized by upregulation of checkpoint ligands such as PD-L1, but also providing an aberrant signal 3, characterized by secreting immunosuppressive cytokines and chemokines that induce a tolerant microenvironment.

In the setting of HNC, overexpressed wild type EGFR induces not only proliferation, resistance to apoptosis and aberrant antigen processing and presentation of tumor cells but also upregulates immunosuppressive signal 2 as shown in chapter 2. Similarly, inhibiting EGFR mediated expression of suppressive cytokines becomes crucial in order to reverse immunoescape. Taking advantage of the large curated TCGA database we are the first to report that HNC tumor specimens have significantly higher expression of signature immunosuppressive cytokines such as TGF β , VEGFA, IL-10 and IDO when compared with normal mucosa (Figure 3.3.1). Furthermore, we also found higher expression IFN γ in tumor specimens than in control tissues, which confirms and further supports our view of an IFN γ /PD-L1 tumor-extrinsic immunosuppressive axis in HNC. In addition, expression of known immunostimulatory/inflammatory cytokines such as IL-12A or IL-17A was significantly lower in tumor specimens than control mucosa (Figure 3.3.2), further providing evidence of the dominant suppressive microenvironment in this type of cancer. Interestingly, previous studies have shown STAT3 as a major transcription factor inducing tumor immune evasion since it not only inhibits production of inflammatory signals from tumor cells but also production of immunosuppressive mediators (194, 195). Because STAT3 mediates the expression of VEGF, IL-6 and IL-10 which in turn activate STAT3 in tumor-associated suppressive immune

infiltrates, providing a feed forward mechanism to ensure a STAT3-dominated microenvironment, we hypothesized that preventing STAT3 activation not only by EGFR blockade but also JAK2 inhibition would downregulate production of STAT3-dependent cytokines. Herein, we show that cetuximab mediated EGFR blockade and specific JAK2 inhibition successfully downregulate STAT3 activation in HNC cells (Figure 3.3.3) and diminish production and secretion of TGF β , VEGF and IL-6 (Figure 3.3.4). Moreover, EGFR and JAK2 inhibition also downregulated production of CCL2 and CCL22, known chemokines that mediate tumor progression, angiogenesis and metastasis (216, 217) and attracts myeloid suppressor cells and regulatory T cells to the tumor microenvironment (218, 219), respectively (Figure 3.3.4D). Interestingly, combined EGR and JAK2 inhibition had an additive effect downregulating IL-6 secretion, further supporting our view that other EGFR-independent pathways, such as IL-6R/gp130 pathway, may play a major role in the synthesis and secretion of immunosuppressive cytokines in the tumor microenvironment. In this regard, further work has to be done in order to investigate the IL-6 effect in the production of these suppressive cytokines as compared to the EGFR pathway.

Our previous work showed that the EGFR/JAK2 pathway induces PD-L1 upregulation in HNC (212), interestingly, PD-L1 not only exists as membrane bound molecule but also as a soluble isoform. In fact, previous reports have shown that soluble PD-L1 (sPD-L1) is present in peripheral blood of gastric, lung and lymphoma patients. Moreover, the concentration detected in these patients was significantly higher than that of the control group, making it a suitable predictive biomarker for anti-PD-1 therapy. Interestingly, whether sPD-L1 is present in peripheral blood of HNC patients is still not known. However, in this study we show that HNC cells secrete sPD-L1 *in vitro* and that EGFR and JAK2 inhibition downregulates sPD-L1 in cell

culture supernatants. Therefore, JAK2 inhibition not only diminishes membrane bound but also secreted soluble PD-L1. This is particularly important, since a previous *in vitro* study in lung cancer cells showed that sPD-L1 actively suppresses T cell proliferation and activation *in vitro* (213). Thus, adding sPD-L1 to the long list of immunosuppressive soluble factors secreted by tumor cells that protect them from lysis.

In order to confirm our TCGA and *in vitro* findings we screened plasma specimens from advanced stage HNC patients that were treated with cetuximab single agent on a neoadjuvant trial (UPCI #08-013, NCT #01218048). We correlated cytokine concentration with clinical response to therapy (as described in section 3.3.5). We found that cetuximab-resistant patients had significantly lower plasma concentrations of Th1 inflammatory cytokines IL-12p70, IL-17 and IFN α 2, opposite to what was seen in cetuximab responders, however statistically non-significant due to the small sample size (Figure 3.3.6). These results most likely reflect that cetuximab mediated activation of effector cells, such as NK cells, triggers a Th1 antitumor response pattern that is clinically effective reducing tumor burden. Importantly, this view is further supported by our finding of a higher frequency of NK cells in peripheral blood of HNC patients than healthy controls that readily infiltrate tumors and get activated after cetuximab:CD16 interaction (See Chapter 4). Moreover, our previous findings where cetuximab reversed the suppressive activity of MDSC *in vitro* and diminished infiltration of granulocytic MDSC in the responder cohort of patients (220) further agree with a Th1 dominant microenvironment induced by cetuximab in those patients who respond to therapy. In addition to determining Th1 cytokines, we also determined TGF β in the same cohort of patients. As shown in figure 3.3.7, cetuximab-resistant patients had significantly higher concentration of TGF β in plasma while the responders had a non-significant change. It is well documented that TGF β is a

strong inducer of immunosuppression by inhibiting NK cytotoxicity, clonal expansion of CTLs and inducing the generation of Tregs. In fact, our findings of a higher TGF β concentration in cetuximab-resistant patients agrees with what our laboratory previously reported, where cetuximab-resistant HNC patients had higher frequencies of Tregs in peripheral blood and in the tumor bed (221).

Overall, our results show that tumors of HNC patients express a higher immunosuppressive cytokine profile including TGF β , IL-10, VEGFA and IDO than control tissues and lower expression of signature inflammatory cytokines such as IL-12A and IL-17A, confirming the view of a dominant immunosuppressive tumor microenvironment that prevents proper immune effector cell activation. We showed that EGFR and JAK2 inhibition effectively downregulate secretion of these immunosuppressive STAT3-dependent cytokines *in vitro*, providing evidence that supports reversing the EGFR/JAK2/STAT3 mediated suppressive pathway in order to enhance tumor lysis. Likewise, targeting not only membrane-bound PD-L1 expression but also sPD-L1 becomes important since HNC cells secrete this soluble immunosuppressive factor. Importantly EGFR and JAK2 inhibition downregulated sPD-L1 secretion further supporting its role reversing tumor-originated immunosuppressive signal 3. Finally, our findings are clinically relevant since HNC patients who are resistant to cetuximab therapy have significantly higher TGF β concentration and a lower immunostimulatory cytokine profile in plasma, which endorses the use of combined therapy in those patients where EGFR blockade is not sufficient to reverse production of immunosuppressive cytokines and chemokines that feed the tolerant cellular network in the tumor microenvironment.

4.0 DISRUPTION OF THE PD-L1/PD-1 AXIS INTERACTION BY JAK2 INHIBITION AND/OR anti-PD-1 mAb BLOCKADE ENHANCES CETUXIMAB MEDIATED NK CELL CYTOTOXICITY IN HEAD AND NECK CANCER

4.1 INTRODUCTION

Immune checkpoint receptors have recently become important targets for cancer immunotherapy. PD-1, an activation marker as well as an immunoinhibitory receptor in the CD28 superfamily, is expressed by several immune subsets including activated CD8⁺ T cells, B cells, NK cells and dendritic cells (DC) in the tumor microenvironment (222, 223), and plays an important role in tumor immunoescape after binding its cognate ligands programmed death ligand 1 or 2 (PD-L1 or PD-L2) (95-97, 224). Blocking the PD-L1/PD-1 axis restores T cell responses and improves clinical outcome in several types of cancer (225, 226). In the setting of head and neck cancer, we previously documented that 50%-70% of tumors express PD-L1 (212) and a high frequency of PD-1 expressing tumor infiltrating T cells (165, 183, 227, 228). Therefore, blocking the PD-L1/PD-1 axis becomes crucial in order to reverse tumor immunoescape.

In chapter 2 we provide evidence that PD-L1 expression in tumor cells is regulated by two major mechanisms. First, an “extrinsic” mechanism where tumor immune infiltrates driven by NK and CD8⁺ T lymphocytes produce IFN γ , which in turn may induce PD-L1 expression on tumor cells. And second, an “intrinsic” mechanism in which constitutive EGFR oncogenic signaling leads to PD-L1 overexpression. Since these extrinsic and intrinsic mechanisms have JAK2 as common signaling relay molecule we hypothesized that JAK2 inhibition on tumor cells may enhance EGFR-specific mAb cetuximab mediated NK cytotoxicity given that PD-L1/PD-1

axis suppression would be reversed by JAK2 inhibition. Furthermore, an equally interesting question is to which extent PD-1, the PD-L1 receptor, is expressed on NK cells and whether its blockade, using PD-1-specific FDA-approved mAb nivolumab, reverses PD-L1/PD-1 mediated NK cell exhaustion/suppression. These findings have particular relevance given the clinical utility of cetuximab, which can both block EGFR signaling and stimulate IFN γ secretion via activation of NK and CTL (100-102).

Interestingly, whether PD-1 is a marker of activation versus exhaustion is still controversial and may differ among various lymphocyte subsets. Indeed, PD-1 expression has been suggested as marker of activated effector T cells (89, 229). Importantly, these data are in concordance with our previous findings where PD-1⁺ TIL co-expressed the Th1 transcription factors STAT1 and T-bet, and cytokines such as IFN γ and IL-12 after CD3/CD28 stimulation (102). While PD-L1/PD-1 axis disruption is important in the clinic and PD-1 expression has been largely characterized in tumor infiltrating T cells, little is known about its expression and function on NK cells despite their importance in bridging innate and adaptive immunity and mediating monoclonal antibody (mAb) specific responses. NK cells are an important subset of innate immune system cells that constitute the first line of defense against pathogens and play a crucial role in immunosurveillance in the tumor microenvironment (230). NK cells mediate cytotoxicity via several distinct mechanisms, being antibody dependent cellular cytotoxicity (ADCC) one of the most studied in the setting of cancer given their availability to bind tumor antigen (TA) specific mAbs and induce objective antitumor responses and increased survival of patients (231). Cetuximab, an EGFR-specific IgG1 mAb, FDA-approved for treatment of HNC patients has shown to activate NK cells via binding of its Fc portion to Fc γ RIIIa expressed on NK cells. The immunostimulatory cytokines secreted into the microenvironment in turn activate

dendritic cells (DC) and promote cross-presentation of TA and the expansion of EGFR-specific CTL (100, 101), linking innate and adaptive antitumor effector mechanisms. However, the benefit of cetuximab-mediated immunotherapy in the clinic is only seen in 20% of patients (101, 232, 233) most likely caused by a dominant immunosuppressive tumor microenvironment where the PD-L1/PD-1 axis interaction between tumor cells and infiltrating dysfunctional NK cells may be present.

PD-1 expression on NK cells has been reported in the setting of infectious diseases such as hepatitis C, HIV and tuberculosis where circulating PD-1 expressing NK cells were higher when compared with healthy controls, and PD-1 blockade enhanced their activation status and cytotoxicity (234-236). Interestingly, in the setting of cancer, multiple myeloma patients showed higher PD-1 expressing NK cells in peripheral blood than healthy individuals, and PD-1 blockade enhanced cytotoxicity of NK cells against tumor targets (237). To our knowledge, there are no reports about PD-1 expression on NK cells in solid tumors, including HNC, and whether it represents a marker of activation or exhaustion. Therefore, we investigate the regulation of cetuximab-activated NK cells by the PD-L1/PD-1 axis in order to reverse potential tumor immunoescape mechanisms and to improve current outcomes of mAb-based immunotherapy (232, 233).

In this study, we investigated the expression of NK activation markers in tumors and correlate these with PD-1 expression in a large cohort of HNC specimens. Moreover, we measured PD-1⁺ circulating and tumor infiltrating NK cells in these cancer patients. We hypothesized that PD-1 expression on NK cells may constitute an activation marker and that cetuximab-mediated activation would further increase PD-1⁺ NK cells *in vitro* and *in vivo*, testing specimens from a novel neoadjuvant cetuximab clinical trial. Thus, JAK2-mediated

inhibition of PD-L1 expression on tumor targets and/or nivolumab-mediated PD-1 blockade on NK cells may enhance cetuximab-mediated NK cell cytotoxicity against PD-L1 expressing HNC targets. Taken together, these findings support the use of combined anti-EGFR and PD-L1/PD-1 axis blockade therapy in the clinic.

4.2 MATERIALS AND METHODS

4.2.1 Patients and specimens

All patients signed an informed consent approved by the Institutional Review Board (IRB #99-06). Peripheral venous blood samples were obtained from HNC patients with stage III/IVA disease, receiving neoadjuvant cetuximab on a prospective phase II clinical trial (UPCI 08-013, NCT 01218048). Tumors were biopsied immediately before, and again after 4 weeks of cetuximab therapy. Clinical response was analyzed by comparing paired CT scans pre/post-cetuximab, and quantifying tumor measurement by a dedicated head and neck radiologist blinded to patient status. Anatomic tumor measurements were recorded in two dimensions and the cohort segregated into clinical “responders,” who showed a reduction in tumor volume, or “nonresponders,” whose tumor grew during this therapy. Tumor biopsies (pre-treatment) or surgical tumor specimens (post-treatment) were preserved for a maximum of 12 hours in complete media until tumor infiltrating lymphocytes were isolated.

4.2.2 Tumor infiltrating lymphocyte (TIL) isolation

Fresh tumors from patients with HNC were minced into small pieces manually or using a gentleMACS dissociator (Miltenyi Biotec), then transferred to 70- μ m cell strainers (BD) and mechanically separated using the plunger of a 5-mL syringe. The cells passing through the cell strainer were collected, washed and subjected to Ficoll–Hypaque gradient centrifugation. After centrifugation, mononuclear cells were recovered and immediately used for experiments.

4.2.3 PBMC and NK isolation from peripheral blood

After approval by our Institutional Review Board [University of Pittsburgh Cancer Institute (UPCI; Pittsburgh, PA) protocol 99-069], informed consent was obtained from each subject before blood withdrawal. Blood from healthy donors (Western Pennsylvania blood bank) or patients with HNC treated with cetuximab during or within 1 month of treatment (UPCI clinical trial #08-013 NCT 01218048). Lymphocytes were purified by Ficoll-Paque PLUS centrifugation following standard protocol (Amersham Biosciences) and subsequently NK cells were purified using NK negative selection magnetic EasySep kits following the manufacturer's protocol (Stemcell technologies). Purity of the selection was more than 95% Fc γ RIIIa+, CD56+, and CD3–.

4.2.4 Co-culture of NK cells using hIgG1 or PD-L1-coupled beads

PD-L1-hIgG1 Fc fusion protein (R&D Systems) or control human IgG1 (Southern Biotech) was covalently coupled to Dynabeads M-450 Epoxy beads according to the manufacturer's protocol (Life Technologies). We kept constant the total amount of protein at 5 μ g per 10⁷ beads as previously described (238). Briefly, 10⁷ beads were coated with 50 μ g/mL of either PD-L1-hIgG1 Fc fusion protein or control human IgG1. Covalent coupling of the proteins to the beads was performed in 0.1mol/L sodium phosphate buffer for 24 hours at room temperature with gentle tilting and 107 rotation. NK cells were freshly isolated from PBMC and subjected to co-culture experiments. NK cells were cultured with beads at a fixed cell:bead ratio of 1:20. Briefly, 0.2 \times 10⁶ NK cells.

4.2.5 Tumor cell lines

HNC cell lines used in this report: JHU022, JHU029, SCC90 and 93VU. JHU022, JHU029 were a kind gift from Dr. James Rocco (Harvard Medical School, Boston, MA) in January of 2006. SCC90 were isolated from patients treated at the University of Pittsburgh Cancer Institute (Pittsburgh, PA) through the explant/culture method, authenticated, and validated as unique using STR profiling and HLA genotyping every 6 months. 93-VU-147 T (called 93VU in this report) was a kind gift from Dr. Henning Bier (Technische Universitat Munchen, Munich, Germany) in October of 2013. All cell lines were routinely tested every 6 months and found to be free of *Mycoplasma* infection and were cultured in IMDM (Invitrogen, Carlsbad, CA) supplemented with 10% FBS (Mediatech, Herndon, VA), 2% L-glutamine and 1% penicillin/streptomycin (Invitrogen Corp, Carlsbad, CA). For treatment with IFN γ , cells were cultured overnight in serum free AIM-V media (Invitrogen, Carlsbad, CA) and IFN γ (10IU/mL) treatment was started when cells reached at least 20% confluence. Adherent tumor cells were detached by warm trypsin-EDTA (0.25%) solution (Invitrogen, Carlsbad, CA) incubated for 5 min at 37. We determined that Trypsin detachment did not cleave surface PD-L1 by comparing with a non-enzymatic detachment method. Surface protein PD-L1 expression was determined by flow cytometry.

4.2.6 Antibodies and treatments

Mouse anti-human PD-L1-PE monoclonal antibody (mAb), CD3-PerCPCy5.5, CD56-PE, CD56-FITC, PD-1-APC (clone MIH4), CD16-PECy7, CD107a-PE, GranzymeB-FITC and IFN γ -APC-Cy7 were purchased from BD Pharmingen (San Jose, CA). Zombie aqua viability dye was purchased from Biolegend (San Diego, CA).

Human recombinant interferon gamma (IFN γ) was purchased from R&D systems (Minneapolis, MN) reconstituted according manufacturer instructions and kept at -80 Celsius freezer in aliquots, for all experiments in this report IFN γ was used at 10IU/mL. rhIL-2 was purchased from R&D systems (Minneapolis, MN) reconstituted according manufacturer instructions and kept at -80 Celsius freezer in aliquots, for NK activation experiments rhIL-2 was used at 130IU/mL for 24h following a previously validated protocol (237). Mouse anti-human anti-IFN γ blocking antibody was purchased from R&D systems (Minneapolis, MN) and used at 50ng/mL in our experiments. Cetuximab (anti-EGFR mAb, IgG1) and nivolumab (anti-PD-1 mAb, IgG4) were kindly provided by Bristol-Meyers Squibb. Panitumumab (anti-EGFR mAb, IgG2) was kindly provided by Amgen. Cetuximab and panitumumab were used at 10ug/mL in all our experiments, while nivolumab was used at 20ug/mL.

4.2.7 Flow cytometry analysis

Surface flow cytometry was performed as follows, cells were harvested and resuspended in PBS containing a 1:50 dilution of a previously validated viability dye Zombie Aqua (174), following the manufacturer's protocol (Biolegend, San Diego, CA), then resuspended in 50uL of fluorescence-activated cell sorting (FACS) buffer and fluorophore conjugated antibodies were added at 1:10 dilution, incubated for 15 minutes at 4 Celsius, then antibodies were washed away twice by sequential centrifugation at 1400 RPM with FACS buffer and resuspended in 2% PFA solution until analyzed in the flow cytometer.

4.2.8 Cellular cytotoxicity assays

Cytotoxicity was determined using a ^{51}Cr release assay. Briefly, target cells were incubated in 100 μL of media with 25 μCi of $\text{Na}_2^{51}\text{CrO}_4$ (Perkin Elmer, Boston MA) for 60 min at 37°C and resuspended in RPMI 1640 medium supplemented with 25 mM HEPES. Cells were thoroughly washed and plated at various effector: target (E:T) ratios in 96-well plates, then treatments (mAbs) and freshly purified NK cells were added at the specified effector:target (E:T) ratios. Plates were incubated for 4 h at 37°C in a 5% CO_2 atmosphere. Controls for spontaneous (cells only) and maximal lysis (cells treated with 1% Triton-X) were included. Each reaction was done in triplicate and repeated three times. The supernatants were collected and analyzed with a Perkin Elmer 96-well plate gamma counter. % specific lysis = $(\text{experimental lysis} - \text{spontaneous lysis}) / (\text{experimental lysis} - \text{maximal lysis}) \times 100$. Results are representative of 3 different donors and were plotted in bar graphs.

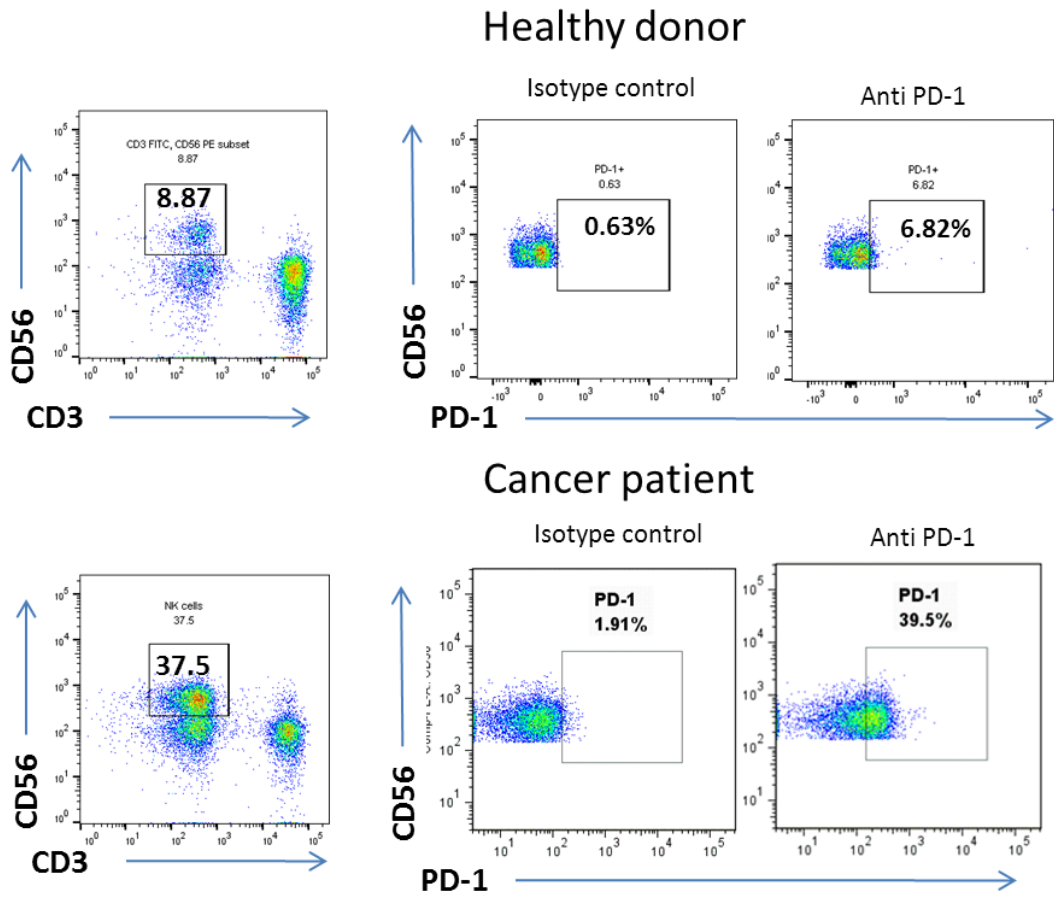
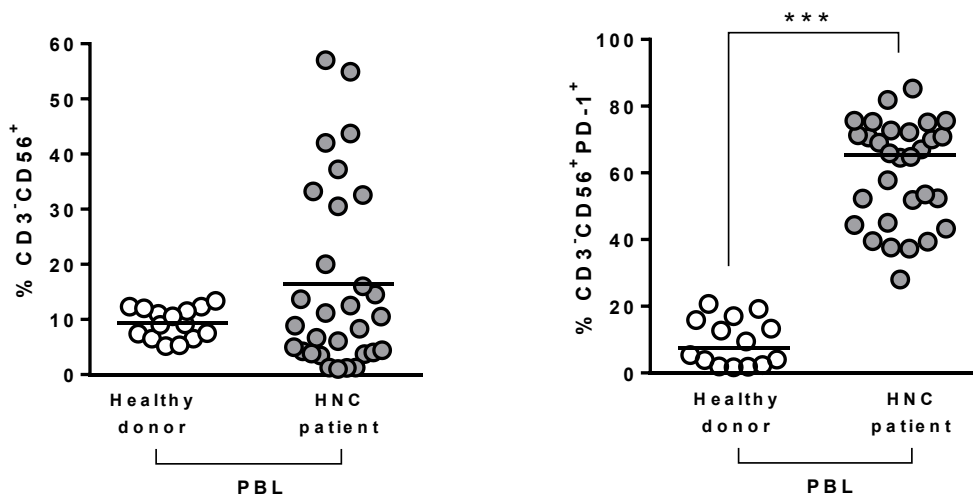
4.2.9 The Cancer Genome Atlas (TCGA) data retrieval and analysis

TCGA data for HNC gene expression by RNAseq were downloaded from the UCSC cancer genomics browser (<https://genome-cancer.ucsc.edu>). The HNC gene expression profile was measured experimentally using the Illumina HiSeq 2000 RNA Sequencing platform. This dataset shows the gene-level transcription estimates, as in RSEM normalized count, percentile ranked within each sample. Genes are mapped onto the human genome coordinates using UCSC cgData HUGO probeMap. The RSEM units to quantitate RNAseq expression data were described and validated previously (179). Correlations and linear regression curve fits from TCGA data were calculated using GraphPad PRISM software version 6 and values were plotted into either graphs or tables.

4.3 RESULTS

4.3.1 HNC patients have higher PD-1⁺ circulating NK cells in healthy individuals, which are enriched in HNC tumors, and predict better survival

Little is known about the frequency of circulating NK cells, their activation status and PD-1 expression in HNC patients. Using freshly isolated PBMC, we observed that circulating NK cells were higher in HNC patients than in healthy individuals (Figure 4.3.1A). More interesting was the finding of a significantly higher frequency of peripheral blood PD-1⁺ NK cells in HNC patients when compared with healthy individuals (Figure 4.3.1B, Mann-Whitney test *** P<0.0001). In the light of these findings, we compared PD-1 expression on CD3⁻CD56⁺ NK cells from peripheral blood and matched HNC tumors in a different subset of patients. This cohort of HNC patients had variable levels of circulating PD-1⁺ NK cells (data not shown), which were significantly enriched at the tumor site (Figure 4.3.1C, Tumor NK cells vs. Peripheral blood, n=8, ** P<0.01). To investigate whether the higher frequency of PD-1⁺ circulating NK cells in HNC patients represented a prognostic biomarker, we segregated NK cells (from the subset of patients shown in Figure 4.3.1 A and B) into % NK PD-1 high or low, according to whether they were above or below the mean frequency cutoff value (mean 60.34% ± SEM 2.817). We observed that patients who had a higher frequency of circulating PD-1⁺ NK cells (above the mean) showed a significantly longer overall survival than those below the mean (Figure 4.3.1D, n=30, P=0.03). This finding showed the same trend but did not reach statistical significance when we analyzed disease free survival (Supplementary figure 4.5.1, n=21, P=0.18).

A**B**

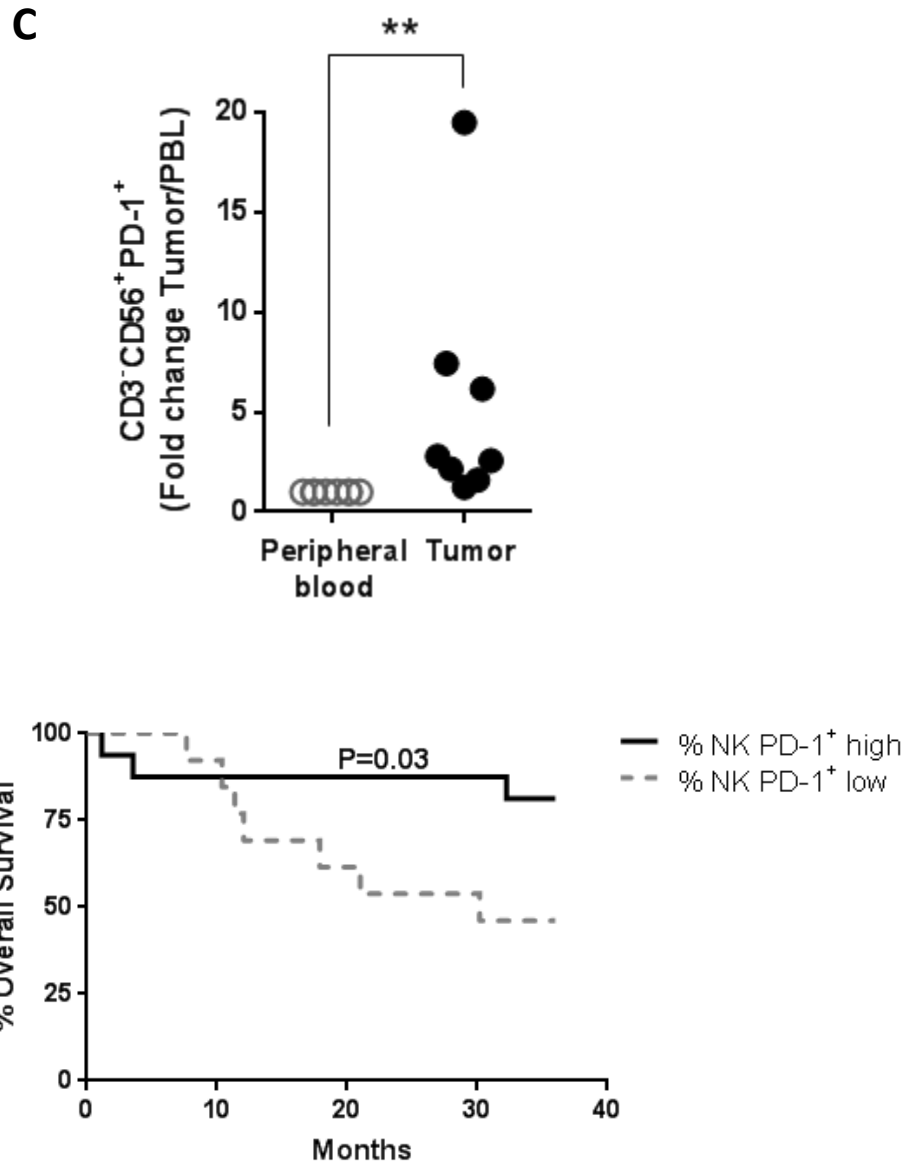
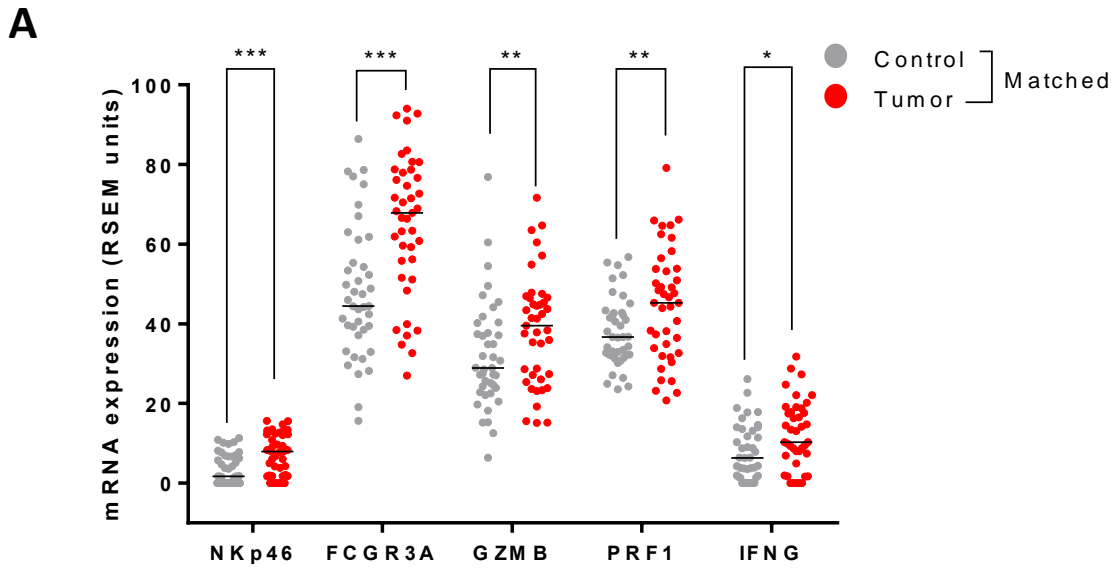


Figure 4.3.1 PD-1⁺ NK cells are higher in HNC patients than in healthy individuals, are enriched in HNC tumors and predict better survival of patients: **A.** Frequency of circulating NK cells (CD3⁺ CD56⁺) from peripheral blood lymphocytes (PBL) is higher in HNC patients than healthy individuals. **B.** Percent of circulating PD-1⁺ NK cells (CD3⁺CD56⁺) is significantly higher in PBL from HNC patients when compared to that of healthy individuals. (Mann-Whitney test *** P<0.001) **C.** Fold change of PD-1⁺ NK cells (CD3⁺CD56⁺) in TIL vs. PBL in HNC patients. Fresh HNC patient TIL or PBL were stained for PD-1 expression on CD3⁺CD56⁺ NK cells by flow cytometry. Fold change increase in tumor over peripheral blood (PBL) was

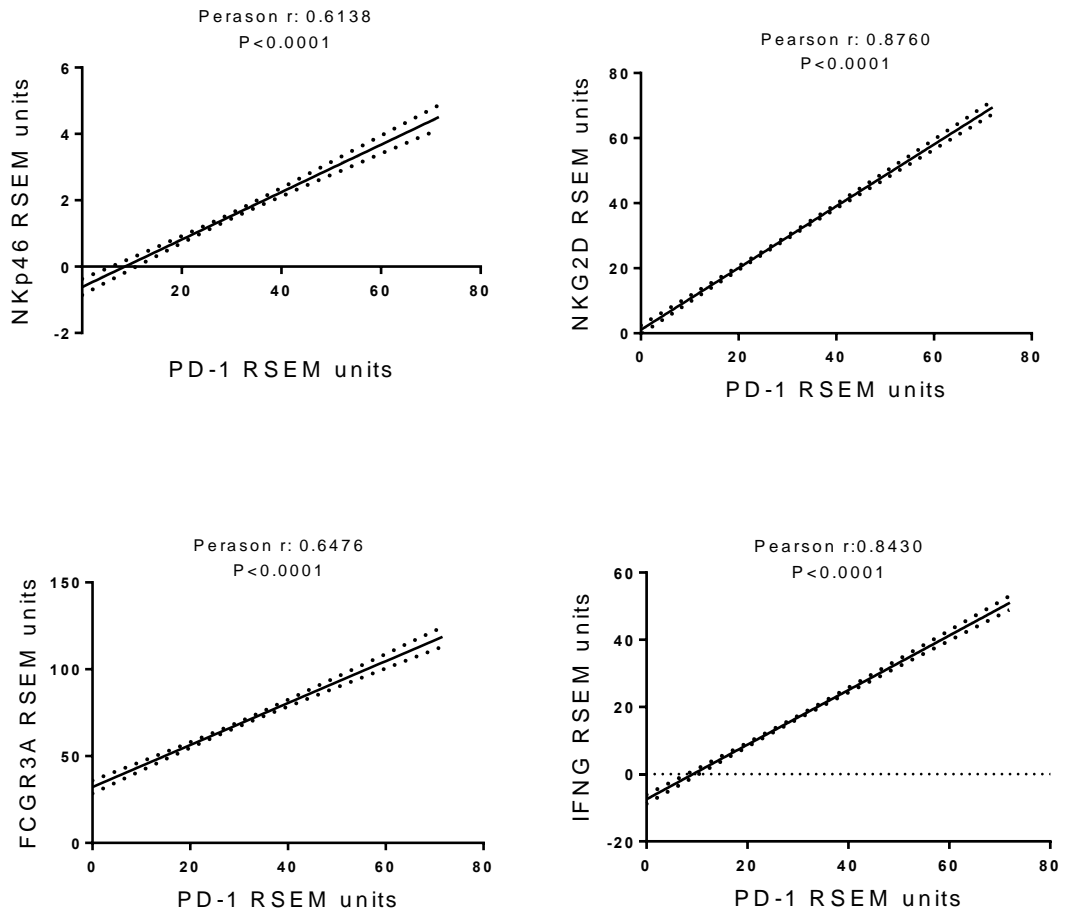
statistically significant. (Mann-Whitney test, ** $P < 0.01$). **D.** Kaplan-Meier survival curve of 30 HNC patients whose PBL were harvested and PD-1 expression was determined on NK (shown in panels A and B), the mean frequency of PD-1⁺ NK cells was set at a cutoff (mean 60.34%± 2.817) and % NK PD-1 high and low refers to frequency of PD-1⁺ NK cells above or below the mean value, respectively. Frequency of PD-1⁺ NK cells was correlated with overall survival of patients, statistical significance was determined by log-rank Mantel-Cox test, $P = 0.03$.

4.3.2 Elevated expression of NK activation markers correlates with that of PD-1 in HNC tumors

In order to corroborate our previous findings, we took advantage of the large curated database of The Cancer Genome Atlas (TCGA) (178) and correlated mRNA expression of the NK cell specific activation marker NKp46, Th1 phenotype activation markers granzyme B (GZMB), perforin (PRF1), interferon- γ (IFNG), and Fc γ RIIIa (FCGR3A) in matched control and tumor tissue from 43 HNC patients. We observed that tumors from HNC patients had higher expression of NKp46 and these well-known NK activation markers when compared with paired control tissues (n=43) (Figure 4.3.2A). Furthermore, we found a strong correlation between PD-1 expression and that of NKp46, NKG2D, FCGR3A, GZMB, PRF1 and IFNG in the entire cohort of HNC in TCGA (n=500) (Figure 4.3.2B and supplementary figure 4.5.2, Pearson r , $P < 0.0001$ for all correlations). These results indicate that activated NK cells infiltrate HNC tumors, strongly correlating with PD-1 expression. Overall, these results extend the finding that PD-1 expressing NK cells are enriched in the tumor microenvironment of HNC patients, and that PD-1 expression may represent a marker of NK cell activation rather than exhaustion, perhaps in distinction to tumor infiltrating T cells.



B



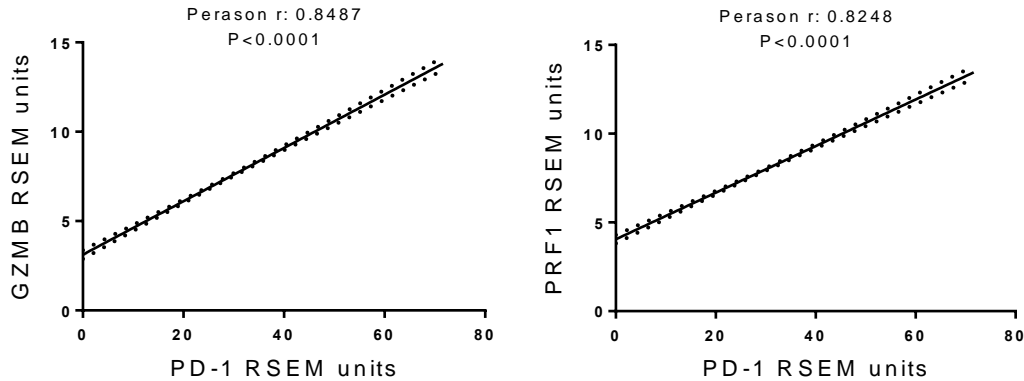


Figure 4.3.2 NK activation markers are higher in HNC tumors than in matched controls and strongly correlate with PD-1 expression: A. NKp46, FcγRIIIA (FCGR3A), granzyme B (GZMB), perforin (PRF1) and IFN γ (IFNG) mRNA expression (RSEM units) is significantly higher in tumor specimens than in normal matched tissues. TCGA mRNA expression data from 43 HNC specimens. (Kruskall-Wallis test *** P<0.001, ** P<0.01, * P<0.05). **B.** PD-1 mRNA expression strongly correlates with that of NK activation markers NKp46, NKG2D, FCGR3A (FcγRIIIA), IFN γ (IFNG), GZMB (granzyme B) and PRF1 (perforin) in HNC tumor specimens. 500 HNC tumor specimens were analyzed from TCGA database (see material and methods), correlation was determined by Pearson r test, graphs show linear regression curve fit (P<0.0001).

4.3.3 PD-1 expressing NK cells display an activated phenotype

In order to test our hypothesis that PD-1 expression on NK cells may reflect an activated rather than an exhausted phenotype, we isolated NK cells from fresh healthy donor PBMC and measured PD-1 expression along with that of NK cell and activation markers such as CD16 (FcγRIIIa), CD107a, IFN γ and Granzyme B at baseline and after activation with IL-2 (130IU/mL, 24h), as described previously (237). PD-1 expression on NK cells significantly increased and concomitantly with that of signature activation markers CD107a, IFN γ , CD16 and Granzyme B, with the first two being significantly upregulated (Figure 4.3.3A, *** P<0.001, **

P<0.01). Furthermore, in order to test whether activated PD-1 expressing NK cells' activated phenotype becomes impaired after PD-L1 ligation, we co-cultured activated NK cells with either isotype control mAb or PD-L1-IgG conjugated beads for 24 hours and then measured the same panel of activation markers on NK cells. When co-cultured with PD-L1-IgG conjugated beads, PD-1⁺ NK cells significantly downregulated CD16, CD107a (P<0.01 and P<0.05, respectively). IFN γ and Granzyme B expression was also decreased but not to a significant extent (Figure 4.3.3B, P>0.05).

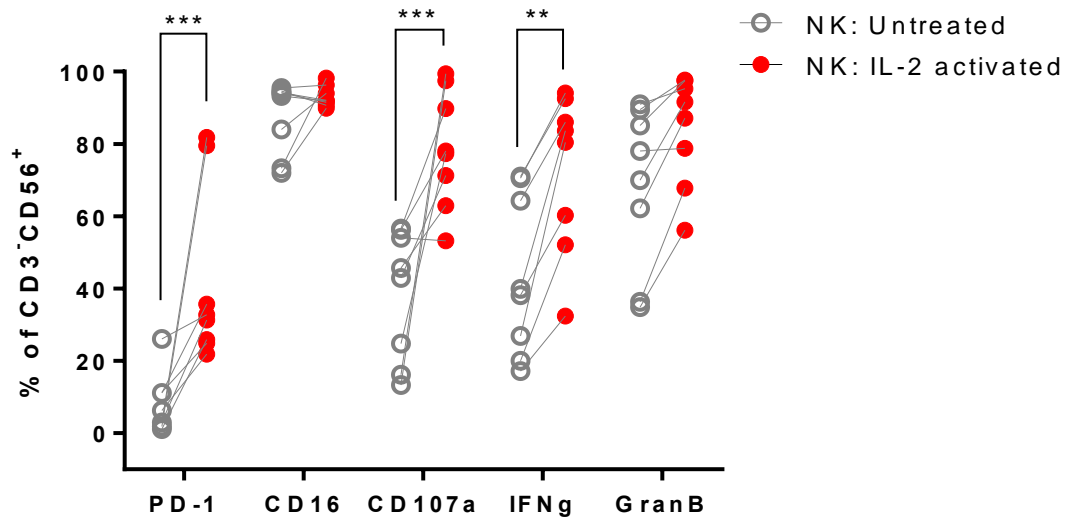
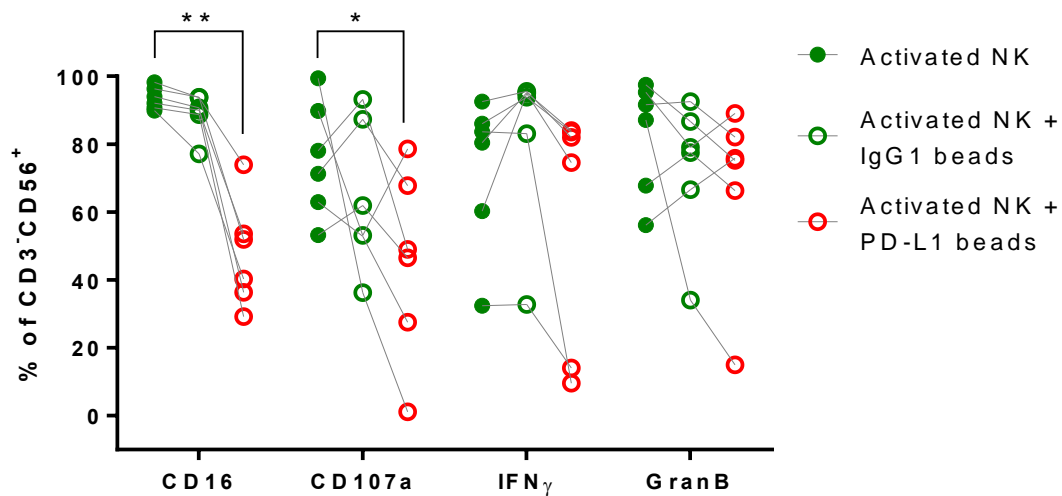
A**B**

Figure 4.3.3 PD-1 upregulated NK cells display an activated phenotype: A. CD3⁺CD56⁺ NK cells concomitantly upregulate PD-1 expression and activation markers such as CD16, CD107a, IFN γ and granzyme B after IL-2 activation. Healthy donor NK cells (CD3⁺CD56⁺) were purified from freshly isolated PBMC and baseline PD-1, CD16, CD107a, IFN γ and granzyme B expression was determined by flow cytometry (open gray circles in graph), a separate aliquot of the same NK cell culture was treated with rhIL-2 (130 IU/mL) for 24 h (For NK activation see material and methods), harvested and the same activation markers were determined by flow

cytometry (closed black circles in graph). Statistical significance between medians was determined by Kruskal-Wallis test (*** $P < 0.001$, ** $P < 0.01$). **B.** PD-1⁺ NK cells downregulate expression of activation markers upon PD-L1 ligation. Healthy donor NK cells (CD3⁻CD56⁺) were purified from freshly isolated PBMC and activated with rhIL-2 (130 IU/mL) for 24 hours (open gray squares), then incubated with either Isotype control (open gray circles) or PD-L1 conjugated beads (closed black circles) for an additional 24 hours, cells were harvested and CD16, CD107a, IFN γ and granzyme B expression was determined by flow cytometry. (Kruskal-Wallis test, ** $P < 0.01$, * $P < 0.05$)

4.3.4 Cetuximab induces NK cell activation, PD-1 expression and IFN γ -dependent PD-L1 upregulation in HNC

We previously reported that cetuximab-coated tumor cells induce NK:DC crosstalk and trigger TA specific CD8⁺ T cell expansion (100, 101). Since cetuximab activates NK cells leading to IFN γ secretion and cytotoxicity, we hypothesized that this activation stimulus could also induce PD-1 upregulation. Indeed, as shown in Figure 4.3.4A, cetuximab but not isotype control (IgG1) or panitumumab (IgG2) induced NK cell activation and IFN γ secretion when co-cultured with EGFR⁺ HNC cells. In turn, NK cell-derived IFN γ secretion led to PD-L1 upregulation on HNC cells from the same co-culture system (Figure 4.3.4B), as well as induced upregulation of PD-1⁺ NK cells (Figure 4.3.4C). Next, we analyzed PD-1 expression on tumor infiltrating NK cells from cetuximab treated HNC tumor specimens. Advanced HNC patients were treated with cetuximab on a prospective neoadjuvant trial (UPCI #08-013, NCT #01218048). Prior to and after 4 weeks of cetuximab therapy, HNC tumors from these patients (n=6) were harvested, tumor infiltrating lymphocytes freshly isolated, and NK cells analyzed by flow cytometry. We found a significant fold change increase in PD-1⁺ tumor infiltrating NK cells in post cetuximab treated specimens when compared with their respective matched samples before treatment

(Figure 4.3.4D, Mann-Whitney test, * $P < 0.05$). Thus, PD-1 expression is strongly upregulated in cetuximab activated NK cells in the tumor microenvironment, where PD-L1 is also present in 50-70% of HNC patients (212), supporting combinational therapy blocking PD-1-mediated NK cell suppression.

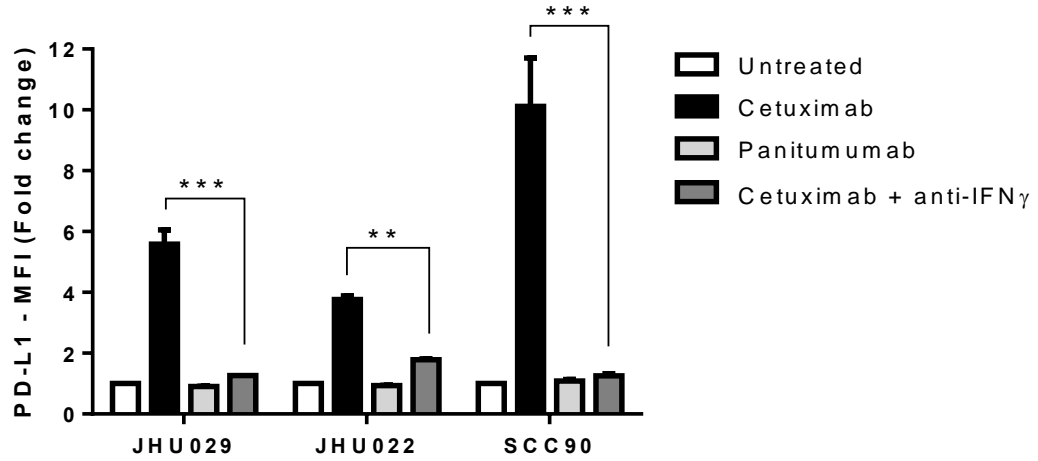
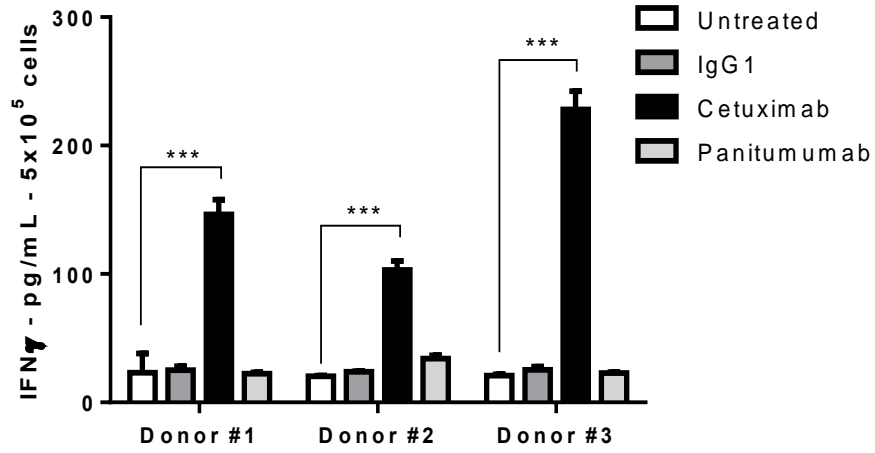
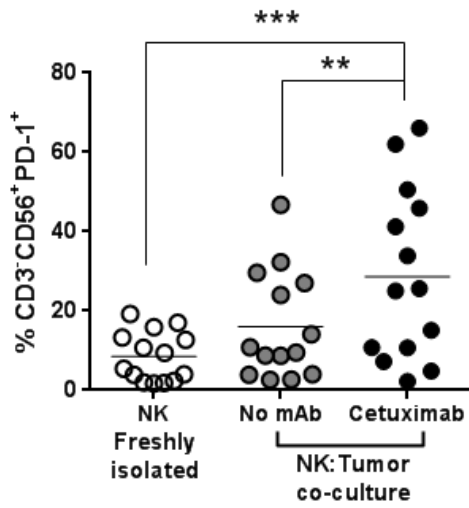
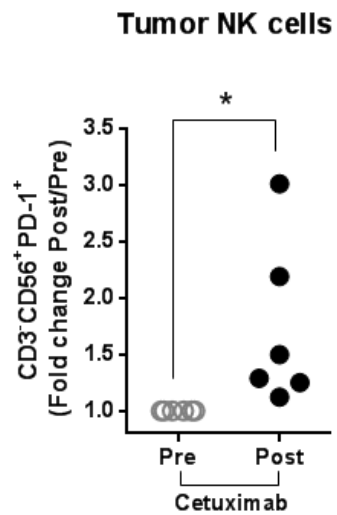
A**B****C****D**

Figure 4.3.4 Cetuximab-activated NK cells increase PD-1 expression, IFN γ secretion, and PD-L1 upregulation in HNC cells: **A.** Higher IFN γ secretion by NK cells when co-cultured with cetuximab-coated HNC cells. Freshly isolated NK cells were co-cultured with JHU029 tumor cells at 1 to 1 ratio for 24h in the absence of mAb or with IgG1 (10ug/mL), cetuximab (10ug/mL) or panitumumab (10ug/mL). IFN γ in the culture supernatants was determined by ELISA. (ANOVA, *** P<0.001). **B.** Cetuximab-activated NK cells upregulate PD-L1 expression in tumor cells in an IFN γ dependent fashion. Freshly isolated NK cells from 3 different healthy donors were co-cultured with JHU029, JHU022 and SCC90 tumor targets for 24h in the absence of mAb or with cetuximab (10ug/mL), panitumumab (10ug/mL) and cetuximab with IFN γ blocking antibody (anti-IFN γ , 50ng/mL). Then harvested and PD-L1 expression on tumor cells was determined by flow cytometry (ANOVA, ** P<0.01, *** P<0.001) **C.** Cetuximab-activated NK cells increase PD-1 expression. Healthy donor peripheral blood NK cells were either stained freshly isolated or co-cultured with tumor targets (JHU029 cells) in the absence of mAb or with cetuximab (10ug/mL) for 24h, harvested and surface PD-1 expression was determined by flow cytometry. (Kruskal-Wallis test *** P<0.001, ** P<0.01). **D.** Cetuximab treatment increases frequency of tumor infiltrating PD-1⁺ NK cells in vivo. Tumor infiltrating NK cells from HNC patients were isolated pre- and post- cetuximab treatment (clinical trial UPCI #08-013, see material and methods) and PD-1 expression on CD3⁺CD56⁺ NK cells was determined by flow cytometry, % NK cell fold change of Post vs. Pre-cetuximab treated specimens was calculated and plotted. (Mann-Whitney test, * P<0.05).

4.3.5 PD-1 blockade enhances NK cell cytotoxicity and cetuximab mediated ADCC in PD-L1 high tumor targets

Next, we determined whether PD-1 blockade using the FDA approved, anti-PD-1 mAb nivolumab could enhance NK cell cytotoxicity against PD-L1 expressing tumor targets. Indeed, cetuximab-activated PBMC increased the frequency of PD-1⁺ NK cells after 24 hours of treatment (Supplementary Figure 4.5.3A and B) and showed a higher specific lysis of tumor targets when co-cultured in the presence of nivolumab (Figure 4.3.5A, left bars). Importantly,

these same effector cells showed a significantly higher cytotoxicity when co-cultured with IFN γ -pretreated, PD-L1^{high} HNC targets (Figure 4.3.5A, right bars) (53% vs 30% specific tumor lysis, ANOVA *** P<0.001). In order to further confirm our interpretation, we isolated fresh NK cells from healthy donor PBMC (n=3), and co-cultured them with either PD-L1^{low} (JHU029 targets) or PD-L1^{high} (93VU targets) (Supplementary Figure 4.5.2C). Under these conditions, PD-1 blockade enhanced cetuximab mediated ADCC, only when tumor targets expressed a higher level of PD-L1 (Figure 4.3.5B and 4.3.5C).

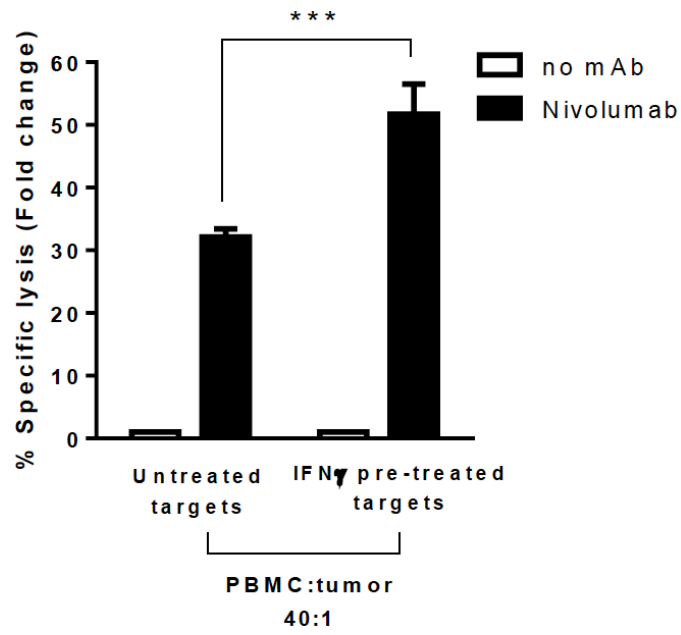
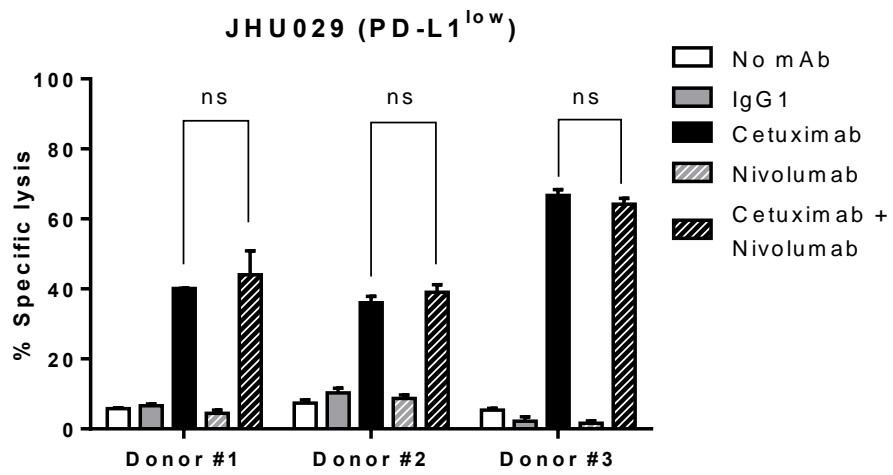
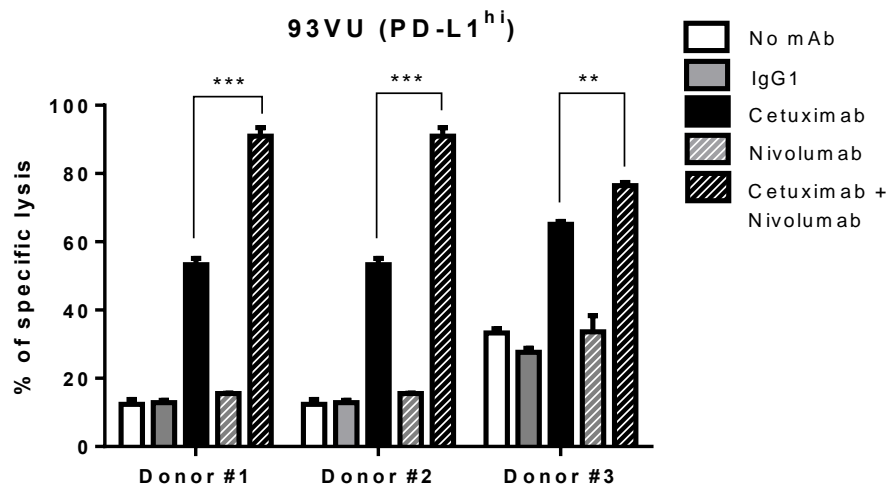
A**B****C**

Figure 4.3.5 PD-1 blockade enhances NK cytotoxicity and cetuximab mediated ADCC of PD-L1^{high} expressing tumor targets: **A.** Nivolumab-mediated PD-1 blockade enhances cytotoxicity of cetuximab pre-activated PBMC. Freshly isolated PBMC were co-cultured with JHU029 tumor cells in a 200:1 ratio in the absence of mAb or with cetuximab (10ug/mL) for 24h, then harvested and co-cultured with either untreated or IFN γ (10IU/mL) pre-treated tumor targets (JHU029 cells, 40:1 ratio, 24h) in the presence or absence of nivolumab for 4 hours. ⁵¹Cr release was determined in a scintillation counter (Perkin-Elmer) and percent specific lysis was calculated. (Two-way ANOVA *** P=0.001) **B.** Nivolumab does not enhance cetuximab mediated ADCC of PD-L1^{low} tumor targets (JHU029 cells, see supplementary figure 2C). Freshly isolated NK cells were co-cultured with tumor targets (⁵¹Cr labeled, 20:1 ratio) with no mAb, IgG1 isotype (10ug/mL), cetuximab (10ug/mL), nivolumab (20ug/mL) or cetuximab + nivolumab for 4 hours. ⁵¹Cr release was determined in a scintillation counter (Perkin-Elmer) and % specific lysis was calculated. (ANOVA, ns=non-significant). **C.** Nivolumab enhances cetuximab mediated ADCC of PD-L1^{high} tumor targets (93VU cells, see supplementary figure 2C). Freshly isolated NK cells were co-cultured with tumor targets (⁵¹Cr labeled, 20:1 ratio) with no mAb, IgG1 isotype (10ug/mL), cetuximab (10ug/mL), nivolumab (20ug/mL) or cetuximab + nivolumab for 4 hours. ⁵¹Cr release was determined in a scintillation counter (Perkin-Elmer) and % specific lysis was calculated. (ANOVA, ** P=0.01, *** P=0.001).

4.3.6 JAK2 inhibition prevents tumor PD-L1 expression and enhances cetuximab mediated NK cell cytotoxicity

Since JAK2 represents a key player in PD-L1 upregulation in both EGFR (intrinsic) and IFN γ (extrinsic) pathways *in vitro*, we tested whether JAK2 inhibition enhanced NK mediated killing via antibody dependent cell cytotoxicity (ADCC) (100) against PD-L1⁺ HNC cells. When NK cells were co-cultured with HNC targets and cetuximab, activated NK cells upregulated tumor PD-L1 expression in an IFN γ dependent fashion (Figure 4.3.6A, open bars). As a control, the EGFR specific mAb panitumumab (IgG2 isotype) which does not bind to CD16 on NK cells, did not induce PD-L1 upregulation, most likely because of a lack of NK cell activation and IFN γ

secretion (137). Importantly, the IFN γ mediated PD-L1 upregulation on HNC cells was prevented when they were pre-treated with the JAK2 inhibitor (top panel, closed bars), but not with a JAK1/3 specific inhibitor (bottom panel, closed bars). We therefore tested the hypothesis that NK cells would more efficiently lyse JAK2 inhibitor pre-treated tumor cells, in the setting of reduced PD-L1 expression. Indeed, NK cells showed approximately 25% higher specific lysis of HNC cells pre-treated with the JAK2 inhibitor (Figure 4.3.6B). Overall, these results confirm that JAK2 is an important regulator of PD-L1 expression in HNC tumor cells, and its inhibition reverses PD-L1 mediated tumor cell escape from cetuximab mediated ADCC.

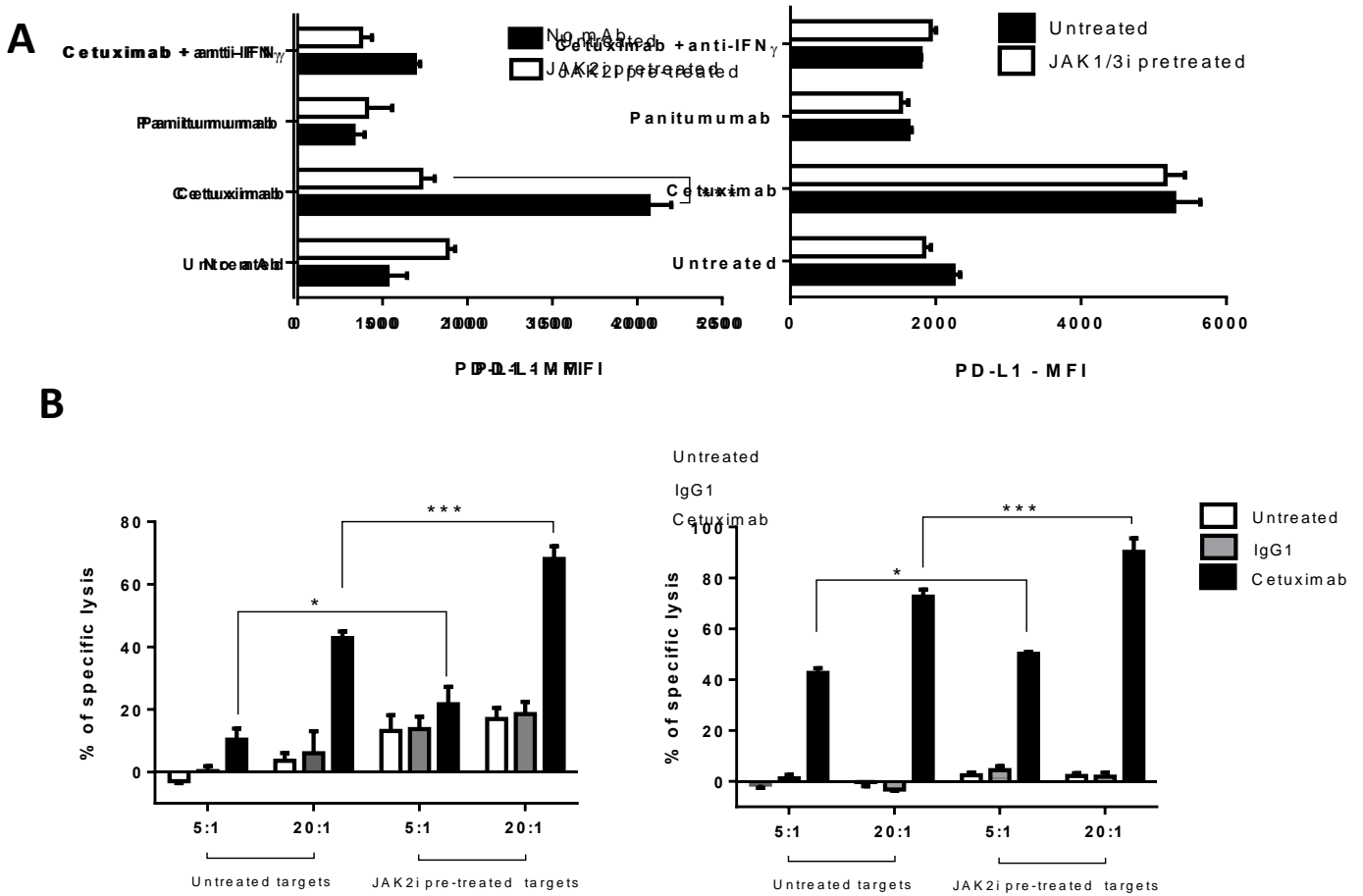


Figure 4.3.6 JAK2 inhibition prevents NK mediated PD-L1 upregulation on tumor cells and enhances cetuximab mediated NK cell cytotoxicity: A. PD-L1 expression is upregulated on tumor cells when co-cultured with cetuximab-activated NK cells in an IFN γ dependent fashion (left panel, open bars). JAK2i pre-treatment of tumor targets prevented PD-L1 upregulation (left panel, closed bars). In contrast, JAK1/3 inhibition did not prevent PD-L1 upregulation under the same conditions (right panel, closed bars). Tumor target cells were incubated in media alone or JAK2i (10uM) supplemented media for 48 hours then co-cultured with NK cells for 24 hours untreated or in the presence of cetuximab (10ug/mL), panitumumab (10ug/mL) or cetuximab +anti-IFN γ blocking antibody (50ug/mL), harvested and PD-L1

expression on tumor cells was determined by FC. Data representative of two independent experiments with similar results **B**. Higher NK-cetuximab mediated lysis of JAK2i pre-treated targets (closed black bars, 5:1 and 20:1 effector:target ratio). Tumor cells were pre-treated with JAK2i (10uM) for 48 hours then labeled with ⁵¹Cr and co-cultured with purified NK cells plus media, IgG1 control (10ug/mL) or cetuximab (10ug/mL) for 4h (ANOVA, * P<0.05, *** P<0.0001).

4.4 DISCUSSION

In the setting of HNC immunotherapy, cetuximab has shown objective responses and improved survival of HNC patients either as single agent or in combination with chemo-radiotherapy. However, its activity is only seen in minority of patients (101). Therefore, investigating and understanding its mechanism of action is crucial in order to improve its clinical outcome. Quantification and phenotypic characterization of immune cell subsets present in the tumor microenvironment is crucial in order to optimize their cytotoxicity against tumor cells. (165). NK cells constitute the first line of defense to respond to tumors without previous sensitization given their ability to recognize and kill targets without receptor gene rearrangement (239-241). While multiple studies implicate the PD-L1/PD-1 axis in tumor immunoevasion of T cell mediated adaptive immune responses in several solid tumors (242, 243), to our knowledge, information regarding the role of PD-L1/PD-1 axis in regards to NK cell-mediated immune responses in cancers, especially HNC is very scarce. Therefore, in the present study we focus in NK cells, which are crucial mediators of cetuximab-mediated therapy given their ability to specifically bind EGFR-overexpressing, cetuximab-coated tumor cells via FcγRIIIa, and to stimulate adaptive T cell responses via NK:DC crosstalk (101). This study demonstrates that NK cell

immune activation markers are highly expressed in tumors of HNC patients, suggesting not only that NK cells can readily infiltrate tumors but also have an important role in immune rejection since they display an activated phenotype. We found that frequency of NK cells in peripheral blood from HNC patients is higher when compared to healthy individuals, concordant with a previous report of a higher percentage and absolute number of circulating NK cells (244). In contrast, others showed a decreased NK cell number in peripheral blood from HNC patients, but that particular study determined NK frequency relying on methylation of NKp46 gene loci from archival DNA samples (245). We directly analyzed NK cell frequency by flow cytometry quantifying CD3⁻CD56⁺ cells, which may represent a more reliable method of measurement. More importantly, we are the first to report that circulating PD-1 expressing NK cells are significantly higher in HNC patients than healthy individuals. These results corroborate those of Benson et al. in which circulating PD-1⁺ NK cells were higher in multiple myeloma patients than in healthy individuals (237). Interestingly, we also found that PD-1⁺ NK cells are enriched in tumors when compared with matched patient peripheral blood, suggesting that NK cells traffic to the tumor microenvironment. More importantly, a significantly better patient survival corresponded with a higher frequency of circulating PD-1⁺ NK cells when compared to those who had lower frequencies (Figure 4.3.1D). In addition, we found significantly higher expression of signature NK activation markers in tumor tissue when compared to matched control mucosa (Figure 4.3.2A), and a strong correlation of these NK activation markers and PD-1 expression in a large cohort of tumors from TCGA database (n=500). All these findings led us to hypothesize that PD-1 expression on NK cells may represent a marker of activation rather than exhaustion. Indeed, when activated PD-1 expressing NK cells were co-cultured with PD-L1 coated beads, activation markers such as CD16 and CD107a as well as IFN γ and Granzyme B showed an

evident downregulation, with the two first in a significant fashion. Thus, confirming our view that PD-1 *per se* is a marker of NK cell activation which only induces an exhausted phenotype after PD-L1 ligation.

Several studies support the view that PD-1 expression represents an activation marker on T cells, namely in the setting of viral infections where PD-1 was co-expressed with CD38 and HLA-DR (229, 236, 246). Furthermore, Badoual et al. showed similar findings in the setting of HNC (165). PD-1 expression depends on the stage of cell differentiation and activation, where early activated CD8⁺ T cells upregulate PD-1 expression along with other signature T cell activation markers (246). Similarly, co-expression of PD-1 and other activation markers have also been shown in tumor infiltrating lymphocytes (TIL) from cancer patients. Regarding NK cells, Alvarez et al. reported a direct correlation between PD-1 and IFN γ expression in the setting of *Mycobacterium tuberculosis* infection, where PD-1 blockade enhanced lytic degranulation and IFN γ production of NK cells that was otherwise reduced when PD-1 was bound by PD-L1 (234). Interestingly, Benson et al. reported that IL-2, a known NK activating cytokine, induced PD-1 expression on NK cells from healthy individuals that were otherwise PD-1 negative (237).

Our laboratory has shown before that cetuximab can activate NK cells (101), herein we demonstrate that cetuximab-activated NK cell-secreted IFN γ induced PD-L1 upregulation on tumor cells (Figure 4.3.4A-B). Likewise, cetuximab treatment induced upregulation of PD-1⁺ NK cells *in vitro* in a co-culture system and *in vivo* in patients from the UPCI #08-013 clinical trial where cetuximab was used as a single agent therapy (Figure 4.3.4D). Overall these data suggest that the otherwise beneficial effect of cetuximab may, in fact, induce a tumor escape mechanism dominated by the PD-L1/PD-1 axis interaction, in which IFN γ secreted from cetuximab-activated NK cells may induce PD-L1 upregulation on the tumor cell and PD-1 expression on the

effector immune cell compartment. Thus, we hypothesized that disruption of PD-L1/PD-1 axis interaction, either by JAK2 mediated inhibition of PD-L1 expression on the tumor end or nivolumab mediated PD-1 blockade on the immune effector cell end, may enhance NK cell cytotoxicity and tumor cell lysis.

In order to test our hypothesis, we co-cultured cetuximab-preactivated PBMC, where PD-1⁺ NK cells were expanded approximately two-fold, with either untreated or IFN γ pre-treated tumor targets in the presence or absence of nivolumab. As expected, PBMCs exhibited a significantly higher cytotoxicity when tumor targets were high expressers of PD-L1 (Figure 4.3.5A). Furthermore, purified activated NK cells showed a significantly higher cytolytic activity with the combination of cetuximab (anti-EGFR) and nivolumab (anti-PD-1) only when co-cultured with PD-L1^{high} but not PD-L1^{low} tumor targets. Taken together, these findings support the view that PD-L1/PD-1 axis disruption is an important strategy to enhance cetuximab-mediated NK cytotoxicity against HNC tumor targets that could be translated into the clinic. Importantly, this strategy most likely will benefit patients that have a higher expression of PD-L1 on tumor cells. Indeed, a recent study showed that anti-PD-1 therapy had a higher response rate (46% vs 11%) when tumors had a very robust PD-L1 expression, thus presenting PD-L1 expression level as a predictor of anti-PD-1 therapy (160). In addition and supporting our view that PD-1 expression on immune cells represents a marker of activation is the finding that PD-1 expression on tumor infiltrating T cells are a favorable prognostic biomarker in HNC (165)

Overall, our results show that PD-1 expressing NK cells in HNC patients readily infiltrate tumors and display an activated phenotype and predicts better survival, that PD-1⁺ NK cells show reduced activation and cytotoxicity only when PD-1 is bound by its cognate ligand PD-L1. Importantly PD-L1/PD-1 axis blockade restores NK cytotoxicity against PD-L1^{high} expressing

tumor targets and enhances cetuximab mediated ADCC. Alternatively, one added benefit of using combined JAK2 inhibition and cetuximab mediated EGFR blockade would be that the JAK2 mediated downregulation of PD-L1 expression on tumor cells would ultimately enhance the effector properties of PD-1⁺ NK cells activated in the tumor microenvironment. Indeed, we show that JAK2 inhibition in tumor targets enhances cetuximab mediated ADCC to a significant extent, therefore reversing PD-L1 mediated immune escape of tumor cells to NK killing (Figure 4.3.6B). Moreover, we may also speculate that JAK2 inhibition might synergize with monoclonal antibodies targeting PD-1 and/or CTLA-4 by enhancing ADCC of PD-1⁺CTLA⁺ lymphoid or myeloid suppressor immune infiltrates in the tumor microenvironment as well as reducing PD-L1 expression. Finally, our findings support novel immunotherapy approaches where combination of PD-L1/PD-1 axis blockade and EGFR blockade should be taken into account to improve clinical outcomes of cetuximab therapy in HNC patients.

4.5. SUPPLEMENTARY DATA

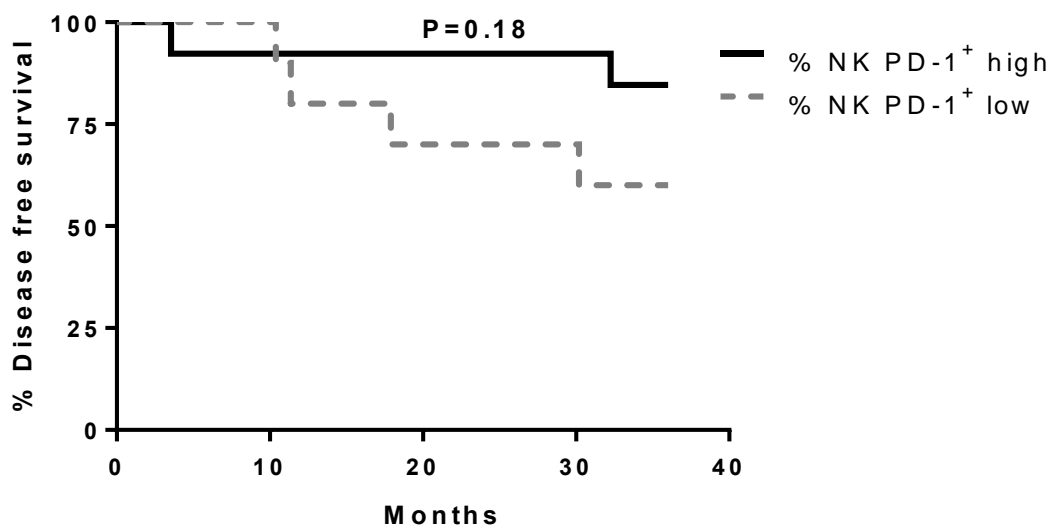
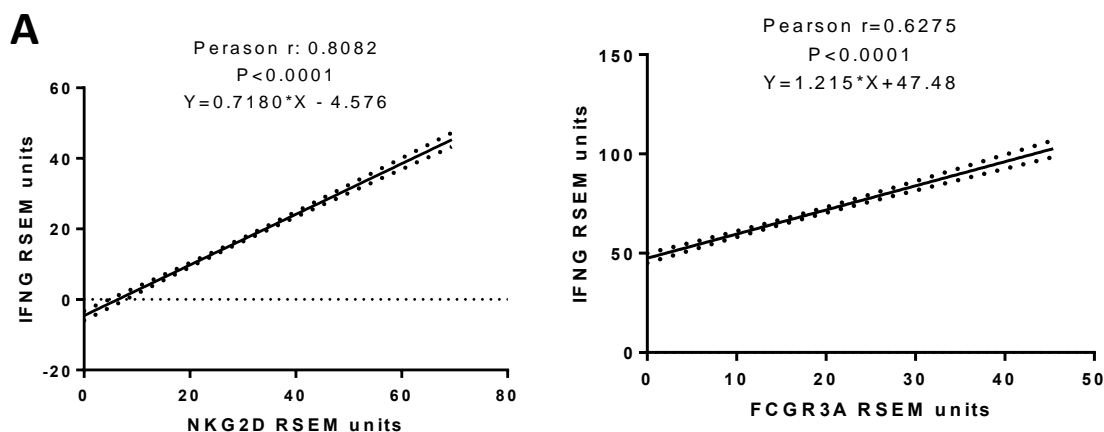


Figure 4.5.1 High frequency of circulating PD-1⁺ NK cells correlates with better survival of patient: A. Kaplan-Meier survival curve of 30 HNC patients whose PBL were harvested and PD-1 expression was determined on NK (shown in Figure 1A and B), the mean frequency of PD-1⁺ NK cells was set at a cutoff (mean 60.34%± 2.817) and % NK PD-1 high and low refers to frequency of PD-1⁺ NK cells above or below the mean value, respectively. Frequency of PD-1⁺ NK cells was correlated with disease free survival of patients, statistical significance was determined by log-rank Mantel-Cox test, P=0.18.



B

Correlation XY	Pearson r	P (two-tailed)
IFNG vs NKp46	0.5579	< 0.0001
IFNG vs NKp44	0.1824	< 0.0001
IFNG vs NKp30	0.5054	< 0.0001
PD-1 vs NKp44	0.2261	< 0.0001
PD-1 vs NKp30	0.6516	< 0.0001

Figure 4.5.2 IFN γ and PD-1 expression correlate with that of NK activation markers in HNC patients: **A.** IFN γ mRNA expression correlates with that of NKG2D, FCGR3A (Fc γ RIIIA). **B.** IFN γ mRNA expression correlates with that of NK activation markers NKp46, NKp44 and NKp30. Likewise, PD-1 mRNA expression correlates with that of other NK activation markers NKp40 and NKp30 in HNC tumor specimens. For all of the above data from 500 HNC tumor specimens were analyzed from the TCGA database. Correlation was determined by Pearson r test, graphs in A show linear regression curve fit.

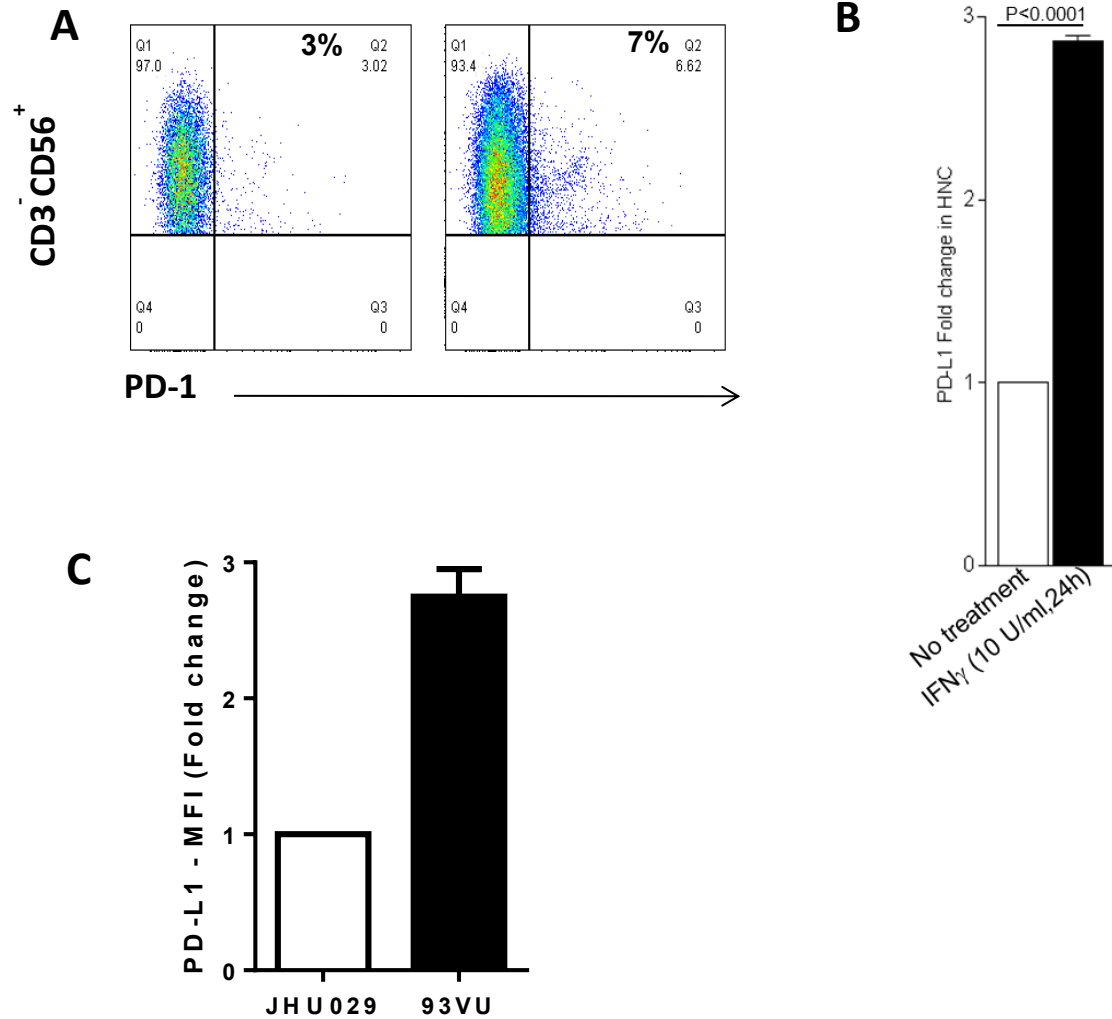


Figure 4.5.3 Increased frequency of PD-1⁺ NK cells in cetuximab-activated PBMC: A. Freshly isolated PBMC were co-cultured with JHU029 tumor cells in a 200:1 ratio in the absence of mAb or with cetuximab (10ug/mL) for 24h, the harvested and frequency of PD-1⁺ NK cells (CD3⁻CD56⁺) was determined by flow cytometry. **B.** IFN γ pre-treatment of target cells (JHU029) increases PD-L1 expression. JHU029 were treated with IFN γ (10IU/mL) for 24h, harvested and PD-L1 surface expression was determined by flow cytometry. **C. PD-L1 expression on JHU29 and 93VU tumor targets.** JHU029 and 93VU cells were harvested and PD-L1 expression was determined by flow cytometry. 93VU cells expresses 3 fold higher PD-L1 than JHU029 and were considered PD-L1^{high} in our experiments as compared to JHU029, which were considered PD-L1^{low}.

BIBLIOGRAPHY

1. Hanahan D, Weinberg RA. Hallmarks of cancer: the next generation. *Cell*. 2011;144:646-74.
2. Burnet FM. The concept of immunological surveillance. *Prog Exp Tumor Res*. 1970;13:1-27.
3. Burnet FM. Implications of immunological surveillance for cancer therapy. *Isr J Med Sci*. 1971;7:9-16.
4. Burnet M. Cancer; a biological approach. I. The processes of control. *Br Med J*. 1957;1:779-86.
5. Stutman O. Tumor development after 3-methylcholanthrene in immunologically deficient athymic-nude mice. *Science*. 1974;183:534-6.
6. Dunn GP, Koebel CM, Schreiber RD. Interferons, immunity and cancer immunoediting. *Nat Rev Immunol*. 2006;6:836-48.
7. Grivennikov SI, Greten FR, Karin M. Immunity, inflammation, and cancer. *Cell*. 2010;140:883-99.
8. Shankaran V, Ikeda H, Bruce AT, White JM, Swanson PE, Old LJ, et al. IFN γ and lymphocytes prevent primary tumour development and shape tumour immunogenicity. *Nature*. 2001;410:1107-11.
9. Schreiber RD, Old LJ, Smyth MJ. Cancer immunoediting: integrating immunity's roles in cancer suppression and promotion. *Science*. 2011;331:1565-70.
10. Diamond MS, Kinder M, Matsushita H, Mashayekhi M, Dunn GP, Archambault JM, et al. Type I interferon is selectively required by dendritic cells for immune rejection of tumors. *J Exp Med*. 2011;208:1989-2003.
11. Fuertes MB, Kacha AK, Kline J, Woo SR, Kranz DM, Murphy KM, et al. Host type I IFN signals are required for antitumor CD8⁺ T cell responses through CD8 α ⁺ dendritic cells. *J Exp Med*. 2011;208:2005-16.
12. Gasser S, Orsulic S, Brown EJ, Raulet DH. The DNA damage pathway regulates innate immune system ligands of the NKG2D receptor. *Nature*. 2005;436:1186-90.
13. Liu XV, Ho SS, Tan JJ, Kamran N, Gasser S. Ras activation induces expression of Raet1 family NK receptor ligands. *J Immunol*. 2012;189:1826-34.

14. Wu X, Peng M, Huang B, Zhang H, Wang H, Huang B, et al. Immune microenvironment profiles of tumor immune equilibrium and immune escape states of mouse sarcoma. *Cancer letters*. 2013;340:124-33.
15. Vesely MD, Kershaw MH, Schreiber RD, Smyth MJ. Natural innate and adaptive immunity to cancer. *Annual review of immunology*. 2011;29:235-71.
16. Gajewski TF, Fuertes M, Spaapen R, Zheng Y, Kline J. Molecular profiling to identify relevant immune resistance mechanisms in the tumor microenvironment. *Curr Opin Immunol*. 2011;23:286-92.
17. Mantovani A, Sica A. Macrophages, innate immunity and cancer: balance, tolerance, and diversity. *Curr Opin Immunol*. 2010;22:231-7.
18. Brahmer JR, Tykodi SS, Chow LQ, Hwu WJ, Topalian SL, Hwu P, et al. Safety and activity of anti-PD-L1 antibody in patients with advanced cancer. *The New England journal of medicine*. 2012;366:2455-65.
19. Topalian SL, Hodi FS, Brahmer JR, Gettinger SN, Smith DC, McDermott DF, et al. Safety, activity, and immune correlates of anti-PD-1 antibody in cancer. *The New England journal of medicine*. 2012;366:2443-54.
20. Wolchok JD, Kluger H, Callahan MK, Postow MA, Rizvi NA, Lesokhin AM, et al. Nivolumab plus ipilimumab in advanced melanoma. *The New England journal of medicine*. 2013;369:122-33.
21. White E, DiPaola RS. The double-edged sword of autophagy modulation in cancer. *Clin Cancer Res*. 2009;15:5308-16.
22. Tang D, Kang R, Coyne CB, Zeh HJ, Lotze MT. PAMPs and DAMPs: signal 0s that spur autophagy and immunity. *Immunol Rev*. 2012;249:158-75.
23. Ciechanover A. Intracellular protein degradation: from a vague idea thru the lysosome and the ubiquitin-proteasome system and onto human diseases and drug targeting. *Biochim Biophys Acta*. 2012;1824:3-13.
24. Watts C. The endosome-lysosome pathway and information generation in the immune system. *Biochim Biophys Acta*. 2012;1824:14-21.
25. Yewdell JW. Not such a dismal science: the economics of protein synthesis, folding, degradation and antigen processing. *Trends Cell Biol*. 2001;11:294-7.
26. Joffre OP, Segura E, Savina A, Amigorena S. Cross-presentation by dendritic cells. *Nat Rev Immunol*. 2012;12:557-69.

27. Koegl M, Hoppe T, Schlenker S, Ulrich HD, Mayer TU, Jentsch S. A novel ubiquitination factor, E4, is involved in multiubiquitin chain assembly. *Cell*. 1999;96:635-44.
28. Aki M, Shimbara N, Takashina M, Akiyama K, Kagawa S, Tamura T, et al. Interferon-gamma induces different subunit organizations and functional diversity of proteasomes. *J Biochem*. 1994;115:257-69.
29. Shin EC, Seifert U, Kato T, Rice CM, Feinstone SM, Kloetzel PM, et al. Virus-induced type I IFN stimulates generation of immunoproteasomes at the site of infection. *J Clin Invest*. 2006;116:3006-14.
30. Gaczynska M, Rock KL, Spies T, Goldberg AL. Peptidase activities of proteasomes are differentially regulated by the major histocompatibility complex-encoded genes for LMP2 and LMP7. *Proc Natl Acad Sci U S A*. 1994;91:9213-7.
31. Toes RE, Nussbaum AK, Degermann S, Schirle M, Emmerich NP, Kraft M, et al. Discrete cleavage motifs of constitutive and immunoproteasomes revealed by quantitative analysis of cleavage products. *J Exp Med*. 2001;194:1-12.
32. Arora S, Lapinski PE, Raghavan M. Use of chimeric proteins to investigate the role of transporter associated with antigen processing (TAP) structural domains in peptide binding and translocation. *Proc Natl Acad Sci U S A*. 2001;98:7241-6.
33. Higgins CF, Linton KJ. The ATP switch model for ABC transporters. *Nat Struct Mol Biol*. 2004;11:918-26.
34. Parcej D, Tampe R. ABC proteins in antigen translocation and viral inhibition. *Nat Chem Biol*. 2010;6:572-80.
35. Ortmann B, Androlewicz MJ, Cresswell P. MHC class I/beta 2-microglobulin complexes associate with TAP transporters before peptide binding. *Nature*. 1994;368:864-7.
36. Grandea AG, 3rd, Lehner PJ, Cresswell P, Spies T. Regulation of MHC class I heterodimer stability and interaction with TAP by tapasin. *Immunogenetics*. 1997;46:477-83.
37. Hatamoto S, Ohama K, Baba E, Awai A, Tominaga M. [Patients with limited life possibilities (1): support of cancer patients. Interactions with patients who suspected cancer]. *Kurinikaru Sutadi*. 1984;5:103-8.
38. Lehner PJ, Surman MJ, Cresswell P. Soluble tapasin restores MHC class I expression and function in the tapasin-negative cell line .220. *Immunity*. 1998;8:221-31.
39. Sant A, Yewdell J. Antigen processing and recognition. *Curr Opin Immunol*. 2003;15:66-8.

40. Meissner M, Reichert TE, Kunkel M, Gooding W, Whiteside TL, Ferrone S, et al. Defects in the human leukocyte antigen class I antigen processing machinery in head and neck squamous cell carcinoma: association with clinical outcome. *Clin Cancer Res.* 2005;11:2552-60.
41. Ogino T, Shigyo H, Ishii H, Katayama A, Miyokawa N, Harabuchi Y, et al. HLA class I antigen down-regulation in primary laryngeal squamous cell carcinoma lesions as a poor prognostic marker. *Cancer Res.* 2006;66:9281-9.
42. Liu Q, Hao C, Su P, Shi J. Down-regulation of HLA class I antigen-processing machinery components in esophageal squamous cell carcinomas: association with disease progression. *Scand J Gastroenterol.* 2009;44:960-9.
43. Qifeng S, Bo C, Xingtao J, Chuanliang P, Xiaogang Z. Methylation of the promoter of human leukocyte antigen class I in human esophageal squamous cell carcinoma and its histopathological characteristics. *J Thorac Cardiovasc Surg.* 2011;141:808-14.
44. Ayshamgul H, Ma H, Ilyar S, Zhang LW, Abulizi A. Association of defective HLA-I expression with antigen processing machinery and their association with clinicopathological characteristics in Kazak patients with esophageal cancer. *Chin Med J (Engl).* 2011;124:341-6.
45. Hirata T, Yamamoto H, Taniguchi H, Horiuchi S, Oki M, Adachi Y, et al. Characterization of the immune escape phenotype of human gastric cancers with and without high-frequency microsatellite instability. *J Pathol.* 2007;211:516-23.
46. Kloor M, Becker C, Benner A, Woerner SM, Gebert J, Ferrone S, et al. Immunoselective pressure and human leukocyte antigen class I antigen machinery defects in microsatellite unstable colorectal cancers. *Cancer Res.* 2005;65:6418-24.
47. Atkins D, Breuckmann A, Schmahl GE, Binner P, Ferrone S, Krummenauer F, et al. MHC class I antigen processing pathway defects, ras mutations and disease stage in colorectal carcinoma. *Int J Cancer.* 2004;109:265-73.
48. Dierssen JW, de Miranda NF, Ferrone S, van Puijenbroek M, Cornelisse CJ, Fleuren GJ, et al. HNPCC versus sporadic microsatellite-unstable colon cancers follow different routes toward loss of HLA class I expression. *BMC Cancer.* 2007;7:33.
49. Romero JM, Jimenez P, Cabrera T, Cozar JM, Pedrinaci S, Tallada M, et al. Coordinated downregulation of the antigen presentation machinery and HLA class I/beta2-microglobulin complex is responsible for HLA-ABC loss in bladder cancer. *Int J Cancer.* 2005;113:605-10.
50. Cathro HP, Smolkin ME, Theodorescu D, Jo VY, Ferrone S, Frierson HF, Jr. Relationship between HLA class I antigen processing machinery component expression and the clinicopathologic characteristics of bladder carcinomas. *Cancer Immunol Immunother.* 2010;59:465-72.

51. Seliger B, Stoehr R, Handke D, Mueller A, Ferrone S, Wullich B, et al. Association of HLA class I antigen abnormalities with disease progression and early recurrence in prostate cancer. *Cancer Immunol Immunother.* 2010;59:529-40.
52. Kageshita T, Hirai S, Ono T, Hicklin DJ, Ferrone S. Down-regulation of HLA class I antigen-processing molecules in malignant melanoma: association with disease progression. *Am J Pathol.* 1999;154:745-54.
53. Kamarashev J, Ferrone S, Seifert B, Boni R, Nestle FO, Burg G, et al. TAP1 down-regulation in primary melanoma lesions: an independent marker of poor prognosis. *Int J Cancer.* 2001;95:23-8.
54. Hasim A, Abudula M, Aimiduo R, Ma JQ, Jiao Z, Akula G, et al. Post-transcriptional and epigenetic regulation of antigen processing machinery (APM) components and HLA-I in cervical cancers from Uighur women. *PLoS One.* 2012;7:e44952.
55. Dovhey SE, Ghosh NS, Wright KL. Loss of interferon-gamma inducibility of TAP1 and LMP2 in a renal cell carcinoma cell line. *Cancer Res.* 2000;60:5789-96.
56. Respa A, Bukur J, Ferrone S, Pawelec G, Zhao Y, Wang E, et al. Association of IFN-gamma signal transduction defects with impaired HLA class I antigen processing in melanoma cell lines. *Clin Cancer Res.* 2011;17:2668-78.
57. Bandoh N, Ogino T, Katayama A, Takahara M, Katada A, Hayashi T, et al. HLA class I antigen and transporter associated with antigen processing downregulation in metastatic lesions of head and neck squamous cell carcinoma as a marker of poor prognosis. *Oncol Rep.* 2010;23:933-9.
58. Feenstra M, Veltkamp M, van Kuik J, Wiertsema S, Slootweg P, van den Tweel J, et al. HLA class I expression and chromosomal deletions at 6p and 15q in head and neck squamous cell carcinomas. *Tissue Antigens.* 1999;54:235-45.
59. Lopez-Albaitero A, Nayak JV, Ogino T, Machandia A, Gooding W, DeLeo AB, et al. Role of antigen-processing machinery in the in vitro resistance of squamous cell carcinoma of the head and neck cells to recognition by CTL. *J Immunol.* 2006;176:3402-9.
60. Pandha H, Rigg A, John J, Lemoine N. Loss of expression of antigen-presenting molecules in human pancreatic cancer and pancreatic cancer cell lines. *Clin Exp Immunol.* 2007;148:127-35.
61. Dissemmond J, Gotte P, Mors J, Lindeke A, Goos M, Ferrone S, et al. Association of TAP1 downregulation in human primary melanoma lesions with lack of spontaneous regression. *Melanoma Res.* 2003;13:253-8.

62. Seliger B, Ritz U, Abele R, Bock M, Tampe R, Sutter G, et al. Immune escape of melanoma: first evidence of structural alterations in two distinct components of the MHC class I antigen processing pathway. *Cancer Res.* 2001;61:8647-50.
63. Yang T, McNally BA, Ferrone S, Liu Y, Zheng P. A single-nucleotide deletion leads to rapid degradation of TAP-1 mRNA in a melanoma cell line. *J Biol Chem.* 2003;278:15291-6.
64. Ayalon O, Hughes EA, Cresswell P, Lee J, O'Donnell L, Pardi R, et al. Induction of transporter associated with antigen processing by interferon gamma confers endothelial cell cytoprotection against natural killer-mediated lysis. *Proc Natl Acad Sci U S A.* 1998;95:2435-40.
65. Ma W, Lehner PJ, Cresswell P, Pober JS, Johnson DR. Interferon-gamma rapidly increases peptide transporter (TAP) subunit expression and peptide transport capacity in endothelial cells. *J Biol Chem.* 1997;272:16585-90.
66. Ferris RL, Whiteside TL, Ferrone S. Immune escape associated with functional defects in antigen-processing machinery in head and neck cancer. *Clinical cancer research : an official journal of the American Association for Cancer Research.* 2006;12:3890-5.
67. Mehta AM, Jordanova ES, van Wezel T, Uh HW, Corver WE, Kwappenberg KM, et al. Genetic variation of antigen processing machinery components and association with cervical carcinoma. *Genes Chromosomes Cancer.* 2007;46:577-86.
68. Fowler NL, Frazer IH. Mutations in TAP genes are common in cervical carcinomas. *Gynecol Oncol.* 2004;92:914-21.
69. Chen HL, Gabrilovich D, Tampe R, Girgis KR, Nadaf S, Carbone DP. A functionally defective allele of TAP1 results in loss of MHC class I antigen presentation in a human lung cancer. *Nat Genet.* 1996;13:210-3.
70. Ogino T, Bandoh N, Hayashi T, Miyokawa N, Harabuchi Y, Ferrone S. Association of tapasin and HLA class I antigen down-regulation in primary maxillary sinus squamous cell carcinoma lesions with reduced survival of patients. *Clin Cancer Res.* 2003;9:4043-51.
71. Liu Y, Komohara Y, Domenick N, Ohno M, Ikeura M, Hamilton RL, et al. Expression of antigen processing and presenting molecules in brain metastasis of breast cancer. *Cancer Immunol Immunother.* 2012;61:789-801.
72. Chang CC, Pirozzi G, Wen SH, Chung IH, Chiu BL, Errico S, et al. Multiple Structural and Epigenetic Defects in the Human Leukocyte Antigen Class I Antigen Presentation Pathway in a Recurrent Metastatic Melanoma Following Immunotherapy. *J Biol Chem.* 2015;290:26562-75.

73. Tang Q, Zhang J, Qi B, Shen C, Xie W. Downregulation of HLA class I molecules in primary oral squamous cell carcinomas and cell lines. *Arch Med Res.* 2009;40:256-63.
74. Yamamoto H, Perez-Piteira J, Yoshida T, Terada M, Itoh F, Imai K, et al. Gastric cancers of the microsatellite mutator phenotype display characteristic genetic and clinical features. *Gastroenterology.* 1999;116:1348-57.
75. de Miranda NF, Nielsen M, Pereira D, van Puijenbroek M, Vasen HF, Hes FJ, et al. MUTYH-associated polyposis carcinomas frequently lose HLA class I expression - a common event amongst DNA-repair-deficient colorectal cancers. *J Pathol.* 2009;219:69-76.
76. Bicknell DC, Kaklamanis L, Hampson R, Bodmer WF, Karran P. Selection for beta 2-microglobulin mutation in mismatch repair-defective colorectal carcinomas. *Curr Biol.* 1996;6:1695-7.
77. Cabrera T, Collado A, Fernandez MA, Ferron A, Sancho J, Ruiz-Cabello F, et al. High frequency of altered HLA class I phenotypes in invasive colorectal carcinomas. *Tissue Antigens.* 1998;52:114-23.
78. Cabrera T, Maleno I, Collado A, Lopez Nevot MA, Tait BD, Garrido F. Analysis of HLA class I alterations in tumors: choosing a strategy based on known patterns of underlying molecular mechanisms. *Tissue Antigens.* 2007;69 Suppl 1:264-8.
79. White CA, Thomson SA, Cooper L, van Endert PM, Tampe R, Coupar B, et al. Constitutive transduction of peptide transporter and HLA genes restores antigen processing function and cytotoxic T cell-mediated immune recognition of human melanoma cells. *Int J Cancer.* 1998;75:590-5.
80. Maleno I, Lopez-Nevot MA, Cabrera T, Salinero J, Garrido F. Multiple mechanisms generate HLA class I altered phenotypes in laryngeal carcinomas: high frequency of HLA haplotype loss associated with loss of heterozygosity in chromosome region 6p21. *Cancer Immunol Immunother.* 2002;51:389-96.
81. Cabrera T, Salinero J, Fernandez MA, Garrido A, Esquivias J, Garrido F. High frequency of altered HLA class I phenotypes in laryngeal carcinomas. *Hum Immunol.* 2000;61:499-506.
82. Seliger B. Molecular mechanisms of MHC class I abnormalities and APM components in human tumors. *Cancer Immunol Immunother.* 2008;57:1719-26.
83. Quezada SA, Jarvinen LZ, Lind EF, Noelle RJ. CD40/CD154 interactions at the interface of tolerance and immunity. *Annual review of immunology.* 2004;22:307-28.

84. Freeman GJ, Gribben JG, Boussiotis VA, Ng JW, Restivo VA, Jr., Lombard LA, et al. Cloning of B7-2: a CTLA-4 counter-receptor that costimulates human T cell proliferation. *Science*. 1993;262:909-11.
85. Larsen CP, Ritchie SC, Hendrix R, Linsley PS, Hathcock KS, Hodes RJ, et al. Regulation of immunostimulatory function and costimulatory molecule (B7-1 and B7-2) expression on murine dendritic cells. *J Immunol*. 1994;152:5208-19.
86. Keir ME, Butte MJ, Freeman GJ, Sharpe AH. PD-1 and its ligands in tolerance and immunity. *Annual review of immunology*. 2008;26:677-704.
87. Dong H, Zhu G, Tamada K, Chen L. B7-H1, a third member of the B7 family, costimulates T-cell proliferation and interleukin-10 secretion. *Nature medicine*. 1999;5:1365-9.
88. Nguyen LT, Radhakrishnan S, Ciric B, Tamada K, Shin T, Pardoll DM, et al. Cross-linking the B7 family molecule B7-DC directly activates immune functions of dendritic cells. *J Exp Med*. 2002;196:1393-8.
89. Agata Y, Kawasaki A, Nishimura H, Ishida Y, Tsubata T, Yagita H, et al. Expression of the PD-1 antigen on the surface of stimulated mouse T and B lymphocytes. *International immunology*. 1996;8:765-72.
90. Nishimura H, Agata Y, Kawasaki A, Sato M, Imamura S, Minato N, et al. Developmentally regulated expression of the PD-1 protein on the surface of double-negative (CD4-CD8-) thymocytes. *International immunology*. 1996;8:773-80.
91. Nishimura H, Honjo T, Minato N. Facilitation of beta selection and modification of positive selection in the thymus of PD-1-deficient mice. *J Exp Med*. 2000;191:891-8.
92. Ansari MJ, Salama AD, Chitnis T, Smith RN, Yagita H, Akiba H, et al. The programmed death-1 (PD-1) pathway regulates autoimmune diabetes in nonobese diabetic (NOD) mice. *J Exp Med*. 2003;198:63-9.
93. Probst HC, McCoy K, Okazaki T, Honjo T, van den Broek M. Resting dendritic cells induce peripheral CD8+ T cell tolerance through PD-1 and CTLA-4. *Nat Immunol*. 2005;6:280-6.
94. Dong H, Strome SE, Salomao DR, Tamura H, Hirano F, Flies DB, et al. Tumor-associated B7-H1 promotes T-cell apoptosis: a potential mechanism of immune evasion. *Nature medicine*. 2002;8:793-800.
95. Tseng SY, Otsuji M, Gorski K, Huang X, Slansky JE, Pai SI, et al. B7-DC, a new dendritic cell molecule with potent costimulatory properties for T cells. *J Exp Med*. 2001;193:839-46.

96. Wang L, Pino-Lagos K, de Vries VC, Guleria I, Sayegh MH, Noelle RJ. Programmed death 1 ligand signaling regulates the generation of adaptive Foxp3+CD4+ regulatory T cells. *Proc Natl Acad Sci U S A*. 2008;105:9331-6.
97. Iwai Y, Ishida M, Tanaka Y, Okazaki T, Honjo T, Minato N. Involvement of PD-L1 on tumor cells in the escape from host immune system and tumor immunotherapy by PD-L1 blockade. *Proc Natl Acad Sci U S A*. 2002;99:12293-7.
98. Sauer S, Bruno L, Hertweck A, Finlay D, Leleu M, Spivakov M, et al. T cell receptor signaling controls Foxp3 expression via PI3K, Akt, and mTOR. *Proc Natl Acad Sci U S A*. 2008;105:7797-802.
99. Terme M, Ullrich E, Aymeric L, Meinhardt K, Coudert JD, Desbois M, et al. Cancer-induced immunosuppression: IL-18-elicited immunoablative NK cells. *Cancer Res*. 2012;72:2757-67.
100. Lee SC, Srivastava RM, Lopez-Albaitero A, Ferrone S, Ferris RL. Natural killer (NK): dendritic cell (DC) cross talk induced by therapeutic monoclonal antibody triggers tumor antigen-specific T cell immunity. *Immunol Res*. 2011;50:248-54.
101. Srivastava RM, Lee SC, Andrade Filho PA, Lord CA, Jie HB, Davidson HC, et al. Cetuximab-activated natural killer and dendritic cells collaborate to trigger tumor antigen-specific T-cell immunity in head and neck cancer patients. *Clin Cancer Res*. 2013;19:1858-72.
102. Li J, Jie HB, Lei Y, Gildener-Leapman N, Trivedi S, Green T, et al. PD-1/SHP-2 inhibits Tc1/Th1 phenotypic responses and the activation of T cells in the tumor microenvironment. *Cancer Res*. 2015;75:508-18.
103. Okazaki T, Honjo T. PD-1 and PD-1 ligands: from discovery to clinical application. *International immunology*. 2007;19:813-24.
104. Balkwill F, Mantovani A. Inflammation and cancer: back to Virchow? *Lancet*. 2001;357:539-45.
105. Hussain SP, Harris CC. Inflammation and cancer: an ancient link with novel potentials. *Int J Cancer*. 2007;121:2373-80.
106. Bates RC, Mercurio AM. Tumor necrosis factor-alpha stimulates the epithelial-to-mesenchymal transition of human colonic organoids. *Mol Biol Cell*. 2003;14:1790-800.
107. Camoglio L, Te Velde AA, Tigges AJ, Das PK, Van Deventer SJ. Altered expression of interferon-gamma and interleukin-4 in inflammatory bowel disease. *Inflamm Bowel Dis*. 1998;4:285-90.
108. Bruewer M, Luegering A, Kucharzik T, Parkos CA, Madara JL, Hopkins AM, et al. Proinflammatory cytokines disrupt epithelial barrier function by apoptosis-independent mechanisms. *J Immunol*. 2003;171:6164-72.

109. Morrison CD, Parvani JG, Schiemann WP. The relevance of the TGF-beta Paradox to EMT-MET programs. *Cancer letters*. 2013;341:30-40.
110. Yang L, Pang Y, Moses HL. TGF-beta and immune cells: an important regulatory axis in the tumor microenvironment and progression. *Trends Immunol*. 2010;31:220-7.
111. Kim BG, Li C, Qiao W, Mamura M, Kasprzak B, Anver M, et al. Smad4 signalling in T cells is required for suppression of gastrointestinal cancer. *Nature*. 2006;441:1015-9.
112. Hodge DR, Hurt EM, Farrar WL. The role of IL-6 and STAT3 in inflammation and cancer. *Eur J Cancer*. 2005;41:2502-12.
113. Braun DA, Fribourg M, Sealfon SC. Cytokine response is determined by duration of receptor and signal transducers and activators of transcription 3 (STAT3) activation. *J Biol Chem*. 2013;288:2986-93.
114. Erdman SE, Rao VP, Poutahidis T, Ihrig MM, Ge Z, Feng Y, et al. CD4(+)CD25(+) regulatory lymphocytes require interleukin 10 to interrupt colon carcinogenesis in mice. *Cancer Res*. 2003;63:6042-50.
115. Chang KJ, Reid T, Senzer N, Swisher S, Pinto H, Hanna N, et al. Phase I evaluation of TNFerade biologic plus chemoradiotherapy before esophagectomy for locally advanced resectable esophageal cancer. *Gastrointest Endosc*. 2012;75:1139-46 e2.
116. Kesselring R, Thiel A, Pries R, Trenkle T, Wollenberg B. Human Th17 cells can be induced through head and neck cancer and have a functional impact on HNSCC development. *British journal of cancer*. 2010;103:1245-54.
117. Chung AS, Wu X, Zhuang G, Ngu H, Kasman I, Zhang J, et al. An interleukin-17-mediated paracrine network promotes tumor resistance to anti-angiogenic therapy. *Nature medicine*. 2013;19:1114-23.
118. Burkholder B, Huang RY, Burgess R, Luo S, Jones VS, Zhang W, et al. Tumor-induced perturbations of cytokines and immune cell networks. *Biochim Biophys Acta*. 2014;1845:182-201.
119. Zhang Q, Bhola NE, Lui VW, Siwak DR, Thomas SM, Gubish CT, et al. Antitumor mechanisms of combined gastrin-releasing peptide receptor and epidermal growth factor receptor targeting in head and neck cancer. *Mol Cancer Ther*. 2007;6:1414-24.
120. Khuri FR, Nemunaitis J, Ganly I, Arseneau J, Tannock IF, Romel L, et al. a controlled trial of intratumoral ONYX-015, a selectively-replicating adenovirus, in combination with cisplatin and 5-fluorouracil in patients with recurrent head and neck cancer. *Nature medicine*. 2000;6:879-85.

121. Grandis JR, Tweardy DJ. Elevated levels of transforming growth factor alpha and epidermal growth factor receptor messenger RNA are early markers of carcinogenesis in head and neck cancer. *Cancer Res.* 1993;53:3579-84.
122. Rubin Grandis J, Melhem MF, Gooding WE, Day R, Holst VA, Wagener MM, et al. Levels of TGF-alpha and EGFR protein in head and neck squamous cell carcinoma and patient survival. *J Natl Cancer Inst.* 1998;90:824-32.
123. Harari PM, Allen GW, Bonner JA. Biology of interactions: antiepidermal growth factor receptor agents. *Journal of clinical oncology : official journal of the American Society of Clinical Oncology.* 2007;25:4057-65.
124. Song JI, Grandis JR. STAT signaling in head and neck cancer. *Oncogene.* 2000;19:2489-95.
125. Schrupp DS, Nguyen DM. The epidermal growth factor receptor-STAT pathway in esophageal cancer. *Cancer J.* 2001;7:108-11.
126. Kijima T, Niwa H, Steinman RA, Drenning SD, Gooding WE, Wentzel AL, et al. STAT3 activation abrogates growth factor dependence and contributes to head and neck squamous cell carcinoma tumor growth in vivo. *Cell growth & differentiation : the molecular biology journal of the American Association for Cancer Research.* 2002;13:355-62.
127. Grandis JR, Drenning SD, Chakraborty A, Zhou MY, Zeng Q, Pitt AS, et al. Requirement of Stat3 but not Stat1 activation for epidermal growth factor receptor-mediated cell growth In vitro. *J Clin Invest.* 1998;102:1385-92.
128. Leeman RJ, Lui VW, Grandis JR. STAT3 as a therapeutic target in head and neck cancer. *Expert opinion on biological therapy.* 2006;6:231-41.
129. Regis G, Pensa S, Boselli D, Novelli F, Poli V. Ups and downs: the STAT1:STAT3 seesaw of Interferon and gp130 receptor signalling. *Seminars in cell & developmental biology.* 2008;19:351-9.
130. Fletcher S, Drewry JA, Shahani VM, Page BD, Gunning PT. Molecular disruption of oncogenic signal transducer and activator of transcription 3 (STAT3) protein. *Biochemistry and cell biology = Biochimie et biologie cellulaire.* 2009;87:825-33.
131. Zhang X, Zhang J, Wang L, Wei H, Tian Z. Therapeutic effects of STAT3 decoy oligodeoxynucleotide on human lung cancer in xenograft mice. *BMC Cancer.* 2007;7:149.

132. Lee TL, Yeh J, Van Waes C, Chen Z. Epigenetic modification of SOCS-1 differentially regulates STAT3 activation in response to interleukin-6 receptor and epidermal growth factor receptor signaling through JAK and/or MEK in head and neck squamous cell carcinomas. *Mol Cancer Ther* 2006;5:8-19.
133. Shim SH, Sung MW, Park SW, Heo DS. Absence of STAT1 disturbs the anticancer effect induced by STAT3 inhibition in head and neck carcinoma cell lines. *Int J Mol Med*. 2009;23:805-10.
134. Harry BL, Eckhardt SG, Jimeno A. JAK2 inhibition for the treatment of hematologic and solid malignancies. *Expert Opin Investig Drugs*. 2012;21:637-55.
135. Purandare AV, McDevitt TM, Wan H, You D, Penhallow B, Han X, et al. Characterization of BMS-911543, a functionally selective small-molecule inhibitor of JAK2. *Leukemia : official journal of the Leukemia Society of America, Leukemia Research Fund, UK*. 2012;26:280-8.
136. Mandic R, Rodgarkia-Dara CJ, Zhu L, Folz BJ, Bette M, Weihe E, et al. Treatment of HNSCC cell lines with the EGFR-specific inhibitor cetuximab (Erbix) results in paradox phosphorylation of tyrosine 1173 in the receptor. *FEBS letters*. 2006;580:4793-800.
137. Lopez-Albaitero A, Ferris RL. Immune activation by epidermal growth factor receptor specific monoclonal antibody therapy for head and neck cancer. *Archives of otolaryngology--head & neck surgery*. 2007;133:1277-81.
138. Lopez-Albaitero A, Lee SC, Morgan S, Grandis JR, Gooding WE, Ferrone S, et al. Role of polymorphic Fc gamma receptor IIIa and EGFR expression level in cetuximab mediated, NK cell dependent in vitro cytotoxicity of head and neck squamous cell carcinoma cells. *Cancer Immunol Immunother*. 2009;58:1853-64.
139. Taylor RJ, Chan SL, Wood A, Voskens CJ, Wolf JS, Lin W, et al. Fc gamma RIIIa polymorphisms and cetuximab induced cytotoxicity in squamous cell carcinoma of the head and neck. *Cancer Immunol Immunother*. 2009;58:997-1006.
140. Marechal R, De Schutter J, Nagy N, Demetter P, Lemmers A, Deviere J, et al. Putative contribution of CD56 positive cells in cetuximab treatment efficacy in first-line metastatic colorectal cancer patients. *BMC Cancer*. 2010;10:340.
141. Banerjee D, Matthews P, Matayeva E, Kaufman JL, Steinman RM, Dhodapkar KM. Enhanced T-cell responses to glioma cells coated with the anti-EGF receptor antibody and targeted to activating Fc gamma Rs on human dendritic cells. *J Immunother*. 2008;31:113-20.
142. Harbers SO, Crocker A, Catalano G, D'Agati V, Jung S, Desai DD, et al. Antibody-enhanced cross-presentation of self antigen breaks T cell tolerance. *J Clin Invest*. 2007;117:1361-9.

143. Rafiq K, Bergtold A, Clynes R. Immune complex-mediated antigen presentation induces tumor immunity. *J Clin Invest.* 2002;110:71-9.
144. Bonner JA, Harari PM, Giralt J, Azarnia N, Shin DM, Cohen RB, et al. Radiotherapy plus cetuximab for squamous-cell carcinoma of the head and neck. *The New England journal of medicine.* 2006;354:567-78.
145. Vermorken JB, Mesia R, Rivera F, Remenar E, Kawecki A, Rottey S, et al. Platinum-based chemotherapy plus cetuximab in head and neck cancer. *The New England journal of medicine.* 2008;359:1116-27.
146. Vermorken JB, Trigo J, Hitt R, Koralewski P, Diaz-Rubio E, Rolland F, et al. Open-label, uncontrolled, multicenter phase II study to evaluate the efficacy and toxicity of cetuximab as a single agent in patients with recurrent and/or metastatic squamous cell carcinoma of the head and neck who failed to respond to platinum-based therapy. *Journal of clinical oncology : official journal of the American Society of Clinical Oncology.* 2007;25:2171-7.
147. Baselga J, Trigo JM, Bourhis J, Tortochaux J, Cortes-Funes H, Hitt R, et al. Phase II multicenter study of the antiepidermal growth factor receptor monoclonal antibody cetuximab in combination with platinum-based chemotherapy in patients with platinum-refractory metastatic and/or recurrent squamous cell carcinoma of the head and neck. *Journal of clinical oncology : official journal of the American Society of Clinical Oncology.* 2005;23:5568-77.
148. Herbst RS, Arquette M, Shin DM, Dicke K, Vokes EE, Azarnia N, et al. Phase II multicenter study of the epidermal growth factor receptor antibody cetuximab and cisplatin for recurrent and refractory squamous cell carcinoma of the head and neck. *Journal of clinical oncology : official journal of the American Society of Clinical Oncology.* 2005;23:5578-87.
149. Leibowitz MS, Andrade Filho PA, Ferrone S, Ferris RL. Deficiency of activated STAT1 in head and neck cancer cells mediates TAP1-dependent escape from cytotoxic T lymphocytes. *Cancer Immunol Immunother.* 2011;60:525-35.
150. Leibowitz MS, Srivastava RM, Andrade Filho PA, Egloff AM, Wang L, Seethala RR, et al. SHP2 is overexpressed and inhibits pSTAT1-mediated APM component expression, T-cell attracting chemokine secretion, and CTL recognition in head and neck cancer cells. *Clinical cancer research : an official journal of the American Association for Cancer Research.* 2013;19:798-808.
151. Lee SK, Seo SH, Kim BS, Kim CD, Lee JH, Kang JS, et al. IFN-gamma regulates the expression of B7-H1 in dermal fibroblast cells. *J Dermatol Sci.* 2005;40:95-103.

152. Han SJ, Ahn BJ, Waldron JS, Yang I, Fang S, Crane CA, et al. Gamma interferon-mediated superinduction of B7-H1 in PTEN-deficient glioblastoma: a paradoxical mechanism of immune evasion. *Neuroreport*. 2009;20:1597-602.
153. Liu J, Hamrouni A, Wolowiec D, Coiteux V, Kuliczowski K, Hetuin D, et al. Plasma cells from multiple myeloma patients express B7-H1 (PD-L1) and increase expression after stimulation with IFN- γ and TLR ligands via a MyD88-, TRAF6-, and MEK-dependent pathway. *Blood*. 2007;110:296-304.
154. Dunn GP, Old LJ, Schreiber RD. The three Es of cancer immunoediting. *Annual review of immunology*. 2004;22:329-60.
155. Jie HB, Gildener-Leapman N, Li J, Srivastava RM, Gibson SP, Whiteside TL, et al. Intratumoral regulatory T cells upregulate immunosuppressive molecules in head and neck cancer patients. *British journal of cancer*. 2013;109:2629-35.
156. Pardoll DM. The blockade of immune checkpoints in cancer immunotherapy. *Nature reviews Cancer*. 2012;12:252-64.
157. Lyford-Pike S, Peng S, Young GD, Taube JM, Westra WH, Akpeng B, et al. Evidence for a role of the PD-1:PD-L1 pathway in immune resistance of HPV-associated head and neck squamous cell carcinoma. *Cancer Res*. 2013;73:1733-41.
158. Topalian SL, Drake CG, Pardoll DM. Targeting the PD-1/B7-H1(PD-L1) pathway to activate anti-tumor immunity. *Curr Opin Immunol*. 2012;24:207-12.
159. Taube JM, Klein A, Brahmer JR, Xu H, Pan X, Kim JH, et al. Association of PD-1, PD-1 ligands, and other features of the tumor immune microenvironment with response to anti-PD-1 therapy. *Clin Cancer Res*. 2014;20:5064-74.
160. Seiwert TY, Burtneß B, Weiss J, Gluck I, Eder JP, Pai SI, et al. A phase Ib study of MK-3475 in patients with human papillomavirus (HPV)-associated and non-HPV-associated head and neck (H/N) cancer. *ASCO Meeting Abstracts*. 2014;32:6011.
161. Ramqvist T, Dalianis T. Oropharyngeal cancer epidemic and human papillomavirus. *Emerging infectious diseases*. 2010;16:1671-7.
162. Chung CH, Gillison ML. Human papillomavirus in head and neck cancer: its role in pathogenesis and clinical implications. *Clinical cancer research : an official journal of the American Association for Cancer Research*. 2009;15:6758-62.
163. Fischer CA, Zlobec I, Green E, Probst S, Storck C, Lugli A, et al. Is the improved prognosis of p16 positive oropharyngeal squamous cell carcinoma dependent of the treatment modality? *International journal of cancer Journal international du cancer*. 2010;126:1256-62.

164. Spanos WC, Nowicki P, Lee DW, Hoover A, Hostager B, Gupta A, et al. Immune response during therapy with cisplatin or radiation for human papillomavirus-related head and neck cancer. *Archives of otolaryngology--head & neck surgery*. 2009;135:1137-46.
165. Badoual C, Hans S, Merillon N, Van Ryswick C, Ravel P, Benhamouda N, et al. PD-1-expressing tumor-infiltrating T cells are a favorable prognostic biomarker in HPV-associated head and neck cancer. *Cancer Res*. 2013;73:128-38.
166. Parsa AT, Waldron JS, Panner A, Crane CA, Parney IF, Barry JJ, et al. Loss of tumor suppressor PTEN function increases B7-H1 expression and immunoresistance in glioma. *Nature medicine*. 2007;13:84-8.
167. Azuma K, Ota K, Kawahara A, Hattori S, Iwama E, Harada T, et al. Association of PD-L1 overexpression with activating EGFR mutations in surgically resected nonsmall-cell lung cancer. *Ann Oncol*. 2014;25:1935-40.
168. Akbay EA, Koyama S, Carretero J, Altabef A, Tchaicha JH, Christensen CL, et al. Activation of the PD-1 pathway contributes to immune escape in EGFR-driven lung tumors. *Cancer discovery*. 2013;3:1355-63.
169. Maiti GP, Mondal P, Mukherjee N, Ghosh A, Ghosh S, Dey S, et al. Overexpression of EGFR in head and neck squamous cell carcinoma is associated with inactivation of SH3GL2 and CDC25A genes. *PLoS One*. 2013;8:e63440.
170. Zhao M, Sano D, Pickering CR, Jasser SA, Henderson YC, Clayman GL, et al. Assembly and initial characterization of a panel of 85 genomically validated cell lines from diverse head and neck tumor sites. *Clin Cancer Res*. 2011;17:7248-64.
171. Heo DS, Snyderman C, Gollin SM, Pan S, Walker E, Deka R, et al. Biology, cytogenetics, and sensitivity to immunological effector cells of new head and neck squamous cell carcinoma lines. *Cancer Res*. 1989;49:5167-75.
172. Curiel TJ, Wei S, Dong H, Alvarez X, Cheng P, Mottram P, et al. Blockade of B7-H1 improves myeloid dendritic cell-mediated antitumor immunity. *Nature medicine*. 2003;9:562-7.
173. Chikamatsu K, Sakakura K, Toyoda M, Takahashi K, Yamamoto T, Masuyama K. Immunosuppressive activity of CD14+ HLA-DR- cells in squamous cell carcinoma of the head and neck. *Cancer science*. 2012;103:976-83.
174. Schmitt NC, Trivedi S, Ferris RL. STAT1 Activation Is Enhanced by Cisplatin and Variably Affected by EGFR Inhibition in HNSCC Cells. *Mol Cancer Ther*. 2015;14:2103-11.

175. Krutzik PO, Nolan GP. Intracellular phospho-protein staining techniques for flow cytometry: monitoring single cell signaling events. *Cytometry Part A : the journal of the International Society for Analytical Cytology*. 2003;55:61-70.
176. Haring M, Offermann S, Danker T, Horst I, Peterhansel C, Stam M. Chromatin immunoprecipitation: optimization, quantitative analysis and data normalization. *Plant Methods*. 2007;3:11.
177. Chen BJ, Chapuy B, Ouyang J, Sun HH, Roemer MG, Xu ML, et al. PD-L1 expression is characteristic of a subset of aggressive B-cell lymphomas and virus-associated malignancies. *Clin Cancer Res*. 2013;19:3462-73.
178. Cancer Genome Atlas N. Comprehensive genomic characterization of head and neck squamous cell carcinomas. *Nature*. 2015;517:576-82.
179. Li B, Dewey CN. RSEM: accurate transcript quantification from RNA-Seq data with or without a reference genome. *BMC bioinformatics*. 2011;12:323.
180. Kel AE, Gossling E, Reuter I, Cheremushkin E, Kel-Margoulis OV, Wingender E. MATCH: A tool for searching transcription factor binding sites in DNA sequences. *Nucleic acids research*. 2003;31:3576-9.
181. Purandare AV, McDevitt TM, Wan H, You D, Penhallow B, Han X, et al. Characterization of BMS-911543, a functionally selective small-molecule inhibitor of JAK2. *Leukemia*. 2012;26:280-8.
182. Ukpo OC, Thorstad WL, Lewis JS, Jr. B7-H1 expression model for immune evasion in human papillomavirus-related oropharyngeal squamous cell carcinoma. *Head and neck pathology*. 2013;7:113-21.
183. Malm IJ, Bruno TC, Fu J, Zeng Q, Taube JM, Westra W, et al. Expression profile and in vitro blockade of programmed death-1 in human papillomavirus-negative head and neck squamous cell carcinoma. *Head & neck*. 2014.
184. Ramkissoon SH, Bi WL, Schumacher SE, Ramkissoon LA, Haidar S, Knoff D, et al. Clinical implementation of integrated whole-genome copy number and mutation profiling for glioblastoma. *Neuro Oncol*. 2015;17:1344-55.
185. McBride SM, Rothenberg SM, Faquin WC, Chan AW, Clark JR, Ellisen LW, et al. Mutation frequency in 15 common cancer genes in high-risk head and neck squamous cell carcinoma. *Head & neck*. 2014;36:1181-8.
186. Stransky N, Egloff AM, Tward AD, Kostic AD, Cibulskis K, Sivachenko A, et al. The mutational landscape of head and neck squamous cell carcinoma. *Science*. 2011;333:1157-60.

187. Sen M, Pollock NI, Black J, DeGrave KA, Wheeler S, Freilino ML, et al. JAK kinase inhibition abrogates STAT3 activation and head and neck squamous cell carcinoma tumor growth. *Neoplasia*. 2015;17:256-64.
188. Yamamoto R, Nishikori M, Tashima M, Sakai T, Ichinohe T, Takaori-Kondo A, et al. B7-H1 expression is regulated by MEK/ERK signaling pathway in anaplastic large cell lymphoma and Hodgkin lymphoma. *Cancer science*. 2009;100:2093-100.
189. Ota K, Azuma K, Kawahara A, Hattori S, Iwama E, Tanizaki J, et al. Induction of PD-L1 Expression by the EML4-ALK Oncoprotein and Downstream Signaling Pathways in Non-Small Cell Lung Cancer. *Clin Cancer Res*. 2015;21:4014-21.
190. Sadzak I, Schiff M, Gattermeier I, Glinitzer R, Sauer I, Saalmuller A, et al. Recruitment of Stat1 to chromatin is required for interferon-induced serine phosphorylation of Stat1 transactivation domain. *Proc Natl Acad Sci U S A*. 2008;105:8944-9.
191. Lee SJ, Jang BC, Lee SW, Yang YI, Suh SI, Park YM, et al. Interferon regulatory factor-1 is prerequisite to the constitutive expression and IFN-gamma-induced upregulation of B7-H1 (CD274). *FEBS letters*. 2006;580:755-62.
192. Lassen P, Overgaard J, Eriksen JG. Expression of EGFR and HPV-associated p16 in oropharyngeal carcinoma: correlation and influence on prognosis after radiotherapy in the randomized DAHANCA 5 and 7 trials. *Radiotherapy and oncology : journal of the European Society for Therapeutic Radiology and Oncology*. 2013;108:489-94.
193. Freeman GJ, Long AJ, Iwai Y, Bourque K, Chernova T, Nishimura H, et al. Engagement of the PD-1 immunoinhibitory receptor by a novel B7 family member leads to negative regulation of lymphocyte activation. *The Journal of experimental medicine*. 2000;192:1027-34.
194. Wang T, Niu G, Kortylewski M, Burdelya L, Shain K, Zhang S, et al. Regulation of the innate and adaptive immune responses by Stat-3 signaling in tumor cells. *Nature medicine*. 2004;10:48-54.
195. Kortylewski M, Kujawski M, Wang T, Wei S, Zhang S, Pilon-Thomas S, et al. Inhibiting Stat3 signaling in the hematopoietic system elicits multicomponent antitumor immunity. *Nature medicine*. 2005;11:1314-21.
196. Gabrilovich DI, Chen HL, Girgis KR, Cunningham HT, Meny GM, Nadaf S, et al. Production of vascular endothelial growth factor by human tumors inhibits the functional maturation of dendritic cells. *Nature medicine*. 1996;2:1096-103.
197. Yang AS, Lattime EC. Tumor-induced interleukin 10 suppresses the ability of splenic dendritic cells to stimulate CD4 and CD8 T-cell responses. *Cancer Res*. 2003;63:2150-7.

198. Yue FY, Dummer R, Geertsen R, Hofbauer G, Laine E, Manolio S, et al. Interleukin-10 is a growth factor for human melanoma cells and down-regulates HLA class-I, HLA class-II and ICAM-1 molecules. *Int J Cancer*. 1997;71:630-7.
199. Salazar-Onfray F, Charo J, Petersson M, Frelund S, Noffz G, Qin Z, et al. Down-regulation of the expression and function of the transporter associated with antigen processing in murine tumor cell lines expressing IL-10. *J Immunol*. 1997;159:3195-202.
200. Mooradian DL, Purchio AF, Furcht LT. Differential effects of transforming growth factor beta 1 on the growth of poorly and highly metastatic murine melanoma cells. *Cancer Res*. 1990;50:273-7.
201. Nishikawa H, Kato T, Tawara I, Ikeda H, Kuribayashi K, Allen PM, et al. IFN-gamma controls the generation/activation of CD4⁺ CD25⁺ regulatory T cells in antitumor immune response. *J Immunol*. 2005;175:4433-40.
202. Larmonier N, Marron M, Zeng Y, Cantrell J, Romanoski A, Sepassi M, et al. Tumor-derived CD4(+)CD25(+) regulatory T cell suppression of dendritic cell function involves TGF-beta and IL-10. *Cancer Immunol Immunother*. 2007;56:48-59.
203. Zorn E, Nelson EA, Mohseni M, Porcheray F, Kim H, Litsa D, et al. IL-2 regulates FOXP3 expression in human CD4⁺CD25⁺ regulatory T cells through a STAT-dependent mechanism and induces the expansion of these cells in vivo. *Blood*. 2006;108:1571-9.
204. Mantovani A, Sica A, Sozzani S, Allavena P, Vecchi A, Locati M. The chemokine system in diverse forms of macrophage activation and polarization. *Trends Immunol*. 2004;25:677-86.
205. Duluc D, Delneste Y, Tan F, Moles MP, Grimaud L, Lenoir J, et al. Tumor-associated leukemia inhibitory factor and IL-6 skew monocyte differentiation into tumor-associated macrophage-like cells. *Blood*. 2007;110:4319-30.
206. Munn DH, Mellor AL. Indoleamine 2,3-dioxygenase and tumor-induced tolerance. *J Clin Invest*. 2007;117:1147-54.
207. Sriuranpong V, Park JI, Amornphimoltham P, Patel V, Nelkin BD, Gutkind JS. Epidermal growth factor receptor-independent constitutive activation of STAT3 in head and neck squamous cell carcinoma is mediated by the autocrine/paracrine stimulation of the interleukin 6/gp130 cytokine system. *Cancer Res*. 2003;63:2948-56.
208. Colomiere M, Ward AC, Riley C, Trenerry MK, Cameron-Smith D, Findlay J, et al. Cross talk of signals between EGFR and IL-6R through JAK2/STAT3 mediate epithelial-mesenchymal transition in ovarian carcinomas. *British journal of cancer*. 2009;100:134-

209. Gao SP, Mark KG, Leslie K, Pao W, Motoi N, Gerald WL, et al. Mutations in the EGFR kinase domain mediate STAT3 activation via IL-6 production in human lung adenocarcinomas. *J Clin Invest*. 2007;117:3846-56.
210. Duffy SA, Taylor JM, Terrell JE, Islam M, Li Y, Fowler KE, et al. Interleukin-6 predicts recurrence and survival among head and neck cancer patients. *Cancer*. 2008;113:750-7.
211. Linkov F, Lisovich A, Yurkovetsky Z, Marrangoni A, Velikokhatnaya L, Nolen B, et al. Early detection of head and neck cancer: development of a novel screening tool using multiplexed immunobead-based biomarker profiling. *Cancer Epidemiol Biomarkers Prev*. 2007;16:102-7.
212. Concha-Benavente F, Srivastava RM, Trivedi S, Lei Y, Chandran U, Seethala RR, et al. Identification of the cell-intrinsic and extrinsic pathways downstream of EGFR and IFN γ that induce PD-L1 expression in head and neck cancer. *Cancer Res*. 2015.
213. Shi MH, Xing YF, Zhang ZL, Huang JA, Chen YJ. [Effect of soluble PD-L1 released by lung cancer cells in regulating the function of T lymphocytes]. *Zhonghua Zhong Liu Za Zhi*. 2013;35:85-8.
214. Rossille D, Gressier M, Damotte D, Maucort-Boulch D, Pangault C, Semana G, et al. High level of soluble programmed cell death ligand 1 in blood impacts overall survival in aggressive diffuse large B-Cell lymphoma: results from a French multicenter clinical trial. *Leukemia*. 2014;28:2367-75.
215. Zheng Z, Bu Z, Liu X, Zhang L, Li Z, Wu A, et al. Level of circulating PD-L1 expression in patients with advanced gastric cancer and its clinical implications. *Chin J Cancer Res*. 2014;26:104-11.
216. Izhak L, Wildbaum G, Jung S, Stein A, Shaked Y, Karin N. Dissecting the autocrine and paracrine roles of the CCR2-CCL2 axis in tumor survival and angiogenesis. *PLoS One*. 2012;7:e28305.
217. Ma J, Wang Q, Fei T, Han JD, Chen YG. MCP-1 mediates TGF-beta-induced angiogenesis by stimulating vascular smooth muscle cell migration. *Blood*. 2007;109:987-94.
218. Curiel TJ, Coukos G, Zou L, Alvarez X, Cheng P, Mottram P, et al. Specific recruitment of regulatory T cells in ovarian carcinoma fosters immune privilege and predicts reduced survival. *Nature medicine*. 2004;10:942-9.
219. Schott AK, Pries R, Wollenberg B. Permanent up-regulation of regulatory T-lymphocytes in patients with head and neck cancer. *Int J Mol Med*. 2010;26:67-75.

220. Li J, Srivastava RM, ETTYREDDY A, Ferris RL. Cetuximab ameliorates suppressive phenotypes of myeloid antigen presenting cells in head and neck cancer patients. *J Immunother Cancer*. 2015;3:54.
221. Jie HB, Schuler PJ, Lee SC, Srivastava RM, Argiris A, Ferrone S, et al. CTLA-4(+) Regulatory T Cells Increased in Cetuximab-Treated Head and Neck Cancer Patients Suppress NK Cell Cytotoxicity and Correlate with Poor Prognosis. *Cancer Res*. 2015;75:2200-10.
222. Okazaki T, Honjo T. The PD-1-PD-L pathway in immunological tolerance. *Trends Immunol*. 2006;27:195-201.
223. Keir ME, Liang SC, Guleria I, Latchman YE, Qipo A, Albacker LA, et al. Tissue expression of PD-L1 mediates peripheral T cell tolerance. *J Exp Med*. 2006;203:883-95.
224. Tsushima F, Yao S, Shin T, Flies A, Flies S, Xu H, et al. Interaction between B7-H1 and PD-1 determines initiation and reversal of T-cell anergy. *Blood*. 2007;110:180-5.
225. Sfanos KS, Bruno TC, Meeker AK, De Marzo AM, Isaacs WB, Drake CG. Human prostate-infiltrating CD8+ T lymphocytes are oligoclonal and PD-1+. *The Prostate*. 2009;69:1694-703.
226. Ahmadzadeh M, Johnson LA, Heemskerk B, Wunderlich JR, Dudley ME, White DE, et al. Tumor antigen-specific CD8 T cells infiltrating the tumor express high levels of PD-1 and are functionally impaired. *Blood*. 2009;114:1537-44.
227. Katou F, Ohtani H, Watanabe Y, Nakayama T, Yoshie O, Hashimoto K. Differing phenotypes between intraepithelial and stromal lymphocytes in early-stage tongue cancer. *Cancer Res*. 2007;67:11195-201.
228. Ferris RL. Immunology and Immunotherapy of Head and Neck Cancer. *Journal of clinical oncology : official journal of the American Society of Clinical Oncology*. 2015;33:3293-304.
229. Petrovas C, Casazza JP, Brenchley JM, Price DA, Gostick E, Adams WC, et al. PD-1 is a regulator of virus-specific CD8+ T cell survival in HIV infection. *J Exp Med*. 2006;203:2281-92.
230. Lanier LL. Up on the tightrope: natural killer cell activation and inhibition. *Nat Immunol*. 2008;9:495-502.
231. Ferris RL, Jaffee EM, Ferrone S. Tumor antigen-targeted, monoclonal antibody-based immunotherapy: clinical response, cellular immunity, and immunoescape. *Journal of clinical oncology : official journal of the American Society of Clinical Oncology*. 2010;28:4390-9.

232. Kim S, Grandis JR, Rinaldo A, Takes RP, Ferlito A. Emerging perspectives in epidermal growth factor receptor targeting in head and neck cancer. *Head & neck*. 2008;30:667-74.
233. Argiris A, Karamouzis MV, Raben D, Ferris RL. Head and neck cancer. *Lancet*. 2008;371:1695-709.
234. Alvarez IB, Pasquinelli V, Jurado JO, Abbate E, Musella RM, de la Barrera SS, et al. Role played by the programmed death-1-programmed death ligand pathway during innate immunity against *Mycobacterium tuberculosis*. *The Journal of infectious diseases*. 2010;202:524-32.
235. Golden-Mason L, Klarquist J, Wahed AS, Rosen HR. Cutting edge: programmed death-1 expression is increased on immunocytes in chronic hepatitis C virus and predicts failure of response to antiviral therapy: race-dependent differences. *J Immunol*. 2008;180:3637-41.
236. Norris S, Coleman A, Kuri-Cervantes L, Bower M, Nelson M, Goodier MR. PD-1 expression on natural killer cells and CD8(+) T cells during chronic HIV-1 infection. *Viral immunology*. 2012;25:329-32.
237. Benson DM, Jr., Bakan CE, Mishra A, Hofmeister CC, Efebera Y, Becknell B, et al. The PD-1/PD-L1 axis modulates the natural killer cell versus multiple myeloma effect: a therapeutic target for CT-011, a novel monoclonal anti-PD-1 antibody. *Blood*. 2010;116:2286-94.
238. Francisco LM, Salinas VH, Brown KE, Vanguri VK, Freeman GJ, Kuchroo VK, et al. PD-L1 regulates the development, maintenance, and function of induced regulatory T cells. *J Exp Med*. 2009;206:3015-29.
239. Herberman RB, Nunn ME, Holden HT, Lavrin DH. Natural cytotoxic reactivity of mouse lymphoid cells against syngeneic and allogeneic tumors. II. Characterization of effector cells. *Int J Cancer*. 1975;16:230-9.
240. Herberman RB, Nunn ME, Lavrin DH. Natural cytotoxic reactivity of mouse lymphoid cells against syngeneic acid allogeneic tumors. I. Distribution of reactivity and specificity. *Int J Cancer*. 1975;16:216-29.
241. Kiessling R, Klein E, Wigzell H. "Natural" killer cells in the mouse. I. Cytotoxic cells with specificity for mouse Moloney leukemia cells. Specificity and distribution according to genotype. *European journal of immunology*. 1975;5:112-7.
242. Brown JA, Dorfman DM, Ma FR, Sullivan EL, Munoz O, Wood CR, et al. Blockade of programmed death-1 ligands on dendritic cells enhances T cell activation and cytokine production. *J Immunol*. 2003;170:1257-66.

243. Strome SE, Dong H, Tamura H, Voss SG, Flies DB, Tamada K, et al. B7-H1 blockade augments adoptive T-cell immunotherapy for squamous cell carcinoma. *Cancer Res.* 2003;63:6501-5.
244. Melioli G, Semino C, Margarino G, Mereu P, Scala M, Cangemi G, et al. Expansion of natural killer cells in patients with head and neck cancer: detection of "noninhibitory" (activating) killer Ig-like receptors on circulating natural killer cells. *Head & neck.* 2003;25:297-305.
245. Accomando WP, Wiencke JK, Houseman EA, Butler RA, Zheng S, Nelson HH, et al. Decreased NK cells in patients with head and neck cancer determined in archival DNA. *Clin Cancer Res.* 2012;18:6147-54.
246. Sauce D, Almeida JR, Larsen M, Haro L, Autran B, Freeman GJ, et al. PD-1 expression on human CD8 T cells depends on both state of differentiation and activation status. *Aids.* 2007;21:2005-13.